UNIVERSITÄT BASEL

DEPARTEMENT PHARMAZEUTISCHE WISSENSCHAFTEN

The Role of the Endoplasmic Reticulum in the Metabolism of *Xenobiotica*

Inauguraldissertation

zur

Erlangung der Würde eines Doktors der Philosophie

vorgelegt der

Philosophisch-Naturwissenschaftlichen Fakultät

der Universität Basel

von

Arne Meyer, eidg. dipl. Apotheker, MSc Pharmazie, BSc Pharmazeutische Wissenschaften

aus Göttingen, Deutschland

Basel, 2013

UNIVERSITÄT BASEL

DEPARTEMENT PHARMAZEUTISCHE WISSENSCHAFTEN

Genehmigt von der Philosophisch-Naturwissenschaftlichen Fakultät

auf Antrag von Prof. Dr. Alex Odermatt (Fakultätsverantwortlicher) und Prof. Dr. Michael Arand (Korreferent)

_____

Fakultätsverantwortlicher

Prof. Dr. Alex Odermatt

Basel, den 23. April 2013

_____

Dekan

Prof. Dr. Jörg Schibler

Summary

Short-chain dehydrogenase/reductase (SDR) enzymes play a key role in the metabolism of steroids, fatty acids, prostaglandins and xenobiotic chemicals. This thesis investigated the role of 11β-hydroxysteroid dehydrogenase type 1 (11β-HSD1) in the metabolism of xenobiotics. It further addressed species-specific differences of the inhibition of 11β-HSD1 and some related microsomal SDRs by xenobiotics. 11β-HSD1 catalyzes the conversion of the inactive glucocorticoids cortisone and 11-dehydrocorticosterone to the active cortisol and corticosterone, respectively. Recently, studies using microsomes and the unspecific inhibitor glycyrrhetinic acid (GA) suggested that 11β-HSD1 metabolizes the antidepressant drug bupropion to erythrohydrobupropion (EHB) and threohydrobupropion (THB), and the fungicide triadimefon to triadimenol. In the present work, the role of human 11β-HSD1 in the reduction of triadimefon and bupropion was studied *in vitro* using the recombinant 11β-HSD1 enzyme, a selective 11β-HSD1 inhibitor and microsomes from liver-specific 11β-HSD1 knock-out mice. Activities were determined using microsomes from human, rat and mouse liver to assess species-specific differences. The results suggest that 11β-HSD1 is the major enzyme responsible for triadimenol formation. Surprisingly, 11β-HSD1 exclusively formed THB but not EHB from bupropion. Due to lower activities of rat and mouse 11β-HSD1 towards these xenobiotics, they are models of limited value to study 11β-HSD1-dependent metabolism of bupropion and triadimefon. A comparison of IC_{50} values suggests that exposure to these compounds is unlikely to impair the 11β-HSD1-dependent activation of glucocorticoids. In contrast, elevated glucocorticoids during stress or upon pharmacological administration are likely to inhibit 11β-HSD1-dependent metabolism of these xenobiotics.

11β-hydroxysteroid dehydrogenase type 2 (11β-HSD2) catalyzes the conversion of the active glucocorticoid cortisol to the inactive cortisone. It has been reported that some organotins and dithiocarbamates are potent inhibitors of human 11β-HSD2. We found that the zebrafish enzyme is not inhibited by these organotins. Furthermore, the dithiocarbamate thiram showed a reduced inhibitory effect on zebrafish 11β-HSD2 compared with the human enzyme. Sequence comparison revealed the presence of an alanine at position 253 on zebrafish 11β-HSD2, corresponding to cysteine-264 in the substrate binding pocket of the human enzyme. Substitution

of alanine-253 by cysteine resulted in a more than 10-fold increased sensitivity of zebrafish 11β-HSD2 to thiram. These findings are important, as the zebrafish is a widely used model in ecotoxicology, and 11β-HSD2 is catalyzing the conversion of 11β-hydroxytestosterone to 11-ketotestosterone, the main androgen in fish.

The gene encoding 11β-HSD1 in zebrafish is absent. Therefore, the mechanism how the ratio between active and inactive glucocorticoids is controlled in fish is unclear. It was suggested by a phylogenetic analysis that one of the two ancestors of 11β-HSD1 might reduce cortisone to cortisol. These ancestors are 11β-HSD3a and 11β-HSD3b. We cloned both zebrafish cDNAs and tested them for 11-oxosteroid reductase activity. Furthermore, we examined the metabolism of cortisone in zebrafish microsomes. Our results indicate that the 11-oxosteroid reductase activity is completely absent in zebrafish.

17β-hydroxysteroid dehydrogenase type 3 (17β-HSD3) catalyzes the conversion of Δ^4-androstenedione to testosterone. We reported earlier that some UV filters inhibit the human enzyme. We tested whether these UV filters also inhibit the zebrafish enzyme. We found interesting species-specific differences of the inhibitory potential of UV filters on human and zebrafish 17β-HSD3. Furthermore, we were able to show additive inhibitory effects of UV filter mixtures and bioaccumulation of UV filters *in vitro*.

In conclusion, the results presented in this thesis significantly extend the knowledge of the role of 11β-HSD1 in the metabolism of xenobiotics. The thesis further emphasizes the importance of considering species-specific differences when trying to extrapolate effects of xenobiotics observed in animal models to humans.

Preface

During this thesis I initiated several projects and successfully completed the majority of them. This thesis is divided into four chapters covering the main findings. In the first chapter, the Yellow Fluorescence Protein project is outlined and possible reasons for its failure are discussed. The second chapter describes a project, where the role of 11β-hydroxysteroid dehydrogenase type 1 in the metabolism of *xenobiotica* was investigated. This chapter is followed by a published paper and a paper draft. In the third chapter, a variety of experiments linked to steroid metabolizing enzymes of the zebrafish (*danio rerio*) are presented, followed by a published paper and a paper draft. The last chapter highlights experiments performed in connection with the 17β-hydroxysteroid dehydrogenase type 2 inhibitor project, followed by a paper where I am a co-author.

I would like to thank Prof. Alex Odermatt for his continuous support and stimulating discussions, my students Petra Strajhar, Céline Murer, Fabio Bachmann and Dominik Vogt for their hard work and contribution of important data, Thierry Da Cunha for his continuous support with the liquid chromatography-tandem mass spectrometry and all members from the Molecular and Systems Toxicology group for their support.

Table of Contents

Chapter 1: YFP-Project: The quest for ER luminal enzymes 6

Introduction 7

Results & Discussion 8

Chapter 2: 11β-HSD1-dependent *xenobiotica* metabolism 10

Introduction 11

Results & Discussion 15

Paper: Carbonyl reduction of triadimefon by human and rodent 11β-hydroxysteroid dehydrogenase 1 16

Paper Draft: Carbonyl reduction of bupropion to threohydrobupropion by human and rodent 11β-hydroxysteroid dehydrogenase 1 52

Chapter 3: Steroid metabolism of zebrafish enzymes 83

Introduction 84

Results & Discussion 86

Paper: Species-specific differences in the inhibition of human and zebrafish 11β-hydroxysteroid dehydrogenase 2 by thiram and organotins 89

Paper Draft: Absence of 11-oxosteroid reductase activity in the model organism zebrafish 97

Chapter 4: 17β-HSD2 inhibitor testing 120

Introduction 121

Results & Discussion 122

Paper: Structural optimization of 2,5-thiophene amides as highly potent and selective 17β-hydroxysteroid dehydrogenase type 2 inhibitors for the treatment of osteoporosis 123

Appendix 139

Protocol: Preparation of intact liver microsomes & cytochrome C reductase assay 140

References 141

Chapter 1: YFP-Project: The quest for ER luminal enzymes

Introduction

The aim of the Yellow Fluorescent Protein (YFP) project was to identify enzymes that interact with hexose-6-phosphate dehydrogenase (H6PDH) in the endoplasmic reticulum (ER) and which might play a role in the metabolism of xenobiotics.

H6PDH is a microsomal enzyme. It has been shown that it interacts directly with 11β-hydroxysteroid dehydrogenase type 1 (11β-HSD1) [1, 2]. H6PDH converts glucose-6-phosphate (G6P) to 6-phosphogluconate and thereby converts $NADP^+$ to NADPH, the cofactor for 11β-HSD1 [3]. Currently, 11β-HSD1 is the only enzyme described which is localized in the lumen of the ER and utilizes NADPH to reduce its substrates. The ER has been described as an oxidative environment compared with the cytosol. We believe that there are additional reductive enzymes inside the ER that need NADPH as a cofactor and we hypothesize that some of these also interact with H6PDH.

In the YFP project we aimed to identify new interacting partners of H6PDH with the use of the protein fragment complementation assay (PCA). We started with the plasmids obtained from the study published by Nyfeler *et al.* [4]. The authors were able to detect protein-protein interactions in the secretory pathway of living cells with the use of the PCA. In the literature the PCA is described as relatively simple assay to perform with the advantage of providing a simple fluorescent readout. The DNA sequence coding for the YFP is split into two parts, one coding for the N-terminal fragment of YFP (YFP1), the other coding for the C-terminal fragment (YFP2). If these fragments are simultaneously expressed in cells and brought into close proximity, the YFP fragments can reconstitute and, upon proper folding, form a complete YFP that serves as a reporter. YFP can be excited at 514 nm and an emission peak of 527 nm can be recorded. The fluorescence can be detected with a fluorescence microscope, or any other fluorescence measuring device. Subcloning of these fragments into two separate vectors each containing an interacting partner, should bring the YFP fragments in close proximity to each other and allow complementation and detection of a fluorescence signal. The YFP fragments are directly linked to the enzymes, either N or C-terminally, with the help of a linker on each of the interacting proteins.

We planned to use H6PDH linked via the C-terminal to the YFP2 fragment with a $(GGGGS)_2$ linker as bait and to construct a cDNA library linked via the C-terminal to the YFP1 with a $(GGGGS)_2$ linker as prey, in order to find new interacting proteins as described by Nyfeler *et al*. [4].

Results & Discussion

Before constructing the cDNA library, we generated a positive and negative control. Therefore, the H6PDH was linked C-terminally to YFP2 with a $(GGGGS)_2$ linker and 11β-HSD1 was linked C-terminally to YFP1 with a $(GGGGS)_2$ linker as a positive control. In this project the enzymes were tagged C-terminally as performed by Atanasov *et al*. [1], using C-terminally tagged H6PDH and 11β-HSD1 for Förster resonance energy transfer (FRET). For the negative control, a chimeric construct of 17β-HSD2 was used. It has previously been shown that 11β-HSD1 interacts with H6PDH [2], while 17β-HSD2 does not, because it is utilizing NAD^+ and therefore no interaction should occur. These constructs have been transfected into HEK-293 and COS-1 cells using the calcium phosphate transfection method and Fugene HD, respectively. Protein expression was verified by western blotting. Although all protein constructs were sequence verified and the expression was controlled, the interaction of H6PDH with 11β-HSD1 could not be monitored with the protein fragmentation assay, since we were not able to detect any fluorescence signal with the positive control. However, the full-length YFP control did show a fluorescence signal under the fluorescence microscope. Unfortunately, taking into account the positive control did not work we decided to stop the YFP project.

In theory the protein fragment complementation assay seems to be a straightforward approach to visualize direct protein interactions in living cells and enables the determination of the subcellular sites of protein interactions. Unfortunately, in our setting we could not confirm a known protein interaction. The specific reasons are unclear. In my opinion, carrying out PCA, the following points need to be considered:

- Steric hindrance,

- N-terminally or C-terminally linkage of YFP fragments,
- Length of the linker,
- Accurate folding of the proteins.

In order to successfully apply the PCA, the two YFP fragments must be close enough for complementation. It could be possible that the two interacting proteins connected to the fragments prevent proper complementation of the two YFP fragments by so called steric hindrance. This problem might be solved with the use of a wide set of linkers of different length. Further, it is important to know the localization of the N- and C-terminal position of the protein. ER membrane-bound proteins can have the N-terminus and C-terminus cytosolic or ER luminal. Soluble proteins might have the termini inside the protein and therefore the YFP fragments are not accessible for complementation, depending on the protein tertiary structure. Therefore two plasmids should be constructed, one N-terminally tagged and one C-terminally tagged, in case the structure is not known. A further pitfall is the accurate folding of the protein if the primary structure of the protein is modified, as it is the case in the PCA, whereby the sequence is prolonged N- or C-terminally, this might ultimately affect the complete folding of the proteins. Incorrectly folded proteins might not be able to interact with each other anymore.

Taking these points into consideration, we realized that the identification of new interacting proteins with H6PDH by this approach was very ambitious. In a cDNA screening approach, the YFP fragment would have been constructed twice (N- and C-terminally), with different length linkers. Another idea would be to create double tagged enzymes, with the same fragments N- and C-terminally tagged. These modifications would lead to a highly time-consuming screening approach, which is still very risky, especially if the H6PDH-YFP2 does not fold properly. For these reasons, we decided to stop the YFP project.

Chapter 2: 11β-HSD1-dependent *xenobiotica* metabolism

Introduction

The pivotal role of 11β-HSD1 has been extensively studied, with its main function in the conversion of the inactive glucocorticoid cortisone to the active cortisol (Fig. 1) and by activating pharmacological applied prednisone to prednisolone. Cortisol and prednisolone are able to activate the glucocorticoid receptor (GR) and therefore are responsible for the expression of GR-dependent genes in metabolically relevant tissues such as the liver, adipose and skeletal muscle [5]. Currently, research is focusing on the development of 11β-HSD1 inhibitors. Several studies suggest that the inhibition of 11β-HSD1 might be beneficial in the treatment of obesity, type 2 diabetes mellitus and metabolic syndrome [6-8].

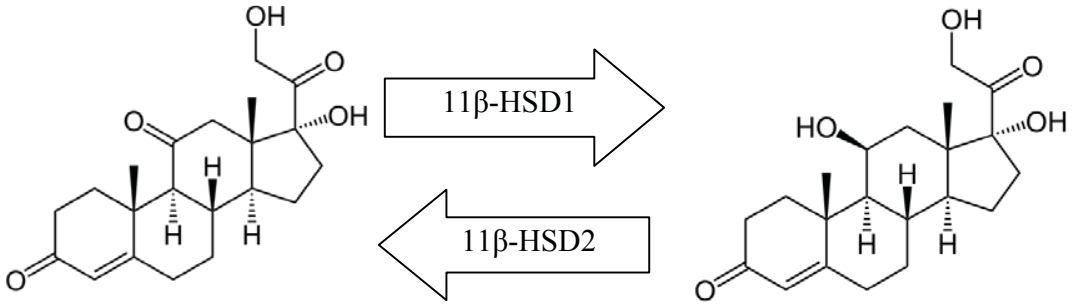

Figure 1: The conversion of inactive cortisone (left) and active cortisol (right) by 11β-hydroxysteroid dehydrogenase type 1 and type 2 (11β-HSD1, 11β-HSD2)

We reported earlier that 11β-HSD1 has a broad substrate spectrum and plays an important role in the metabolism of 7-ketodehydroepiandrosterone [9], 7-ketocholesterol [10] and the secondary bile acid 7-oxolithocholic acid [11]. In addition, several xenobiotics have been identified as substrates of 11β-HSD1 like oracin [12], metyrapone [13] and ketoprofen [14].

Lately, by the use of rat liver microsomes and the unspecific 11β-HSD inhibitor glycyrrhetinic acid (GA), it has been suggested that the triazole fungicide triadimefon is reduced to its metabolite triadimenol by 11β-HSD1 (Fig. 2) [15, 16]. Barton *et al*. showed the involvement of cytochrome P450 in the metabolism of triadimefon in human and rat liver microsomal preparations [17]. Triadimefon and the active metabolite triadimenol are extensively used as broad-spectrum fungicides in agriculture and landscaping [16]. The wide use of triadimefon and the long degradation half-life of around 23 days under controlled laboratory conditions [18]

demonstrates the need to not only study the effects on mammalian models, but also to investigate the metabolism of this fungicide in humans.

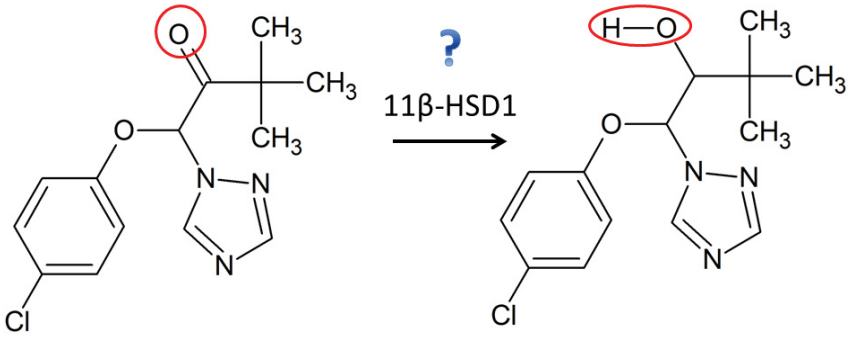

Figure 2: Suggested carbonyl reduction of triadimefon (left) to triadimenol (right) by 11β-HSD1

Another interesting compound is climbazole, which is used in anti-dandruff shampoos. It is structurally similar to triadimefon, with the exception of belonging to the imidazoles and having therefore only two nitrogens in the ring system instead of three (Fig. 3). Due to the structural similarity of climbazole and triadimefon, it can be assumed that climbazole is metabolized by 11β-HSD1. Unfortunately, the theoretically reduced metabolite of climbazole by 11β-HSD1 is not commercially available. Therefore, a quantitation of the product is inaccurate and further testing was put on hold.

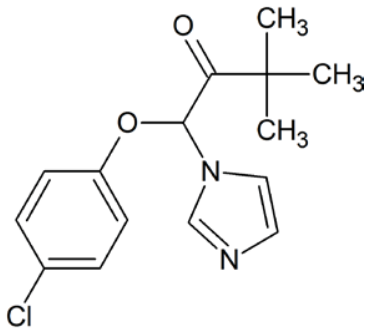

Figure 3: Structure of climbazole

It has been suggested that bupropion (Wellbutrin®) is metabolized by 11β-HSD1 [19-21]. Bupropion is used as a racemic mixture of *R*- and *S*-bupropion (Fig. 4). Bupropion is used for more than 20 years for the treatment of depression by approximately 40 million people [22, 23]. Cytochrome P450 2B6 has been identified to be responsible for hydroxybupropion formation [24, 25]. Lately, it was thought that the antidepressant bupropion might be metabolized by one of the

11β-HSDs to erythrohydrobupropion (EHB) and threohydrobupropion (THB) by human placental microsomes [20], baboon hepatic and placental microsomes [19] and human liver microsomes [21]. This hypothesis was based on observations from experiments with human microsomes of liver and placenta with bupropion and the unspecific 11β-HSD inhibitor GA. Incubations with GA yielded lower amounts of THB and EHB. These studies suggested the involvement of 11β-HSD in the carbonyl reduction of bupropion.

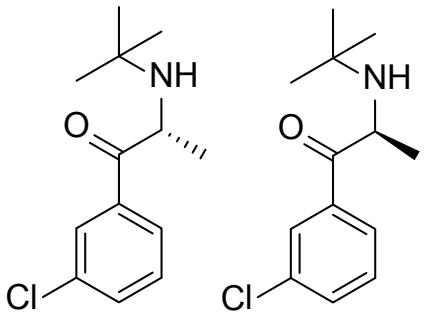

Figure 4: Structure of *R*-bupropion (left) and *S*-bupropion (right)

We performed several experiments in order to elucidate the 11β-HSD1-dependent metabolism of these three xenobiotics. This is interesting for three reasons: First, the metabolism of these xenobiotics might be impaired by the future therapeutic use of 11β-HSD1 inhibitors. Second, as it is suggested that substances metabolized by 11β-HSD1 in the ER could undergo direct phase II metabolism in the ER, *i.e.* glucuronidation. Third, if under circumstances of glucocorticoid treatment the metabolism of these xenobiotica might be impaired or *vice versa*. The results of triadimefon and bupropion are included in the paper and the paper draft at the end of this chapter.

We obtained livers from liver-specific 11β-HSD1 knockout mice from Prof. Lavery (University of Birmingham, UK) to investigate the relative contribution of 11β-HSD1 to the metabolism of xenobiotics by microsomal incubations. First, I optimized the protocol for the preparation of microsomes from liver tissue. Important in the preparation of microsomes is the intactness of the microsomal vesicles, which allows afterwards in the microsomal incubations to distinguish between luminal enzymes and microsomal enzymes facing the cytoplasm. If the microsomal vesicles are intact, 11β-HSD1 activity can be measured upon incubation with G6P, as G6P is transported by glucose-6-phosphate translocase (G6PT) into the lumen of the ER, where it is used by H6PDH, which then produces NADPH. Whereas upon addition of NADPH, NADPH will be

exclusively utilized by enzymes facing the cytoplasm, since the ER membrane is a barrier for NADPH (Fig 5).

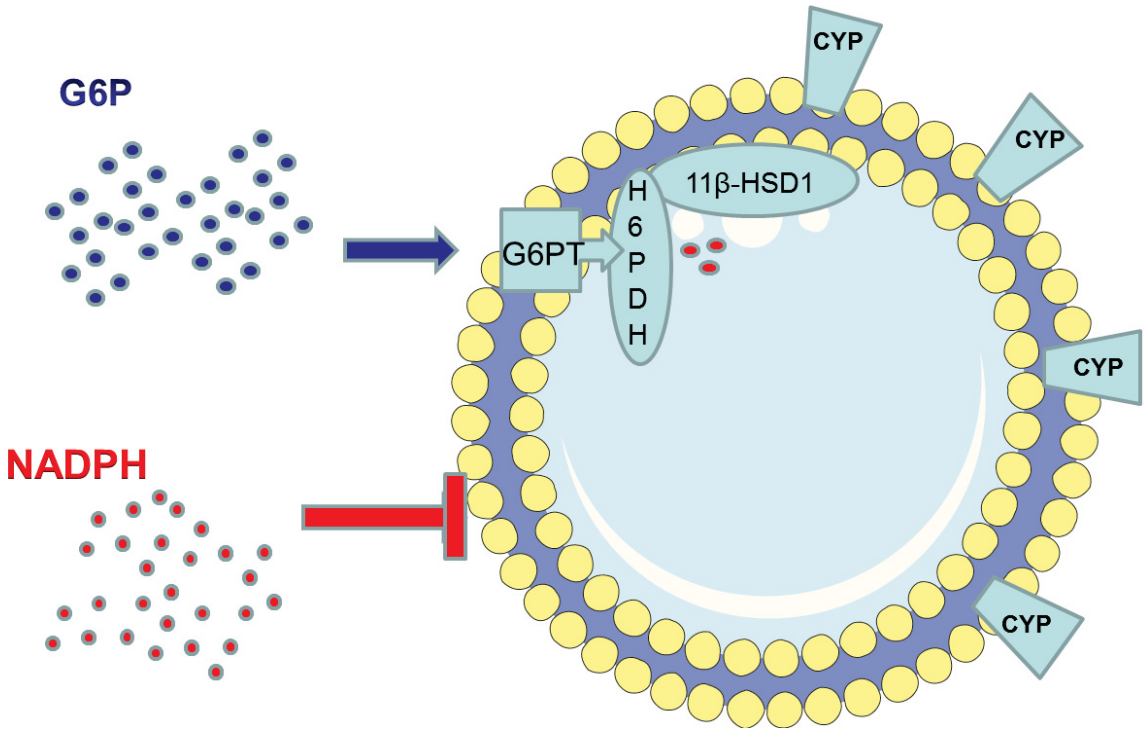

Figure 5: Schematic picture of microsomal incubations. Glucose-6-phosphate (G6P) is transported by glucose-6-phosphate translocase (G6PT) into the lumen of the ER, where it is used by hexose-6-phosphate dehydrogenase (H6PDH), which then produces NADPH. Addition of NADPH will only stimulate enzymes facing the cytosol, *i.e.* cytochrome P450 reductase leading to cytochrome P450 (CYP) mediated metabolism. Figure was produced using Servier Medical Art (www.servier.com).

Results & Discussion

The protocol to prepare microsomes was optimized, the final protocol can be found in the appendix. By following the optimized protocol, the latency of 11β-HSD1 activity in microsomes was about 90%, whereas the latency of commercially available human liver microsomes (Celsis In Vitro Inc (Baltimore, MD)) was around 75%. In order to generate intact microsomal vesicles from frozen liver tissue, the pieces should be homogenized with a Potter-Elvehjem PTFE pestle and glass tube, and ultrasonification should be avoided. No more than 12 strokes should be applied. The buffer should be of physiological ionic strength. If these points are taken into consideration, a high degree of intactness of the microsomal vesicles can be achieved.

Microsomal incubations with climbazole have been performed as for triadimefon and bupropion. We were able to monitor the disappearance of the climbazole peak by liquid chromatography-tandem mass spectrometry (LC-MS/MS), but since no authentic standard of the product is commercially available, the hydroxyclimbazole peak cannot be verified and no quantitation of the peak is possible. Nevertheless, our results indicate that climbazole is metabolized by 11β-HSD1. Ultimately, this has to be tested with an authentic standard. This finding is interesting from a mechanistic point of view, although I would assume that it is biologically less relevant, because anti-dandruff shampoos contain only concentrations up to 2% climbazole, and the human exposure to climbazole is expected to be very low.

Paper: Carbonyl reduction of triadimefon by human and rodent 11β-hydroxysteroid dehydrogenase 1

Carbonyl reduction of triadimefon by human and rodent 11β-hydroxysteroid dehydrogenase 1

Arne Meyer[1], Anna Vuorinen[2], Agnieszka E. Zielinska[3], Thierry Da Cunha[1], Petra Strajhar[1], Gareth G. Lavery[3], Daniela Schuster[2] and Alex Odermatt[1]

[1]Swiss Center for Applied Human Toxicology and Division of Molecular and Systems Toxicology, Department of Pharmaceutical Sciences, University of Basel, Klingelbergstrasse 50, 4056 Basel, Switzerland

[2]Institute of Pharmacy/Pharmaceutical Chemistry and Center for Molecular Biosciences Innsbruck – CMBI, University of Innsbruck, Innrain 80/82, 6020 Innsbruck, Austria

[3]Centre for Endocrinology Diabetes and Metabolism (CEDAM), Institute of Biomedical Research, Medical School Building, School of Clinical and Experimental Medicine, College of Medical and Dental Sciences, University of Birmingham, Edgbaston, Birmingham, B15 2TT, UK

Corresponding author:
Dr. Alex Odermatt, Division of Molecular and Systems Toxicology, Department of Pharmaceutical Sciences, University of Basel, Klingelbergstrasse 50, 4056 Basel, Switzerland
Phone: +41 61 267 1530, Fax: +41 61 267 1515, E-mail: alex.odermatt@unibas.ch

Abstract

11β-hydroxysteroid dehydrogenase 1 (11β-HSD1) catalyzes the conversion of inactive 11-oxo glucocorticoids (endogenous cortisone, 11-dehydrocorticosterone and synthetic prednisone) to their potent 11β-hydroxyl forms (cortisol, corticosterone and prednisolone). Besides, 11β-HSD1 accepts several other substrates. Using rodent liver microsomes and the unspecific inhibitor glycyrrhetinic acid, it has been proposed earlier that 11β-HSD1 catalyzes the reversible conversion of the fungicide triadimefon to triadimenol. In the present study, recombinant human, rat and mouse enzymes together with a highly selective 11β-HSD1 inhibitor were applied to assess the role of 11β-HSD1 in the reduction of triadimefon and to uncover species-specific differences. To further demonstrate the role of 11β-HSD1 in the carbonyl reduction of triadimefon, microsomes from liver-specific 11β-HSD1-deficient mice were employed. Molecular docking was applied to investigate substrate binding. The results revealed important species differences and demonstrated the irreversible 11β-HSD1-dependent reduction of triadimefon. Human liver microsomes showed 4 and 8 times higher activity than rat and mouse liver microsomes. The apparent V_{max}/K_m of recombinant human 11β-HSD1 was 5 and 15 times higher than that of mouse and rat 11β-HSD1, respectively, indicating isoform-specific differences and different expression levels for the three species. Experiments using inhibitors and microsomes from 11β-HSD1-deficient mice indicated that 11β-HSD1 is the major if not only enzyme responsible for triadimenol formation. The IC_{50} values of triadimefon and triadimenol for cortisone reduction suggested that exposure to these xenobiotica unlikely impairs the 11β-HSD1-dependent glucocorticoid activation. However, elevated glucocorticoids during stress or upon pharmacological administration likely inhibit 11β-HSD1-dependent metabolism of triadimefon in humans.

Keywords

Triadimefon, 11β-hydroxysteroid dehydrogenase, metabolism, liver microsomes, azole fungicide, molecular docking

1. Introduction

Triadimefon and to a lesser extent the active metabolite triadimenol are used as broad-spectrum fungicides in agriculture and landscaping, with annual application rates of about 135,000 and 24,000 lbs/year, respectively [1]. Humans can be exposed through consumption of foods containing triadimefon or triadimenol residues [2]. More critical is occupational exposure through dermal contact and inhalation of sprays by field workers applying these fungicides [3]. The wide use of triadimefon and its long half-life of around 23 days under controlled laboratory conditions [4] emphasizes the need to investigate both the environmental fate and the potentially hazardous effects on animals and humans.

Toxicological studies revealed neurotoxic effects of triadimefon and triadimenol in rats, mice and rabbits [1]. Teratogenic effects were observed at very low concentrations in experiments using rat embryos [5]. Furthermore, triadimefon and triadimenol were shown to cause thyroid and liver tumors in rats, and they are considered as potential human carcinogens [1]. They act by inhibiting the activity of fungal lanosterol-14α-demethylase, a cytochrome P450 enzyme (CYP51), thereby blocking ergosterol biosynthesis which is essential for fungal cell wall integrity [6]. Like other azole fungicides, triadimefon and triadimenol can inhibit some of the mammalian cytochrome P450 enzymes involved in steroidogenesis, which may lead to endocrine disturbances [7].

According to conclusions by the US Environmental Protection Agency (EPA), the mechanisms of toxicity of triadimefon and triadimenol differ from those of other azole fungicides [1]. Kenneke et al. proposed that differences in the metabolism of triadimefon compared with other azole fungicides may be involved [8]. Experiments by Barton et al. with liver microsomes revealed that triadimefon can be metabolized by CYPs, whereby CYP2B6, CYP2C19 and CYP3A4 were the most active enzymes in human liver [9]. The authors mentioned very low

formation of triadimenol; however, they used assay conditions that do not allow to measure luminal carbonyl reductase activity. Kenneke et al., using rat liver microsomes and the unselective inhibitor glycyrrhetinic acid, then provided evidence that triadimefon is mainly metabolized to triadimenol and that this reaction is catalyzed by 11β-hydroxysteroid dehydrogenase 1 (11β-HSD1, SDR26C1) [8, 10, 11]. Interestingly, in a follow-on study they reported the conversion of triadimefon to triadimenol by rainbow trout microsomes [12], although it is known that the gene encoding 11β-HSD1 is absent in teleost species [13], thus suggesting the involvement of another enzyme.

11β-HSD1 plays a pivotal role in the regulation of energy metabolism through the activation of endogenous glucocorticoids in tissues such as liver, adipose and skeletal muscle [14]. Moreover, it essentially regulates the balance of mineralocorticoid receptor (MR)- and glucocorticoid receptor (GR)-mediated modulation of inflammatory parameters in macrophage-derived cells [15-17]. 11β-HSD1 is required for the pharmacological effect of cortisone and prednisone, which do not bind to corticosteroid receptors. Since 11β-HSD1 is considered as a promising target for the treatment of metabolic disorders, there is great interest in the development of 11β-HSD1 inhibitors [14, 18]. Besides its role in glucocorticoid activation, 11β-HSD1 catalyzes the carbonyl reduction of several endogenous oxidized sterols such as 7-ketocholesterol [19, 20], 7-ketodehydroepiandrosterone [21] and the secondary bile acid 7-oxolithocholic acid [22], as well as that of several xenobiotics including oracin [23], metyrapone [24], ketoprofen [25], 4-(methylnitrosamino)-1-(3-pyridyl)-1-butanone (NNK) [26], and as mentioned above, triadimefon [8, 10, 11].

Since the evidence for a role of 11β-HSD1 in the metabolism of triadimefon was based on rat microsomal activities and inhibition by the unselective inhibitor glycyrrhetinic acid (GA), we aimed in the present study to 1) optimize the assay conditions to distinguish between luminal

enzymes and microsomal enzymes facing the cytoplasm, 2) compare carbonyl reduction activity in human, rat and mouse liver microsomes in the presence and absence of a selective 11β-HSD1 inhibitor, 3) assess whether other enzymes contribute to the carbonyl reduction of triadimefon in human, rat and mouse liver microsomes, 4) assess activities of the corresponding recombinant 11β-HSD1 enzymes, and 5) investigate the binding of triadimefon to 11β-HSD1 by molecular modeling.

2. Materials and Methods

2.1. Chemicals and reagents

Human liver microsomes were purchased from Celsis In Vitro Inc (Baltimore, MD) and were obtained from a 77 year old male Caucasian. Human embryonic kidney (HEK-293) cells from ATCC (No CRL-1573) were obtained through LGC Standards S.a.r.l., Molsheim Cedex, France. Cell culture medium was from Invitrogen (Carlsbad, CA) and 5H-1,2,4-triazolo(4,3-a)azepine,6,7,8,9-tetrahydro-3-tricyclo(3·3·1·13·7)dec-1-yl (T0504) from Enamine (Kiev, Ukraine). BNW16 was kindly provided by Dr. Thomas Wilckens, BioNetWorks GmbH, Munich, Germany. Steroids were purchased from Steraloids (Newport, RI). Triadimefon, triadimenol, glycyrrhetinic acid (GA) and all other chemicals were from Sigma-Aldrich Chemie GmbH (Buchs, Switzerland). The solvents were of analytical and high performance liquid chromatography grade and the reagents of the highest grade available.

2.2. Cell culture, transfection and enzyme expression

HEK-293 cells were cultivated in Dulbecco's modified Eagle medium (DMEM) containing 4.5 g/L glucose, 10% fetal bovine serum, 100 U/ml penicillin, 0.1 mg/mL streptomycin, 1 × MEM non-essential amino acids and 10 mM HEPES buffer, pH 7.4. Cells were incubated at 37°C in a humidified 5% CO_2 atmosphere. Cells were transiently transfected by the calcium phosphate transfection method with plasmids for C-terminally FLAG-tagged human, rat or mouse 11β-HSD1 [27], or human 11β-HSD2 [28]. Briefly, HEK-293 cells at 70% confluence on a 10 cm^2 dish with 10 mL of culture medium were transfected with 10 µg plasmid. The plasmid was diluted in 430 µL sterile water, followed by drop wise addition of 62.5 µL of 2 M $CaCl_2$. This mixture was then added drop wise to 500 µL BEST buffer (500 mL H_2O containing 8.0 g NaCl, 0.198 g Na_2HPO_4-heptahydrate, 5.3 g BES (N, N-bis [2-hydroxyethyl] -2 amino ethane sulfonic acid), pH 7.0). After incubation for 10 min at room temperature, this mixture was added to the cells. Medium was changed at 6 h post-transfection. The transfection efficiency was approximately 20%. Cells were trypsinized 48 h post-transfection, followed by centrifugation at 900 × g for 4 min. Cell pellets (4 pellets per 10 cm^2 dish) were immediately shock frozen on dry ice and stored at -80°C. Upon determination of the protein concentration using the Pierce BCA protein assay kit (Thermo Fisher Scientific Inc., Rockford, IL, USA), 20 µg of total protein were loaded onto SDS-PAGE and expression of FLAG-tagged enzymes was semi-quantitatively analyzed by Western blotting and immune-detection using mouse monoclonal M2 anti-FLAG antibody (Sigma-Aldrich Chemie GmbH) and horseradish peroxidase-conjugated secondary antibodies as described previously [29]. β-actin was used as a loading control and was detected using rabbit anti-actin IgG from Santa Cruz Biotechnology Inc. (Santa Cruz, CA, USA).

2.3. Preparation of liver microsomes

Sprague Dawley rats were obtained from Charles River, Paris, France, and housed in the breeding facility of the Biocenter, University of Basel, in groups of four in a 12:12-h light-dark cycle with standard laboratory chow and tap water *ad libitum*. Mice on a mixed C57BL/6J/129vJ background and liver-specific knock-out mice (LKO) generated by crossing albumin-Cre transgenic mice on a C57BL/6J background with floxed homozygous *HSD11B1* mice on a mixed C57BL/6J/129SvJ background were bred at the breeding facility of the University of Birmingham, UK, as described earlier [30]. Pooled microsomes were prepared from the livers of three adult male Sprague Dawley rats or three C57BL/6J/129vJ parental mice or LKO mice. Liver pieces were homogenized in solution A (0.3 M sucrose, 10 mM imidazole, pH 7.0; 2 mL per 100 mg tissue) with a Potter-Elvehjem PTFE pestle with 10 – 12 strokes and at 220 rpm. Debris and nuclei were removed by two centrifugation steps for 10 min at 1,000 × g. The supernatant was centrifuged twice for 10 min at 12,000 × g to remove mitochondria, followed by ultracentrifugation for 1 h at 100,000 × g to obtain microsomes. The pellet was resuspended in solution B (0.6 M potassium chloride, 0.3 M sucrose, 20 mM tris-maleate, pH 7.0; 500 µL per 100 mg tissue) and the ultracentrifugation step was repeated. The final pellet was resuspended in solution C (0.15 M potassium chloride, 0.25 M sucrose, 10 mM tris-maleate, pH 7.0; 200 µL per 100 mg tissue). The microsomes were then aliquoted, shock frozen on dry ice and stored at -80°C until further use. The microsomal protein concentration was measured using the Pierce BCA protein assay kit. The quality of the microsomal preparations was analyzed using the cytochrome C reductase assay kit (Sigma-Aldrich Chemie GmbH) and by assessing the latent activity of the 11β-HSD1-dependent oxoreduction of cortisone in the presence of glucose-6-phosphate (G6P).

2.4. Determination of enzyme activities using microsomal preparations

In order to measure the oxoreduction of cortisone, microsomes of human liver (final concentration (f.c.) 0.5 mg/mL), rat liver (f.c. 0.25 mg/mL), mouse liver (f.c. 0.5 mg/mL) and LKO mouse liver (f.c. 0.5 mg/mL) were incubated in a final reaction volume of 22 µL of TS2 buffer (100 mM NaCl, 1 mM EGTA, 1 mM EDTA, 1 mM $MgCl_2$, 250 mM sucrose, 20 mM Tris–HCl, pH 7.4), supplemented with 1 µM cortisone and either 1 mM G6P or 1 mM NADPH in the presence or absence of 20 µM of the selective 11β-HSD1 inhibitor T0504 for 15 min at 37°C. For measuring the metabolism of triadimefon, 1 µM triadimefon and rat liver microsomes (f.c. 1 mg/mL), mouse liver microsomes (f.c. 1 mg/mL) or human liver microsomes (f.c. 0.2 mg/mL) were incubated for 1 h at 37°C. Reactions were stopped by the addition of 200 µL 0.3 M zinc sulfate in a 1:1 (v/v) mixture of water and methanol. The internal standard (atrazine for triadimefon and deuterized d4-cortisol for cortisone) was added at a final concentration of 50 nM, followed by vortexing for 10 sec and centrifugation for 10 min at 12,000 × g on a table top centrifuge. Supernatants (180 µL) were transferred onto solid phase extraction columns (Oasis HBL 1cc (30 mg) Waters WAT094225, Waters, Milford, MA, USA) pre-conditioned with 1 mL of methanol and 1 mL of distilled water. After washing with 1 mL water, compounds were eluted with 1 mL methanol. The eluate was evaporated to dryness, reconstituted in 100 µL methanol and stored at -20°C until analysis by liquid chromatography–tandem mass spectrometry (LC–MS/MS) (section 2.6).

2.5. Determination of enzyme activities using lysates of transfected HEK-293 cells

Frozen pellets of HEK-293 cells transiently transfected with human, rat or mouse 11β-HSD1 were resuspended in TS2 buffer and immediately sonicated at 4°C using a Branson sonicator (5 pulses, output 2, and duty cycles 20). Lysates were incubated for 1 h at 37°C in the presence of 1 mM NADPH and different concentrations of triadimefon (8 µM, 4 µM, 2 µM, 1 µM, 500 nM, 250 nM and 125 nM) in a final volume of 22 µL to estimate apparent K_M and apparent V_{max} values for the three species. Substrate conversion in all experiments was kept below 25%. Reactions were stopped and processed as described in section 2.4.

Alternatively, the oxidation of triadimenol was assessed by incubating lysates of cells, transiently transfected with human 11β-HSD1 or 11β-HSD2 (SDR9C3), with 1 µM triadimenol and 1 mM $NADP^+$ to measure the oxidation capacity of 11β-HSD1, or with 1 µM triadimenol and 1 mM NAD^+ to measure 11β-HSD2 activity. The conversion of cortisol (at a concentration of 1 µM) was determined as a positive control.

For determination of the reductase activity of human 11β-HSD1, cell lysates were incubated in the presence of 1 µM cortisone or 1 µM triadimefon as substrate and various concentrations of either triadimefon and triadimenol or cortisone as the respective inhibitor. IC_{50} values were calculated by non-linear regression using four parametric logistic curve fitting (GraphPad Prism software).

2.6. Liquid chromatography-tandem mass spectrometry measurements

All chromatographic separations (HPLC) were performed using an Atlantis T3 column (3 μm, 2.1 × 150 mm, Waters) and an Agilent 1200 Infinity Series chromatograph (Agilent Technologies, Basel, Switzerland). The mobile phase consisted of solvent A (water:acetonitrile, 95:5 (v/v), containing 0.1% formic acid) and solvent B (water:acetonitrile, 5:95 (v/v), containing 0.1% formic acid), at a total flow rate of 0.4 mL/min. Triadimefon and triadimenol were separated using 25% solvent B for 1 min, followed by a linear gradient from 1 to 20 min to reach 70% solvent B, and then 100% solvent B for 3min. The column was then re-equilibrated with 25% solvent B. Cortisone and cortisol were resolved using 30% solvent B from 0 to 4 min, followed by a linear gradient from 30% solvent B to 40% solvent B from 4 to 7 min, solvent B was then increased to 100% from 7 to 7.5 min and then continued for another 2.5 min, followed by re-equilibration with 30% solvent B for 3 min.

The LC was interfaced to an Agilent 6490 triple quadropole tandem mass spectrometer (MS/MS). The entire LC-MS/MS system was controlled by Mass Hunter workstation software (version B.01.05). The injection volume of each sample was 10 μL. The mass spectrometer was operated in electrospray ionization (ESI) positive ionization mode, with the source temperature of 350°C, with nebulizer pressure of 20 psi. The capillary voltage was set at 4000 V. The compounds were analyzed using multiple-reaction monitoring (MRM) and identified by comparing their retention time and mass to charge ratio (*m/z*) with those of authentic standards. The transitions, collision energy and retention time were *m/z* 294.8/197, 12 V, 13 min for triadimefon; *m/z* 296.8/70, 12 V, 11.0 and 11.5 min (R/S enantiomer) for triadimenol; *m/z* 216/174, 16 V, 5 min for atrazine; *m/z* 361/163, 25 V, 4.6 min for cortisone; *m/z* 363/121, 26 V, 4.3 min for cortisol; and *m/z* 367.2/121.1, 36 V, 4.3 min for the internal standard d4-cortisol.

The LC-MS/MS method was validated for accuracy, precision, sensitivity, stability, recovery, and calibration range. Acceptable inter-day assay precision (≤ 5.2%) and accuracy (95.0 – 103.9 %) were achieved over a linear range of 50 to 5000 nM for both triadimefon and triadimenol. Recovery of triadimefon was close to 100% and that of triadimenol >60% in all solid phase extractions. For each experiment a new calibration curve was determined.

2.7. Molecular modeling

Triadimefon and triadimenol were docked to the X-ray crystal structure of 11β-HSD1 using AutoDock4 [31]. The 3D-structures of the ligands were downloaded from PubChem [32] (CID-codes: 39385 for triadimefon and 41368 for triadimenol, respectively), and the structure of the protein was obtained from Protein Data Bank (PDB, www.pdb.org [33], entry: 2BEL [34]). The selected protein structure contains the tetrameric form of the protein; however, the docking studies were performed only with chain A. The protein was prepared for docking by removing the cocrystallized ligand carbenoxolone and water molecules from the protein structure as well as by adding hydrogens. The atom types of the protein and the ligands were automatically created by the program. During the docking, the ligand conformations were set flexible (with five rotatable bonds for triadimefon and six for triadimenol, respectively) and the protein was handled as rigid. The binding site was defined as a 3D-grid, centered at the binding site point X=8.858, Y= 22.143, and Z=15.547, with 30, 40, and 30 points in the respective dimensions. The grid spacing was set to 0.375 Å. The genetic algorithm was selected as search method with default settings, except for the maximum number of evaluations, which was set to short (250,000). The default settings for docking run were kept, with one exception: the RMS cluster tolerance was set

to 1.0 Å. Using these settings, the docking program was able to reproduce the binding orientation of the cocrystallized ligand, carbenoxolone, which validated the docking settings.

3. Results

3.1. Optimization of assay conditions and measurement of cortisone reduction in liver microsomes

In a first step, the assay conditions were optimized in order to distinguish between NADPH-dependent activities of microsomal enzymes facing the cytoplasm and enzymes facing the ER-lumen. The preparation employed in the present study yielded microsomes with approximately 90% inside-out orientation, based on the latency of 11β-HSD1-dependent reduction of cortisone as well as the latent activity of hexose-6-phosphate dehydrogenase (H6PDH) [35]. Thus, the luminal compartment is protected by the microsomal membrane, and enzymes with a cytoplasmic orientation such as CYPs and 17β-HSD1 or 17β-HSD3 can be readily measured upon addition of NADPH to the reaction mixture [36]. A NADPH regenerating system using bacterial G6PDH and G6P, widely used for measurements of CYP activities, further stimulates microsomal enzymes with cytoplasmic orientation when high substrate concentrations (> 10 μM) are applied. In contrast, carbonyl reductases such as 11β-HSD1 that protrude into the ER-lumen are dependent on the NADPH pool present in the microsomal vesicle [37-39]. The high endogenous expression of H6PDH in the liver represents an endogenous NADPH regenerating system, and we found that the addition of G6P to the assay mixture was required and sufficient to stimulate 11β-HSD1 reductase activity. Due to the relatively small vesicle volume, the capacity of this endogenous regenerating system is limited, however, and substrate concentrations have to be kept below 5-10

μM. Therefore, a substrate concentration of 1 μM was chosen for the experiments with liver microsomes.

A comparison of the cortisone reduction in human, rat and mouse liver microsomes yielded comparable activities of human and mouse liver microsomes and approximately two-fold higher activity of rat microsomes ($p < 0.001$) (Fig. 1). The latency of 11β-HSD1 activity was about 90% for rat and mouse microsomes and about 75% for the commercially available human liver microsomes (data not shown). To compare the activity of liver microsomes from wild-type and 11β-HSD1-deficient mice, cytochrome C reductase activity was determined. Comparable activities were obtained for microsomes of wild-type and knock-out mice with 3.35 U/mL and 3.13 U/mL, respectively. Importantly, microsomes of 11β-HSD1-deficient mice were devoid of cortisone reductase activity as expected, and cortisone reductase activity in hepatic microsomes from wild-type mice was completely blocked upon coincubation with the selective 11β-HSD1 inhibitor T0504.

3.2. Reduction of triadimefon in liver microsomes

In the presence of G6P triadimefon was efficiently converted to triadimenol by mouse liver microsomes (Fig. 2). In contrast, much lower activity was detected when microsomes were incubated with NADPH ($p < 0.001$), an activity corresponding to the low percentage of right-side out vesicles. Importantly, the conversion of triadimefon to triadimenol could be completely blocked with the specific 11β-HSD1 inhibitors T0504 (Fig. 2) and BNW16 (not shown) as well as with the unspecific inhibitor glycyrrhetinic acid (GA). Further excluding the possibility that other enzymes might be involved in the observed carbonyl reduction of triadimefon, microsomes of liver-specific 11β-HSD1 knock-out mice showed no conversion of triadimefon to triadimenol.

A species comparison revealed about 4-fold higher triadimefon carbonyl reductase activity of human liver microsomes compared with rat liver microsomes ($p < 0.001$) and 8-fold higher activity than mouse liver microsomes ($p < 0.001$) (Fig. 3). The fact that the selective inhibitor T0504 completely abolished triadimefon reductase activity indicated that 11β-HSD1 is the major if not only microsomal enzyme catalyzing this reaction.

3.3. Reduction of triadimefon by recombinant 11β-HSD1 measured in cell lysates

The different microsomal activities can potentially be due to differences in 11β-HSD1 expression levels, differences in the expression of H6PDH and/or its interaction with 11β-HSD1, or species-specific differences in the kinetic properties of 11β-HSD1. Significant species-specific differences in the substrate and inhibitor specificity of 11β-HSD1 have been reported [27, 40]. Therefore, in a next step, the carbonyl reduction of triadimefon by recombinant human, rat and mouse 11β-HSD1 was measured in lysates of transiently transfected HEK-293 cells. HEK-293 cells were chosen because they do not express endogenous steroid-metabolizing enzymes and to be able to compare the enzymes of the three species in the same cellular background. Because HEK-293 cells express no or very low H6PDH levels [37], lysates were prepared by sonication, which leads to microsomal vesicles with mixed orientation and allows measuring 11β-HSD1 activity in the presence of NADPH. Lysates of untransfected HEK-293 cells did not metabolize triadimefon. A comparison of the triadimefon reduction revealed a 3-4 fold higher affinity of human compared with rat and mouse 11β-HSD1 (Table 1). The expression levels of 11β-HSD1 in transiently transfected cells were semi-quantitatively analyzed by Western blotting and densitometry and did not vary significantly between species (data not shown). Human 11β-HSD1

was most active with 2-fold and 4-fold higher V_{max} and 5-fold and 15-fold higher V_{max}/K_m values than mouse and rat 11β-HSD1, respectively (Table 1).

3.4. Inhibition of 11β-HSD1-dependent cortisone reduction by triadimefon and *vice versa*

In order to estimate the potential of triadimefon and triadimenol to interfere with glucocorticoid activation, inhibition of human 11β-HSD1-dependent cortisone reduction by the azole fungicides was measured. IC_{50} values of 15.3 ± 7.0 μM and 56 ± 14 μM were obtained for triadimefon and triadimenol, respectively (Fig. 4). The 11β-HSD1-dependent reduction of triadimefon was inhibited by cortisone with an IC_{50} of 289 ± 54 nM (Fig. 5).

3.5. 11β-HSD1 and 11β-HSD2 do not catalyze the oxidation of triadimenol

11β-HSD1 is a reversible enzyme *in vitro* and catalyzes the interconversion of cortisone/cortisol, 11-dehydrocorticosterone/corticosterone, prednisone/prednisolone, 7β-hydroxycholesterol/7-oxocholesterol, and 7α- and 7β-hydroxydehydroepiandrosterone/7-oxodehydroepiandrosterone [41]. However, we reported recently that 11β-HSD1 irreversibly catalyzes the reduction of the secondary bile acid 7-oxolithocholic acid to chenodeoxycholic acid [22]. Therefore, the potential oxidation of triadimenol by 11β-HSD1 was tested in the presence of the cofactor $NADP^+$. Triadimenol was not oxidized by 11β-HSD1 (Fig. 6). As a control to verify enzyme activity, the reduction of triadimefon was measured, resulting in efficient formation of triadimenol, with 70% substrate conversion. Furthermore, incubation of triadimenol with lysates of cells expressing 11β-HSD2 in the presence of NAD^+ did not result in the formation of any triadimefon. Under similar conditions, cortisol was converted by 90% to cortisone (not shown).

3.6. Analysis of the binding of triadimefon and triadimenol to 11β-HSD1 by molecular modeling

Using molecular docking, the binding orientations were predicted for triadimefon and triadimenol. The binding orientation of triadimefon is comparable to that reported by Mazur et al. [10], while triadimenol is observed in the binding pocket in a flipped way compared with triadimefon (Fig. 7). Triadimefon is located in the binding pocket with the carbonyl-oxygen facing towards the catalytic amino acids Tyr183 and Ser170, and forming hydrogen bonds with them (Fig. 8A and B). In contrast, triadimenol is located in the same area with the alcohol group pointing away from Tyr183 and Ser170 (Fig. 8A, C and D). Instead, the alcohol group forms a hydrogen bond with the cofactor molecule.

4. Discussion

Almost all studies on the assessment of NADPH-dependent enzyme activities reported in the literature so far used either NADPH or an NADPH-regenerating system (NRS), consisting of $NADP^+$, G6P and purified bacterial G6PDH. Mazur et al. compared different conditions to measure 11β-HSD1 reductase activity and observed highest activity upon incubation of microsomes with an NRS in the presence of the pore forming agent alamethicin [10]. However, in this setting NADPH is produced in the extra-vesicular space and can be readily utilized by cytochrome P450 enzymes.

In the present study, optimized assay conditions have been applied to distinguish between activities of NADPH-dependent microsomal enzymes facing the cytoplasm and enzymes protruding into the ER luminal compartment. Intact liver microsomes contain an endogenous

NRS, consisting of the luminal pyrimidine nucleotide pool, the glucose-6-phosphate translocase (G6PT) and H6PDH. Because of the neglectible permeability of the ER membrane for pyridine nucleotides, the NADPH generated by H6PDH upon addition of G6P into the assay buffer is exclusively available for ER luminal enzymes. The intactness of microsomal vesicles and the percentage of inside-out vesicles (approximately 90% in the protocol used) can be tested by comparing 11β-HSD1-dependent cortisone reduction in the presence of either NADPH or G6P. The quality of microsomal preparations can be further assessed by measuring cytochrome C reductase activity. This approach should be valuable for the characterization of enzymatic conditions of other luminal carbonyl reductases.

In mouse liver microsomes the NADPH-dependent conversion of triadimefon to metabolites other than triadimenol was almost two times higher than the G6P-dependent formation of triadimenol. This ratio was significantly different in rat and human liver microsomes, where the carbonyl reduction of triadimefon was 2- and 8-fold higher than in mice. The cytochrome P450-mediated metabolism of triadimefon has been described earlier [9, 42]. Barton et al. reported a role for cytochrome P450 subfamilies 2C and 3A in the hydroxylation of triadimefon by rat liver microsomes [9]. Iyer et al. identified the two metabolites 1-(4-chlorophenoxy)-4-hydroxy-3,3-dimethyl-1-(1H-1,2,4-triazol-1-yl)-2-butanone (kwg1323) and β-(4-chlorophenoxy)-α-(1,1-dimethylethyl)-1H-1,2,4-triazole-1-ethanol (desmethyl kwg1342) in experiments using cultured rat hepatocytes.

The use of selective 11β-HSD1 inhibitors demonstrates that the carbonyl reduction of triadimefon is catalyzed exclusively by 11β-HSD1. This is further substantiated by the fact that no triadimenol formation could be observed in microsomes from livers of 11β-HSD1-deficient mice. The analysis of the kinetic properties of recombinant 11β-HSD1 revealed clearly higher triadimefon reductase activity of the human isoform compared with the rodent isoforms.

Although it must be taken into consideration that the rat and mouse enzymes were expressed in a human cell line, and that it cannot be fully excluded that the lower activities might emerge from protein folding disturbances, or the lack of some mouse- or rat-specific factors in human cells, comparable cortisone reductase activities for the three enzymes have been observed in this cell system in previous experiments [27]. The present study revealed similar affinities for triadimefon of rat and mouse 11β-HSD1. The fact that the recombinant mouse enzyme had three-fold higher catalytic efficiency (V_{max}/K_m) than the rat enzyme but rat microsomes were twice as active as mouse microsomes (in line with a previous study by Crowell et al. [11]) suggests a higher expression of 11β-HSD1 in rats. Indeed, approximately two times higher cortisone reductase activity was obtained in rat liver microsomes compared with mouse liver microsomes. A reliable comparison of 11β-HSD1 protein expression levels in human, rat and mouse is difficult due to significant species specificity of available antibodies. The present study suggests that rats and mice are of limited use to study the possible consequences of impaired carbonyl reduction of triadimefon for humans; however, 11β-HSD1-deficient mice turned out to be very useful for solving mechanistic questions.

Crowell et al. recently developed a physiologically based pharmacokinetic model for triadimefon and triadimenol in rats and humans [43]. The model showed good results for peak blood and tissue levels, but the clearance of both compounds was over estimated. Better results were obtained by a reverse metabolism model, based on the assumption that 11β-HSD1, or alternatively 11β-HSD2, might catalyze the oxidation of triadimenol. However, our results revealed that neither 11β-HSD1 nor 11β-HSD2 catalyze the oxidation of triadimenol. Previous studies demonstrated that 11β-HSD1 is a reversible enzyme that catalyzes the interconversion of endogenous glucocorticoids as well as 7-oxigenated cholesterol and 7-oxigenated DHEA in vitro, and molecular modelling revealed the close proximity of the carbonyl and the respective

hydroxyl on C7 and C11 of the steroid backbone to the catalytic Tyr183 [21, 44, 45]. However, a recent study reported the irreversible reduction of 7-oxolithocholic acid by 11β-HSD1, whereby molecular modelling suggested that only 7-oxolithocholic acid has optimal binding of substrate and cofactor to Tyr183 and Lys187, thus allowing electron transfer with the cofactor [22]. Similarly, the docking studies of the present study support our experimental findings that triadimenol is not oxidized by 11β-HSD1 (Fig. 7, 8). Triadimefon binds to 11β-HSD1 in an orientation, where the carbonyl-oxygen is pointing towards the catalytic amino acids Tyr183 and Ser170, and forming hydrogen bonds with them. This orientation is essential, since in the reduction reaction, the hydrogen is transferred from Tyr183 to the substrate [46]. Thus, the binding orientation of triadimefon allows the reduction reaction to take place. In contrast, triadimenol has a flipped binding mode compared to triadimefon, suggesting why this compound is not oxidized by 11β-HSD1. These findings suggest that after reduction of triadimefon to triadimenol, the compound rotates away from the catalytic amino acids, thus preventing its oxidation. However, the fact that triadimenol fits to the binding pocket and forms hydrogen bonds with the catalytic amino acid Ser170 and the cofactor, could explain the weak inhibitory activity of this compound.

In an attempt to estimate whether exposure to triadimefon or triadimenol might affect 11β-HSD1-dependent glucocorticoid activation, we determined IC_{50} values of the two fungicides for cortisone reduction. Regarding the expected exposure levels upon intake of contaminated food or water or upon occupational exposure of field workers and uptake through skin, it is highly unlikely that concentrations as high as 10 µM are reached to significantly inhibit 11β-HSD1-dependent cortisone reduction. On the other side, cortisone efficiently inhibited the carbonyl reduction of triadimefon. Under the conditions applied, an apparent K_m of 300-400 nM for cortisone reduction has been obtained [47]. Thus, the IC_{50} of about 300 nM obtained in the

present study suggests that at elevated concentrations of 11-oxoglucocorticoids, i.e. during stress situations or therapeutic treatment, the carbonyl reduction of triadimefon may be significantly lowered. The competition of cortisone (or 11-dehydrocorticosterone) and triadimefon for binding to 11β-HSD1 may explain the lower than expected clearance of triadimefon based on the physiologically-based pharmacokinetic model in the study by Crowell et al. [43]. The observation suggests that the circadian rhythm of glucocorticoids should be considered for estimation of the clearance of triadimefon.

In conclusion, the use of recombinant enzymes demonstrated the ability of 11β-HSD1 to irreversibly catalyze the carbonyl reduction of triadimefon. Comparison of human, rat and mouse 11β-HSD1 revealed at least five times higher catalytic efficiency of the human compared with the rodent enzymes, which is relevant regarding an improved cross-species extrapolation for risk assessment. Absence of triadimenol formation upon incubation of microsomes from livers of 11β-HSD1-deficient mice and of liver microsomal preparations with selective 11β-HSD1 inhibitors indicate that 11β-HSD1 is the major if not only enzyme catalyzing the conversion of triadimefon to triadimenol. Finally, inhibition studies suggest that the carbonyl reduction of triadimefon is impaired by elevated cortisone levels.

Acknowledgements

This work was supported by the Swiss National Science Foundation (PDFMP3_127330) to Alex Odermatt and a BBSRC David Philips fellowship (BB/G023468/1) to Gareth G. Lavery. Alex Odermatt has a Chair for Molecular and Systems Toxicology by the Novartis Research Foundation. Anna Vuorinen thanks the University of Innsbruck, Nachwuchsförderung for financial support.

Conflict of interest statement

The authors declare that there are no conflicts of interest.

References

[1] Agency USEP. Triadimefon Reregistration Eligibility Decision (RED) and Triadimenol Tolerance Reassessment and Risk Management Decision (TRED) Fact Sheet. In: Office of Pesticide Programs USEPA, editor. Washington, DC, 2006.

[2] Yess NJ, Houston MG, Gunderson EL. Food and Drug Administration pesticide residue monitoring of foods: 1983-1986. J Assoc Off Anal Chem 1991;74:273-80.

[3] Lavy TL, Mattice JD, Massey JH, Skulman BW. Measurements of year-long exposure to tree nursery workers using multiple pesticides. Arch Environ Contam Toxicol 1993;24:123-44.

[4] Fang H, Tang FF, Zhou W, Cao ZY, Wang DD, Liu KL, et al. Persistence of repeated triadimefon application and its impact on soil microbial functional diversity. J Environ Sci Health B 2012;47:104-10.

[5] Menegola E, Broccia ML, Di Renzo F, Prati M, Giavini E. In vitro teratogenic potential of two antifungal triazoles: triadimefon and triadimenol. In Vitro Cell Dev Biol Anim 2000;36:88-95.

[6] Robinson JF, Tonk ECM, Verhoef A, Piersma AH. Triazole induced concentration-related gene signatures in rat whole embryo culture. Reproductive Toxicology 2012;34:275-83.

[7] Vinggaard AM, Hnida C, Breinholt V, Larsen JC. Screening of selected pesticides for inhibition of CYP19 aromatase activity in vitro. Toxicol In Vitro 2000;14:227-34.

[8] Kenneke JF, Mazur CS, Ritger SE, Sack TJ. Mechanistic investigation of the noncytochrome P450-mediated metabolism of triadimefon to triadimenol in hepatic microsomes. Chemical research in toxicology 2008;21:1997-2004.

[9] Barton HA, Tang J, Sey YM, Stanko JP, Murrell RN, Rockett JC, et al. Metabolism of myclobutanil and triadimefon by human and rat cytochrome P450 enzymes and liver microsomes. Xenobiotica 2006;36:793-806.

[10] Mazur CS, Kenneke JF, Goldsmith M-R, Brown C. Contrasting Influence of NADPH and a NADPH-Regenerating System on the Metabolism of Carbonyl-Containing Compounds in Hepatic Microsomes. Drug Metabolism and Disposition 2009;37:1801-5.

[11] Crowell SR, Henderson WM, Fisher JW, Kenneke JF. Gender and species differences in triadimefon metabolism by rodent hepatic microsomes. Toxicol Lett 2010;193:101-7.

[12] Kenneke JF, Ekman DR, Mazur CS, Konwick BJ, Fisk AT, Avants JK, et al. Integration of metabolomics and in vitro metabolism assays for investigating the stereoselective transformation of triadimefon in rainbow trout. Chirality 2010;22:183-92.

[13] Baker ME. Evolutionary analysis of 11[beta]-hydroxysteroid dehydrogenase-type 1, -type 2, -type 3 and 17[beta]-hydroxysteroid dehydrogenase-type 2 in fish. FEBS Letters 2004;574:167-70.

[14] Atanasov AG, Odermatt A. Readjusting the glucocorticoid balance: an opportunity for modulators of 11beta-hydroxysteroid dehydrogenase type 1 activity? Endocrine, metabolic & immune disorders drug targets 2007;7:125-40.

[15] Chantong B, Kratschmar DV, Nashev LG, Balazs Z, Odermatt A. Mineralocorticoid and glucocorticoid receptors differentially regulate NF-kappaB activity and pro-inflammatory cytokine production in murine BV-2 microglial cells. J Neuroinflammation 2012;9:260.

[16] Chapman KE, Odermatt A. Steroids: Modulators of inflammation and immunity. The Journal of Steroid Biochemistry and Molecular Biology 2010;120:67-8.

[17] Staab CA, Maser E. 11beta-Hydroxysteroid dehydrogenase type 1 is an important regulator at the interface of obesity and inflammation. J Steroid Biochem Mol Biol 2010;119:56-72.

[18] Hughes KA, Webster SP, Walker BR. 11-Beta-hydroxysteroid dehydrogenase type 1 (11beta-HSD1) inhibitors in type 2 diabetes mellitus and obesity. Expert opinion on investigational drugs 2008;17:481-96.

[19] Schweizer RA, Zurcher M, Balazs Z, Dick B, Odermatt A. Rapid hepatic metabolism of 7-ketocholesterol by 11beta-hydroxysteroid dehydrogenase type 1: species-specific differences between the rat, human, and hamster enzyme. J Biol Chem 2004;279:18415-24.

[20] Hult M, Elleby B, Shafqat N, Svensson S, Rane A, Jornvall H, et al. Human and rodent type 1 11beta-hydroxysteroid dehydrogenases are 7beta-hydroxycholesterol dehydrogenases involved in oxysterol metabolism. Cell Mol Life Sci 2004;61:992-9.

[21] Nashev LG, Chandsawangbhuwana C, Balazs Z, Atanasov AG, Dick B, Frey FJ, et al. Hexose-6-phosphate dehydrogenase modulates 11beta-hydroxysteroid dehydrogenase type 1-dependent metabolism of 7-keto- and 7beta-hydroxy-neurosteroids. PLoS One 2007;2:e561.

[22] Odermatt A, Da Cunha T, Penno CA, Chandsawangbhuwana C, Reichert C, Wolf A, et al. Hepatic reduction of the secondary bile acid 7-oxolithocholic acid is mediated by 11β-hydroxysteroid dehydrogenase 1. Biochemical Journal 2011;436:621-9.

[23] Wsol V, Szotakova B, Skalova L, Maser E. Stereochemical aspects of carbonyl reduction of the original anticancer drug oracin by mouse liver microsomes and purified 11beta-hydroxysteroid dehydrogenase type 1. Chemico-Biological Interactions 2003;143-144:459-68.

[24] Maser E, Bannenberg G. 11 beta-hydroxysteroid dehydrogenase mediates reductive metabolism of xenobiotic carbonyl compounds. Biochem Pharmacol 1994;47:1805-12.

[25] Hult M, Nobel CS, Abrahmsen L, Nicoll-Griffith DA, Jornvall H, Oppermann UC. Novel enzymological profiles of human 11beta-hydroxysteroid dehydrogenase type 1. Chemico-Biological Interactions 2001;130-132:805-14.

[26] Maser E, Friebertshauser J, Volker B. Purification, characterization and NNK carbonyl reductase activities of 11beta-hydroxysteroid dehydrogenase type 1 from human liver: enzyme cooperativity and significance in the detoxification of a tobacco-derived carcinogen. Chem Biol Interact 2003;143-144:435-48.

[27] Arampatzis S, Kadereit B, Schuster D, Balazs Z, Schweizer RA, Frey FJ, et al. Comparative enzymology of 11beta-hydroxysteroid dehydrogenase type 1 from six species. J Mol Endocrinol 2005;35:89-101.

[28] Odermatt A, Arnold P, Stauffer A, Frey BM, Frey FJ. The N-terminal anchor sequences of 11beta-hydroxysteroid dehydrogenases determine their orientation in the endoplasmic reticulum membrane. J Biol Chem 1999;274:28762-70.

[29] Meyer A, Strajhar P, Murer C, Da Cunha T, Odermatt A. Species-specific differences in the inhibition of human and zebrafish 11beta-hydroxysteroid dehydrogenase 2 by thiram and organotins. Toxicology 2012;301:72-8.

[30] Lavery GG, Zielinska AE, Gathercole LL, Hughes B, Semjonous N, Guest P, et al. Lack of significant metabolic abnormalities in mice with liver-specific disruption of 11beta-hydroxysteroid dehydrogenase type 1. Endocrinology 2012;153:3236-48.

[31] Morris GM, Huey R, Lindstrom W, Sanner MF, Belew RK, Goodsell DS, et al. AutoDock4 and AutoDockTools4: Automated docking with selective receptor flexibility. J Comput Chem 2009;30:2785-91.

[32] Bolton E, Wang Y, Thiessen PA, Bryant SH. PubChem: integrated platform of small molecules and biological activities. Annual Reports in Computational Chemistry. Washington, DC: American Chemical Society, 2008.

[33] Berman HM, Westbrook J, Feng Z, Gililand G, Bhat TN, Weissig H, et al. The Protein Data Bank. Nucleic Acids Res 2000;28:235-42.

[34] Wu X, Kavanagh K, Svensson S, Elleby B, Hult M, Von Delft F, et al. The High Resolution Structures of Human, Murine and Guinea Pig 11-Beta-Hydroxysteroid Dehydrogenase Type 1 Reveal Critical Differences in Active Site Architecture. DOI:102210/pdb2bel/pdb

[35] Senesi S, Legeza B, Balazs Z, Csala M, Marcolongo P, Kereszturi E, et al. Contribution of fructose-6-phosphate to glucocorticoid activation in the endoplasmic reticulum: possible implication in the metabolic syndrome. Endocrinology 2010;151:4830-39.

[36] Legeza B, Balazs Z, Nashev LG, Odermatt A. The Microsomal Enzyme 17beta-Hydroxysteroid Dehydrogenase 3 Faces the Cytoplasm and Uses NADPH Generated by Glucose-6-Phosphate Dehydrogenase. Endocrinology 2013,154:205-13.

[37] Atanasov AG, Nashev LG, Gelman L, Legeza B, Sack R, Portmann R, et al. Direct protein-protein interaction of 11beta-hydroxysteroid dehydrogenase type 1 and hexose-6-phosphate dehydrogenase in the endoplasmic reticulum lumen. Biochim Biophys Acta 2008;1783:1536-43.

[38] Atanasov AG, Nashev LG, Schweizer RA, Frick C, Odermatt A. Hexose-6-phosphate dehydrogenase determines the reaction direction of 11beta-hydroxysteroid dehydrogenase type 1 as an oxoreductase. FEBS letters 2004;571:129-33.

[39] Banhegyi G, Benedetti A, Fulceri R, Senesi S. Cooperativity between 11beta-hydroxysteroid dehydrogenase type 1 and hexose-6-phosphate dehydrogenase in the lumen of the endoplasmic reticulum. J Biol Chem 2004;279:27017-21.

[40] Hult M, Shafqat N, Elleby B, Mitschke D, Svensson S, Forsgren M, et al. Active site variability of type 1 11beta-hydroxysteroid dehydrogenase revealed by selective inhibitors and cross-species comparisons. Mol Cell Endocrinol 2006;248:26-33.

[41] Odermatt A, Nashev LG. The glucocorticoid-activating enzyme 11β-hydroxysteroid dehydrogenase type 1 has broad substrate specificity: Physiological and toxicological considerations. The Journal of Steroid Biochemistry and Molecular Biology 2010;119:1-13.

[42] Iyer VV, Ovacik MA, Androulakis IP, Roth CM, Ierapetritou MG. Transcriptional and metabolic flux profiling of triadimefon effects on cultured hepatocytes. Toxicology and Applied Pharmacology 2010;248:165-77.

[43] Crowell SR, Henderson WM, Kenneke JF, Fisher JW. Development and application of a physiologically based pharmacokinetic model for triadimefon and its metabolite triadimenol in rats and humans. Toxicol Lett 2011;205:154-62.

[44] Balazs Z, Nashev LG, Chandsawangbhuwana C, Baker ME, Odermatt A. Hexose-6-phosphate dehydrogenase modulates the effect of inhibitors and alternative substrates of 11beta-hydroxysteroid dehydrogenase 1. Mol Cell Endocrinol 2009;301:117-22.

[45] Odermatt A, Atanasov AG, Balazs Z, Schweizer RA, Nashev LG, Schuster D, et al. Why is 11beta-hydroxysteroid dehydrogenase type 1 facing the endoplasmic reticulum lumen? Physiological relevance of the membrane topology of 11beta-HSD1. Mol Cell Endocrinol 2006;248:15-23.

[46] Kavanagh KL, Jornvall H, Persson B, Oppermann U. Medium- and short-chain dehydrogenase/reductase gene and protein families : the SDR superfamily: functional and structural diversity within a family of metabolic and regulatory enzymes. Cellular and molecular life sciences 2008;65:3895-906.

[47] Frick C, Atanasov AG, Arnold P, Ozols J, Odermatt A. Appropriate function of 11beta-hydroxysteroid dehydrogenase type 1 in the endoplasmic reticulum lumen is dependent on its N-terminal region sharing similar topological determinants with 50-kDa esterase. J Biol Chem 2004;279:31131-8.

Figure Legends

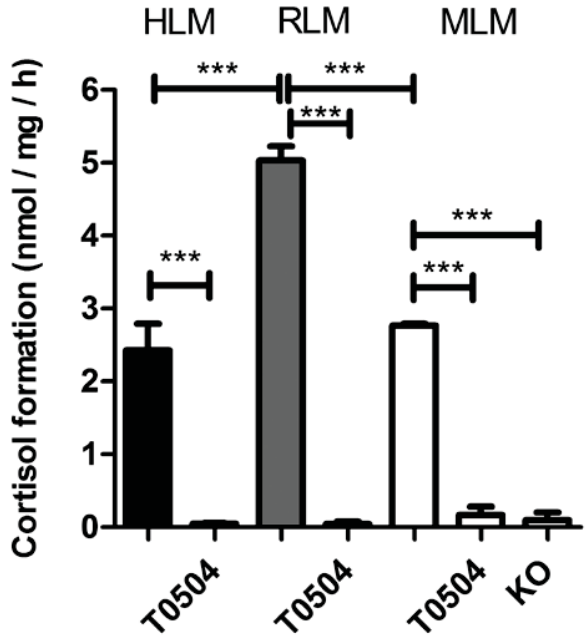

Fig. 1. Conversion of cortisone to cortisol by liver microsomes. Human liver microsomes (HLM, black bars, f.c. 0.5 mg/mL), rat liver microsomes (RLM, grey bars, f.c. 0.25 mg/mL) and mouse liver microsomes (MLM, white bars, f.c. 0.5 mg/mL) were incubated for 15 min at 37°C in the presence of 1 μM cortisone and 1 mM glucose-6-phosphate, in the absence or presence of 20 μM of the 11β-HSD1 inhibitor T0504. The amount of cortisone and cortisol was then quantitated. Lack of activity of liver microsomes from 11β-HSD1-deficient mice is indicated by KO. Data (mean ± SD) were obtained from at least three independent experiments using pooled samples. Repeated measures ANOVA found significant species differences in cortisone reduction. Post hoc analysis by Tukey test was used for multiple comparisons. *** $P < 0.001$.

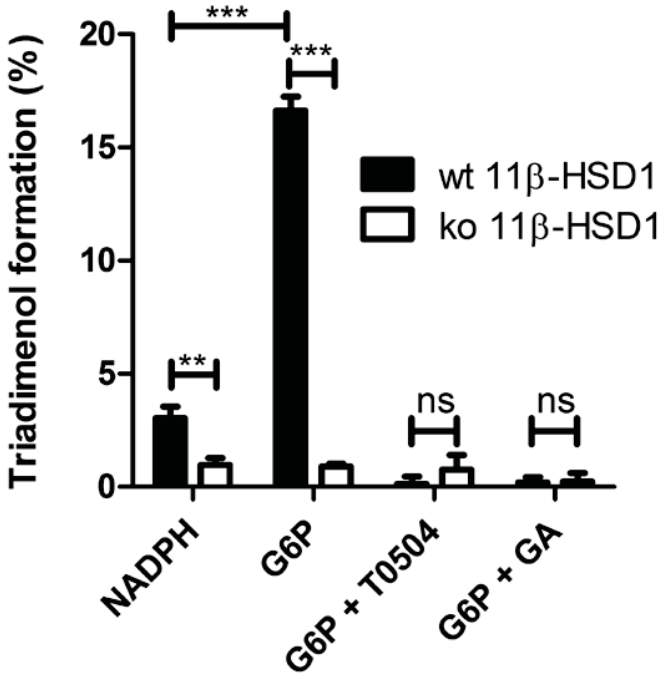

Fig. 2. Conversion of triadimefon to triadimenol by mouse liver microsomes. Microsomes (1 mg/mL), prepared from wild-type (wt) and liver-specific 11β-HSD1 knock-out mice (ko), were incubated for 1 h at 37°C in the presence of 1 μM triadimefon and either 1 mM of NADPH or 1 mM of glucose-6-phosphate (G6P), in the absence or presence of 20 μM T0504 or glycyrrhetinic acid (GA). Data represent mean ± SD from at least three independent experiments using pooled samples. Repeated measures ANOVA found significant differences in the groups. Post hoc analysis by Tukey test was used for multiple comparisons. ** $p < 0.01$, *** $p < 0.001$, ns = not significant.

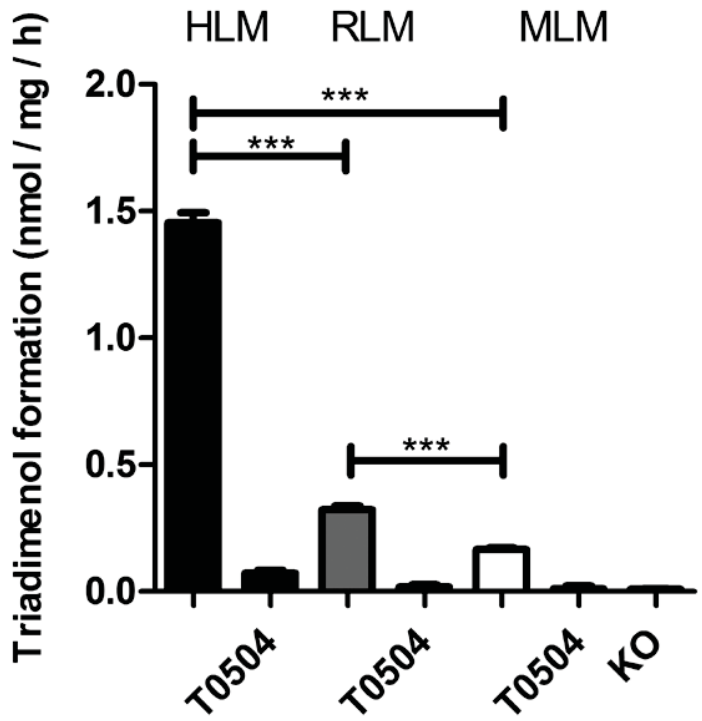

Fig. 3. Triadimenol formation in liver microsomes. Human liver microsomes (HLM, black bars, f.c. 0.2 mg/mL), rat liver microsomes (RLM, grey bars, f.c. 1 mg/mL) and mouse liver microsomes (MLM, white bars, f.c. 1 mg/mL) were incubated for 1 h at 37°C with 1 µM triadimefon and 1 mM G6P, in the absence or presence of 20 µM T0504. Lack of activity of MLM of 11β-HSD1-deficient mice is indicated by KO. Data (mean ± SD) were obtained from at least three independent experiments using pooled samples. Repeated measures ANOVA found significant species differences in triadimefon reduction. Post hoc analysis by Tukey test was used for multiple comparisons. *** $P < 0.001$.

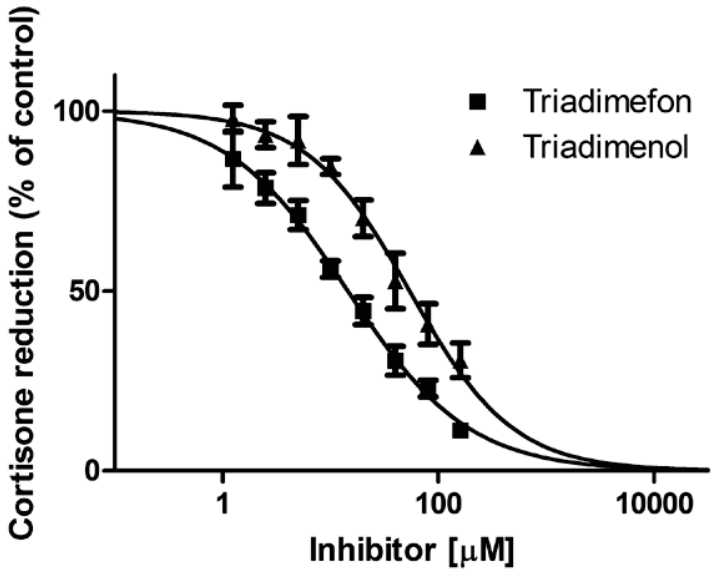

Fig. 4. Inhibition of 11β-HSD1-dependent cortisone reduction by triadimefon and triadimenol. Inhibition of the 11β-HSD1-dependent conversion of cortisone to cortisol by various concentrations of triadimefon and triadimenol was measured in lysates of HEK-293 cells transfected with the human enzyme as described in Section 2. Lysates were simultaneously incubated with cortisone (1 μM) and triadimefon or triadimenol for 15 min at 37°C. Data were normalized to vehicle control (0.05% DMSO) and represent mean ± SD from three independent experiments.

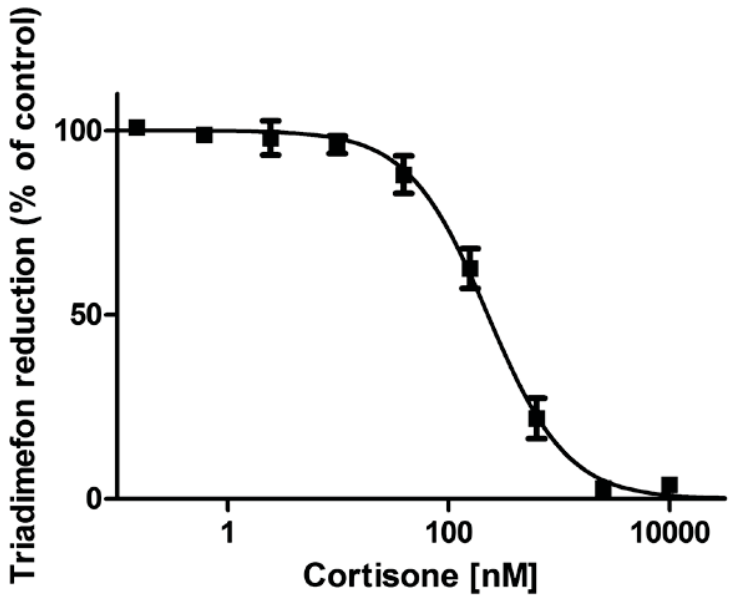

Fig. 5. Inhibition of 11β-HSD1-dependent triadimefon reduction by cortisone. Inhibition of the 11β-HSD1-dependent conversion of triadimefon to triadimenol by various concentrations of cortisone was measured in lysates of HEK-293 cells transfected with the human enzyme as described in Section 2. Lysates were simultaneously incubated with triadimefon (1 μM) and cortisone for 60 min at 37°C. Data were normalized to vehicle control (0.05% DMSO) and represent mean ± SD from three independent experiments.

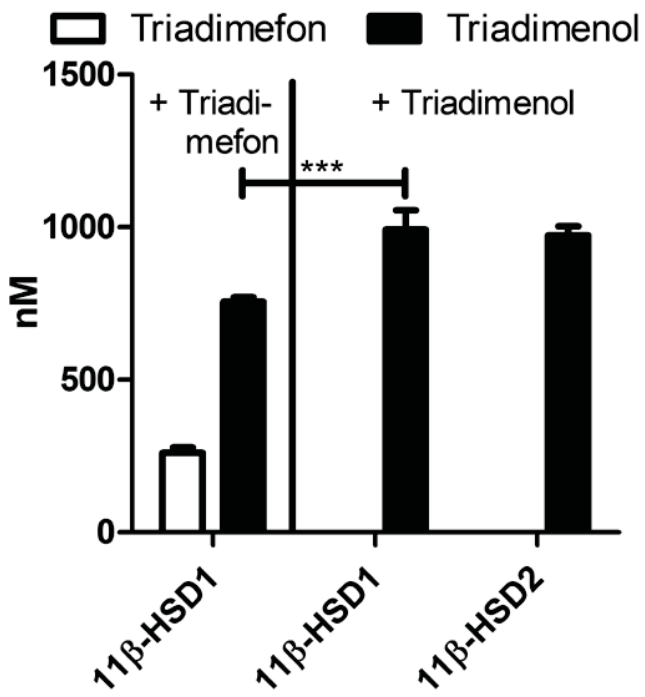

Fig. 6. Triadimenol is not oxidized by 11β-HSD1 and 11β-HSD2. Recombinant human 11β-HSD1 and 11β-HSD2 were expressed in HEK-293 cells. Cells were lysed by sonication to obtain vesicles with mixed orientation. 11β-HSD1 activity was measured by incubation of lysates for 1 h at 37°C with 1 μM triadimefon and 1 mM NADPH or with 1 μM triadimenol and 1 mM $NADP^+$. 11β-HSD2 activity was measured in the presence of 1 μM triadimenol and 1 mM NAD^+. Data (mean ± SD) were obtained from at least three independent experiments. Repeated measures ANOVA found significant differences. Post hoc analysis by Tukey test was used for multiple comparisons. *** $P < 0.001$.

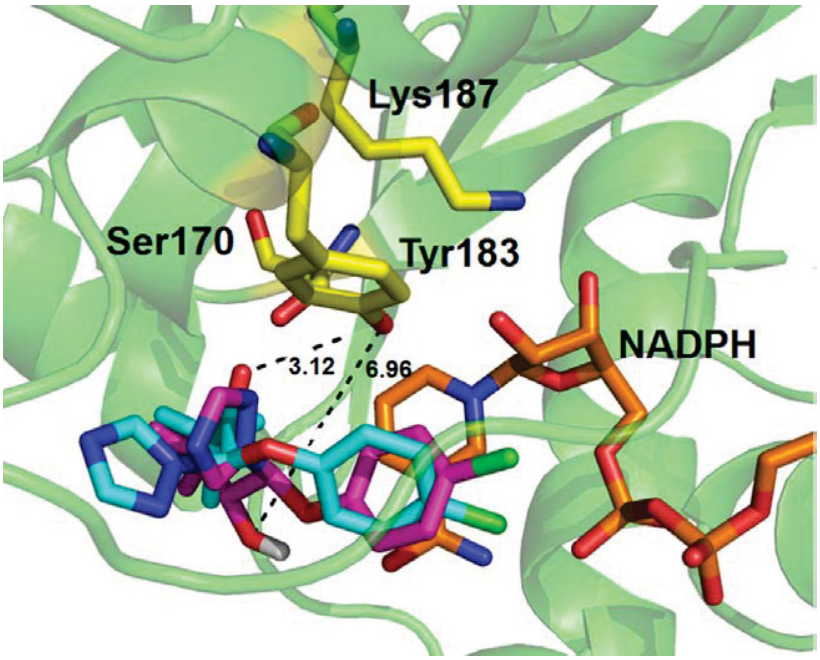

Fig. 7. The binding orientations of triadimefon (cyan) and triadimenol (magenta) in the 11β-HSD1 binding site. The carbonyl-oxygen of triadimefon is facing towards catalytic residues, with a distance of the hydroxyl on Tyr183 to the carbonyl-oxygen of 3.12 Å. Triadimenol is predicted to have a flipped binding orientation, where the reduced carbonyl-oxygen faces away from the catalytic residues, with a distance of the hydroxyl on Tyr183 to the carbonyl-oxygen of 6.96 Å.

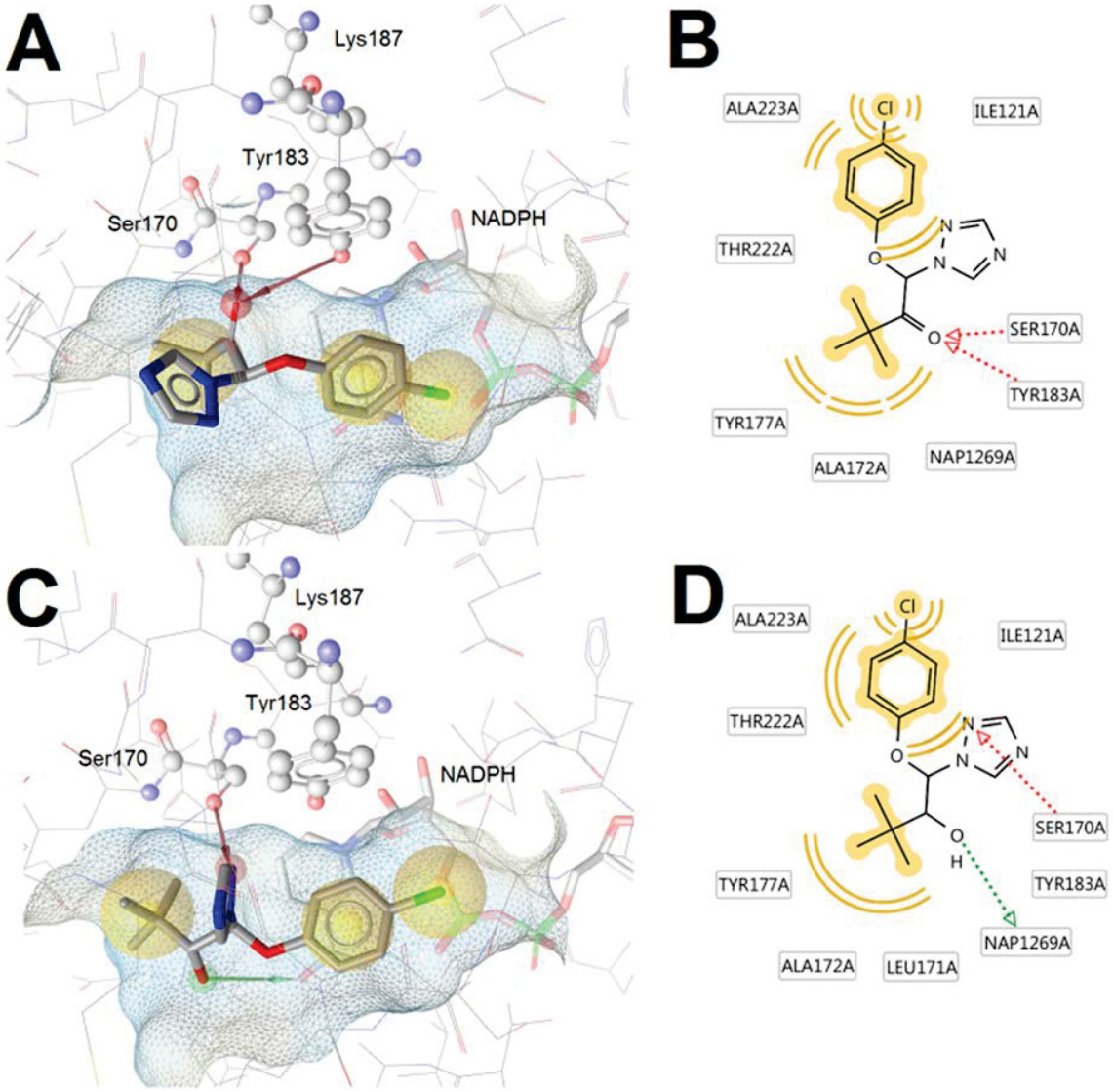

Fig. 8. The predicted binding orientations of triadimefon (A and B) and triadimenol (C and D) in 11β-HSD1. The ligand-protein interactions are color-coded: hydrogen bond acceptor – red arrow, hydrophobic – yellow sphere. The ligand binding pocket is colored by aggregated lipophilicity. The catalytic amino acids are highlighted in ball- and stick style and the cofactor NADPH in stick style.

Table 1

Kinetic parameters of 11β-HSD1-dependent carbonyl reduction of triadimefon. HEK-293 cells were transiently transfected with either human, rat or mouse 11β-HSD1, followed by measuring the carbonyl reduction of triadimefon and determination of apparent V_{max} and apparent K_M values as described in Section 2. The appV_{max} values are expressed relative to total protein concentration of the lysates used. Data were calculated by non-linear regression using four parametric logistic curve fitting (GraphPad Prism) and represent mean ± SD of three independent experiments. One-way ANOVA found significant differences ($P < 0.01$) in appV_{max} values, post hoc analysis by Tukey test was used for multiple comparison. Human appV_{max} value was significant higher then rat appV_{max} ($p < 0.01$) and mouse appV_{max} ($p < 0.05$). Other comparisons were not significant.

11β-HSD1	appV_{max}	appK_M	appV_{max}/ appK_M
Human	0.54 ± 0.060 nmol × mg^{-1} × h^{-1}	3.5 ± 0.8 µM	154 × 10^{-6} l × mg^{-1} × h^{-1}
Rat	0.14 ± 0.031 nmol × mg^{-1} × h^{-1}	12.8 ± 4.2 µM	11 × 10^{-6} l × mg^{-1} × h^{-1}
Mouse	0.31 ± 0.129 nmol × mg^{-1} × h^{-1}	10.4 ± 6.5 µM	30 × 10^{-6} l × mg^{-1} × h^{-1}

Paper Draft: Carbonyl reduction of bupropion to threohydrobupropion by human and rodent 11β-hydroxysteroid dehydrogenase 1

Carbonyl reduction of bupropion to threohydrobupropion by human and rodent 11β-hydroxysteroid dehydrogenase 1

Arne Meyer[1], Anna Vuorinen[2], Agnieszka E. Zielinska[3], Thierry Da Cunha[1], Petra Strajhar[1], Gareth G. Lavery[3], Daniela Schuster[2] and Alex Odermatt[1]

[1]Swiss Center for Applied Human Toxicology and Division of Molecular and Systems Toxicology, Department of Pharmaceutical Sciences, University of Basel, Klingelbergstrasse 50, 4056 Basel, Switzerland

[2]Institute of Pharmacy/Pharmaceutical Chemistry and Center for Molecular Biosciences Innsbruck – CMBI, University of Innsbruck, Innrain 80/82, 6020 Innsbruck, Austria

[3]Centre for Endocrinology Diabetes and Metabolism (CEDAM), Institute of Biomedical Research, Medical School Building, School of Clinical and Experimental Medicine, College of Medical and Dental Sciences, University of Birmingham, Edgbaston, Birmingham, B15 2TT, UK

Correspondence to:
Dr. Alex Odermatt, Division of Molecular and Systems Toxicology, Department of Pharmaceutical Sciences, University of Basel, Klingelbergstrasse 50, 4056 Basel, Switzerland
Phone: +41 61 267 1530, Fax: +41 61 267 1515, E-mail: alex.odermatt@unibas.ch

Abstract

Bupropion is widely used for treatment of depressions and as smoking cessation drug. Despite of more than 20 years of therapeutic use, its metabolism is not fully understood. While CYP2B6 has been shown to form hydroxybupropion, the enzyme(s) generating erythro- and threohydrobupropion remained unclear. Experiments using the unspecific inhibitor glycyrrhetinic acid (GA) and human liver and placenta microsomes suggested a role for 11β-hydroxysteroid dehydrogenases (11β-HSDs) in the formation of erythro- and threohydrobupropion. 11β-HSD2 converts the active glucocorticoids cortisol and prednisolone to the inactive cortisone and prednisone. 11β-HSD1 catalyzes the reverse reaction and, in addition, accepts several other substrates. In the present study, we used human, rat and mouse liver microsomes, recombinant enzymes and a selective inhibitor to assess the role of 11β-HSD1 in the carbonyl reduction of bupropion and to characterize species-specific differences. The results revealed 11β-HSD1 as the major enzyme converting bupropion to threohydrobupropion. The reaction was irreversible and stereoselective. Human liver microsomes showed 10 and 80 times higher activity than rat and mouse liver microsomes. 11β-HSD1 did not form erythrohydrobupropion, indicating the existence of another carbonyl reductase that generates erythrohydrobupropion. In line with this observation, erythrohydrobupropion formation was not altered in experiments with microsomes from 11β-HSD1-deficient mice or upon incubation with 11β-HSD1 inhibitor. Molecular docking supported the experimental findings, suggesting that 11β-HSD1 selectively converts *R*-bupropion to threohydrobupropion. Enzyme inhibition experiments suggested that exposure to bupropion unlikely impairs 11β-HSD1-dependent glucocorticoid activation but that pharmacological administration of cortisone or prednisone inhibits 11β-HSD1-dependent bupropion metabolism.

Keywords

Bupropion, 11β-hydroxysteroid dehydrogenase, metabolism, liver microsomes, carbonyl reduction, molecular docking

1. Introduction

Bupropion (Wellbutrin®) is used since more than 20 years in the treatment of depressions and as an efficient smoking cessation drug (Zyban®) [1]. Further, it has been proposed for the treatment of attention-deficit/hyperactivity disorders [2]. According to a recent review, approximately 40 million patients worldwide are treated with bupropion [3]. Despite of its frequent use, the mechanisms of bupropion metabolism are not fully understood. The identification and characterization of the enzymes involved may help to optimize the therapeutic use of bupropion and avoid potential drug-drug interactions.

Bupropion is used as a racemic mixture of *R*- and *S*-bupropion (Fig. 1) and acts as a dopamine and norepinephrine reuptake inhibitor. The first studies with bupropion in humans in the 1980s led to the identification of the three major metabolites hydroxybupropion, erythrohydrobupropion and threohydrobupropion [4-7]; however, the enzymes responsible for the metabolism remained unknown. A decade later, cytochrome P450 2B6 (CYP2B6) was identified as the enzyme responsible for the formation of hydroxybupropion [8, 9]. Another ten years later, experiments with human and baboon placental and liver microsomes and the unspecific 11β-hydroxysteroid dehydrogenase (11β-HSD) inhibitor 18β-glycyrrhetinic acid (GA) suggested that bupropion is metabolized by one of the 11β-HSDs to erythrohydrobupropion and threohydrobupropion [5, 10, 11]. Incubations with the unspecific inhibitor GA yielded lower amounts of both threohydrobupropion and erythrohydrobupropion, suggesting the involvement of 11β-HSD1 in the carbonyl reduction of bupropion.

Two distinct 11β-HSD enzymes are known; 11β-HSD1 is responsible for the conversion of the inactive 11-ketoglucocorticoids cortisone (humans) and 11-dehydrocorticosterone (rodents) to the active 11β-hydroxyglucocorticoids cortisol (humans) and corticosterone (rodents), whereas 11β-HSD2 catalyzes the reverse reaction [12]. 11β-HSD2 is known to inactivate cortisol by

conversion to cortisone. It plays a crucial role in protecting mineralocorticoid receptors (MR) from activation by glucocorticoids [13]. Although 11β-HSD2 is able to act as a reversible enzyme for some substrates such as dexamethasone/11-ketodexamethasone under *in vitro* conditions [14], 11β-HSD2 functions exclusively as a dehydrogenase *in vivo* and a role in the reduction of bupropion can be excluded. 11β-HSD1 is expressed in many metabolically active tissues such as liver, adipose and skeletal muscle [15]. In addition to the reduction of cortisone, 11β-HSD1 essentially converts the pro-drug prednisone to its active form prednisolone [16], thereby enabling binding to and activation of the glucocorticoid receptor (GR) and regulation of GR-dependent target genes. Due to the adverse metabolic effects of prolonged periods of exposure to excessive glucocorticoid levels and the observed metabolic disturbances in transgenic mice overexpressing 11β-HSD1 in adipose tissue [17], there are considerable efforts to develop inhibitors for therapeutic applications [18, 19]. Nevertheless, 11β-HSD1 is a multi-functional carbonyl reductase with broad substrate specificity [20]. It is able to reduce endogenous sterols such as 7-ketocholesterol [21, 22], the secondary bile acid 7-oxolithocholic acid [23], 7-ketodehydroepiandrosterone [24] and several xenobiotics, including triadimefon [25], 4-(methylnitrosamino)-1-(3-pyridyl)-1-butanone (NNK) [26] oracin [27], metyrapone [28] and ketoprofen [29].

The evidence from earlier studies using microsomes and the unspecific inhibitor GA suggested a role for 11β-HSD1 in the formation of the two metabolites erythrohydrobupropion and threohydrobupropion. Since it still remained unclear whether indeed 11β-HSD1 is responsible for the generation of these two metabolites, and whether it has a major or minor contribution, we used hepatic microsomes, a selective 11β-HSD1 inhibitor, and recombinant enzyme to assess the role of 11β-HSD1 in bupropion metabolism. Furthermore, we investigated species-specific differences in the carbonyl reduction of bupropion by human, rat and mouse liver microsomes as

well as the corresponding recombinant enzymes. The contribution of 11β-HSD1 was further assessed using microsomes from liver-specific 11β-HSD1 knockout mice. Finally, the putative binding of bupropion to 11β-HSD1 was investigated by molecular modeling, providing an explanation for the selective carbonyl reduction of bupropion to threohydrobupropion by human 11β-HSD1.

2. Materials and Methods

2.1. Chemicals and reagents

Microsomes from a liver of a 77 year old male Caucasian were purchased from Celsis In Vitro Inc (Baltimore, MD). Human embryonic kidney (HEK-293) cells from ATCC (No CRL-1573) were purchased from LGC Standards S.a.r.l. (Molsheim Cedex, France). Cell culture medium was purchased from Invitrogen (Carlsbad, CA), 5H-1,2,4-triazolo(4,3-a)azepine,6,7,8,9-tetrahydro-3-tricyclo(3·3·1·13·7)dec-1-yl (T0504) from Enamine (Kiev, Ukraine), and steroids from Steraloids (Newport, RI). The metabolites hydroxybupropion, erythrohydrobupropion and threohydrobupropion were purchased from Toronto Research Chemicals Inc. (North York, Canada), and bupropion and all other chemicals from Sigma-Aldrich Chemie GmbH (Buchs, Switzerland). The solvents were of analytical and high performance liquid chromatography grade and reagents of the highest grade available.

2.2. Cell culture and transfection

HEK-293 cells were grown at 37 °C in Dulbecco's modified Eagle medium (DMEM, containing 4.5 g/L glucose, 10% fetal bovine serum, 100 U/ml penicillin, 0.1 mg/mL streptomycin, 1 × MEM non-essential amino acids and 10 mM HEPES buffer, pH 7.4). For the experiments with recombinant 11β-HSD1, HEK-293 cells were transiently transfected by the calcium phosphate

transfection method as described earlier [25] with plasmids for human, rat or mouse 11β-HSD1 [30]. Cells were harvested 48 h post-transfection, centrifuged at 900 × g for 4 min, and cell pellets were immediately shock frozen and stored at -80°C until further use. Protein concentration was determined using the Pierce BCA protein assay kit (Thermo Fisher Scientific Inc., Rockford, IL, USA).

2.3. Preparation of liver microsomes

Microsomes were prepared as described earlier [25]. Livers were taken from adult male Sprague Dawley rats, C57BL/6J mice and liver-specific knock-out mice (LKO) generated by crossing albumin-Cre transgenic mice on a C57BL/6J background with floxed homozygous *HSD11B1* mice on a mixed C57BL/6J/129SvJ background [31]. Liver tissue was homogenized, and microsomes were obtained after differential centrifugation as described [25]. Microsomes were finally resuspended in a buffer containing 0.15 M potassium chloride, 0.25 M sucrose, and 10 mM Tris-maleate, pH 7.0. Aliquots were stored at -80°C until further use. The microsomal protein concentration was measured using the Pierce BCA protein assay kit. The quality of the microsomal preparations was analyzed using the cytochrome C reductase assay kit (Sigma-Aldrich Chemie GmbH) and by assessing the latent activity of the 11β-HSD1-dependent oxoreduction of cortisone in the presence of glucose-6-phosphate (G6P).

2.4. Enzyme activity measurements using liver microsomes

The oxoreduction of cortisone by liver microsomes was measured as reported earlier [25]. The metabolism of bupropion was determined at 37 °C (1 h incubation) in a final reaction volume of 22 µL of TS2 buffer (100 mM NaCl, 1 mM EGTA, 1 mM EDTA, 1 mM $MgCl_2$, 250 mM sucrose, 20 mM Tris–HCl, pH 7.4) containing 1 µM of bupropion and either human liver

microsomes (final concentration (f.c.) of 0.4 mg/mL) or rat, mouse or LKO mouse liver microsomes (all at a f.c. of 1 mg/mL), supplemented with either 1 mM G6P or 1 mM NADPH in the presence or absence of 20 µM of the selective 11β-HSD1 inhibitor T0504. Reactions were stopped by adding 200 µL 0.3 M zinc sulfate in a 1:1 (v/v) mixture of water and methanol. Atrazine was added as an internal standard at an f.c. of 50 nM, followed by vortexing for 10 s and centrifugation for 10 min at 12,000 × g on a table top centrifuge. Samples were further purified by an ethyl acetate extraction. Supernatants (180 µL) were added to 600 µL ethyl acetate and incubated for 10 min on a thermomixer at 700 rpm. Following centrifugation for 10 min at 12,000 × g, supernatants (550 µL) were evaporated to dryness, reconstituted in 100 µL methanol and stored at -20°C until analysis by liquid chromatography–tandem mass spectrometry (LC–MS/MS) (section 2.6).

2.5. Enzyme activity measurements using lysates of transfected HEK-293 cells

Frozen pellets of HEK-293 cells transiently expressing human, rat or mouse 11β-HSD1 were resuspended in TS2 buffer and sonicated. Lysates were then incubated for 1 h at 37 °C in the presence of 1 mM NADPH and different concentrations of bupropion (8 µM, 4 µM, 2 µM, 1 µM, 500 nM, 250 nM and 125 nM) in a final volume of 22 µL to estimate apparent K_M and apparent V_{max} values. Substrate conversion was kept below 25% in all experiments. Reactions were stopped and processed as described in section 2.4.

For measuring the reductase activity of 11β-HSD1, cell lysates were incubated in the presence of 1 µM cortisone or 1 µM bupropion as substrate and various concentrations of either bupropion or cortisone and prednisone as the respective inhibitor. IC_{50} values were calculated by non-linear regression using four parametric logistic curve fitting (GraphPad Prism software).

2.6. Liquid chromatography-tandem mass spectrometry measurements

An Acquity UPLC BEH C18 column (1.7 μm, 2.1 × 150 mm ID Waters, Milford, MA) and an Agilent 1290 Infinity Series chromatograph (Agilent Technologies, Basel, Switzerland) were used for chromatographic separations.

The mobile phase consisted of solvent A (H_2O/acetonitrile, 95:5 (v/v), containing 0.1% formic acid, and solvent B (H_2O/acetonitrile, 5:95 (v/v), containing 0.1% formic acid, at a flow rate of 0.5 mL/min. Bupropion, hydroxybupropion, threohydrobupropion and erythrohydrobupropion were separated using 15% solvent B for 6 min, followed by a linear gradient from 6 to 10 min to reach 100% solvent B, and then 100% solvent B for 3 min. The column was then re-equilibrated with 15% solvent B. Cortisone and cortisol were resolved as described earlier [25].

The UPLC was interfaced to an Agilent 6490 triple quadropole tandem mass spectrometer (MS/MS). The entire UPLC-MS/MS system was controlled by Mass Hunter workstation software (version B.01.05). The injection volume of each sample was 5 μL. The mass spectrometer was operated in electrospray ionization (ESI) positive ionization mode, a source temperature of 350°C, a nebulizer pressure of 20 psi and a capillary voltage of 4000 V.

The compounds were analyzed using multiple-reaction monitoring (MRM) and identified by comparing their retention time and mass to charge ratio (*m/z*) with those of authentic standards. The transitions, collision energy and retention time were *m/z* 240.1/184.1, 19 V and 4.9 min for bupropion; *m/z* 242/168, 20 V and 5.4 min for threohydrobupropion, *m/z* 242/168, 20 V and 4.8 min for erythrohydrobupropion; *m/z* 256/238.1, 17 V and 3.0 min for hydroxybupropion and *m/z* 216/174, 16 V and 5 min for the internal standard atrazine.

The UPLC-MS/MS method was validated for accuracy, precision, sensitivity, recovery, and calibration range. Acceptable inter-day assay precision (≤ 6.2%) and accuracy (94.1 – 105.0%)

were achieved over a linear range of 50 to 5000 nM for bupropion, hydroxybupropion, threohydrobupropion and erythrohydrobupropion. Recovery of bupropion, hydroxybupropion, threohydrobupropion and erythrohydrobupropion were 96%, 80%, 79% and 82%, respectively in all extractions. For each experiment a new calibration curve was determined.

2.7. Molecular modeling

The 2D structures of *R*- and *S*-Bupropion were generated using ChemBioDraw Ultra 12.0 (1986-2010 CambridgeSoft). The 2D-structures were converted into 3D-structures using ChemBio3D Ultra 12.0 (1986-2010 CambridgeSoft). The docking studies were performed using GOLD [32, 33], which uses a genetic algorithm to produce low-energy binding solutions for small molecules in the ligand binding pocket. The X-ray crystal structure of 11β-HSD1 was obtained from the Protein Data Bank (www.pdb.org [34]). Both stereoisomers of bupropion were docked into the ligand binding site of 11β-HSD1 (PDB code 2BEL, Chain A [35]). The binding site was defined as a 10 Å sphere, centered on the hydroxyl-oxygen of Ser170 (x: 3.84, y: 22.49, and z: 13.34). The protein side chains were handled as rigid and the ligand conformations as flexible during the docking run. The program was set to define the atom types of the ligands and the protein automatically. GoldScore was selected as a scoring function. The program was allowed to terminate the docking run in cases where three best-ranked solutions were within an RMSD of 1.0 Å from each other. Using these settings, the program successfully reproduced the binding mode of the cocrystallized ligand carbenoxolone, thus validating the docking settings.

3. Results

3.1. Species-specific differences in the metabolism of bupropion

Earlier studies using the unspecific 11β-HSD inhibitor GA and microsomes prepared from human placenta [5] and liver [11] or from baboon liver [10] suggested a role for 11β-HSD enzymes in the metabolism of bupropion. To test our assumption that 11β-HSD1 catalyzes the oxoreduction of bupropion and to study the stereo-selectivity of the reaction, we first measured the metabolism of bupropion in human liver microsomes that were incubated in the presence of G6P. We recently reported that intact liver microsomes, where the ER lumen is protected by the microsomal membrane, contain an endogenous NADPH regenerating system consisting of H6PDH, and that 11β-HSD1 reductase activity can be measured by incubation of microsomes with the substrate and G6P [25]. Upon incubation with G6P and bupropion, human liver microsomes efficiently formed threohydrobupropion and to a lesser extent (4-5 fold) erythrohydrobupropion (Fig. 2). Surprisingly, the selective 11β-HSD1 inhibitor T0504 completely blocked the formation of threohydrobupropion but had no effect on the formation of erythrohydrobupropion. To assess possible species-specific differences, we compared the activities of human, rat and mouse liver microsomes. The rat and mouse liver microsomes showed 10- and 80-fold lower activities to generate threohydrobupropion. Significant changes were identified by multiple measures ANOVA ($p < 0.0001$) between threohydrobupropion formation comparing human against rodent species with Tukey test (*** $p < 0.001$). It is important to note that under the same conditions rat liver microsomes showed a two-fold higher activity to reduce the substrate cortisone than human and mouse liver microsomes, which had comparable activities [25]. Rat liver microsomes formed equal amounts of threohydrobupropion and erythrohydrobupropion and mouse liver microsomes about 2-fold more erythrohydrobupropion than threohydrobupropion. As with the human liver microsomes, the 11β-HSD1 inhibitor T0504 selectively blocked threohydrobupropion, suggesting

that 11β-HSD1 stereo-selectively reduces bupropion to threohydrobupropion. To further support a role for 11β-HSD1, we used liver microsomes from liver-specific 11β-HSD1 knockout mice (LKO). Threohydrobupropion formation was completely abolished, while erythrohydrobupropion formation was comparable to that in wild-type mice, suggesting that another enzyme is responsible for the formation of erythrohydrobupropion.

3.2. Impact of cofactor on bupropion metabolism

As reported recently, the preparation of rodent microsomes yielded approximately 90% inside-out vesicles (*e.g.* luminal compartment protected by the vesicle membrane and cytoplasmic side facing the solution), whereas the commercially available human liver microsomes show 75% latency [25]. Incubation of human liver microsomes with G6P yielded approximately 8-fold higher amounts of threohydrobupropion than erythrohydrobupropion, but only minor amounts of hydroxybupropion (Fig. 3). As expected, incubation of microsomes with NADPH mainly led to the cytochrome P450-dependent formation of hydroxybupropion. The formation of threohydrobupropion is probably due to the microsomal fraction with reverse orientation. Similar observations were made with mouse and rat liver microsomes, and even higher differences between NADPH- and G6P-dependent formation of hydroxybupropion *versus* erythro- and threohydrobupropion, respectively, were measured (data not shown).

To compare the relative activities of cytochrome P450-dependent hydroxylation and 11β-HSD1-dependent carbonyl reduction *in vitro*, human liver microsomes were incubated in the presence of both NADPH and G6P (Fig. 4). Threohydrobupropion was the major product formed, followed by hydroxybupropion and erythrohydrobupropion.

3.3. Carbonyl reduction of bupropion by recombinant human 11β-HSD1 measured in cell lysates

The lysates of HEK-293 cells transiently transfected with human 11β-HSD1 efficiently converted bupropion to threohydrobupropion (Fig. 5). Importantly, no other metabolites were detected and lysates of untransfected HEK-293 cells did not metabolize bupropion. These incubations were performed in the presence of NADPH, because the cells were lysed by sonication, which generates microsomal vesicles with mixed (inside-out and rightside-out) orientation. Therefore, 11β-HSD1 activity can be easily measured upon incubation with NADPH, which is not the case if cells are homogenized by a more gentle procedure. An apparent K_m of 2.1 ± 0.9 μM and V_{max} of 0.22 ± 0.03 nmol/mg/h for the carbonyl reduction of bupropion was obtained for human 11β-HSD1, suggesting that bupropion is less efficiently reduced by 11β-HSD1 than cortisone.

Furthermore, we assessed whether 11β-HSD1 catalyzes the reverse reaction by incubating cell lysates with threohydrobupropion and $NADP^+$. No bupropion could be detected, indicating that the reaction is irreversible (data not shown).

3.4. Inhibition of 11β-HSD1-dependent cortisone reduction by bupropion and *vice versa*

To test whether the substrates influence each other, we first assessed the effect of bupropion on glucocorticoid activation. The reduction of cortisone was inhibited with an IC_{50} value of 165 ± 51 μM (Fig. 6). Next, we tested the impact of cortisone and the widely used synthetic glucocorticoid prednisone on the carbonyl reduction of bupropion. The conversion of bupropion to threohydrobupropion was inhibited by cortisone and prednisone with IC_{50} of 193 ± 40 nM (Fig. 7A) and 2.9 ± 0.3 μM, respectively (Fig. 7B).

3.5. Binding mode prediction of bupropion to 11β-HSD1 by molecular docking

Both isomers of bupropion geometrically fit to the binding site of 11β-HSD1 and both are predicted to bind next to the catalytic triad Ser170-Tyr183-Lys187 and the cofactor NADPH. However, the stereochemistry of these two isomers allows only one of them, *R*-bupropion, to be metabolized by 11β-HSD1. Since the hydrogens in the reduction reaction are transferred to the substrate *via* the cofactor and Tyr183 [36, 37], it is essential that the carbonyl-oxygen of bupropion is located next to these residues. This is the case for *R*-bupropion (Fig. 8A): the carbonyl oxygen points towards Tyr183 and the cofactor is at 2.46 Å distance from the carbonyl-carbon. In contrast, *S*-bupropion is located in the same place, but because of the different stereochemistry, the *tert*-butyl-group points towards the cofactor, thus pushing the carbonyl-group further away from the cofactor and Tyr183 (Fig. 8B). Thus, the *S*-bupropion carbonyl group is more distant from the catalytic H-donors and has a non-favorable interaction angle with the Tyr183 hydroxyl group. These docking results support our biological findings that only threohydrobupropion is formed by 11β-HSD1. Erythrohydrobupropion is not formed because of steric hindrance coming from the stereochemistry of *S*-bupropion.

4. Discussion

Based on earlier studies using microsomes from human and baboon liver and placenta together with the unspecific inhibitor GA it was suggested that 11β-HSD enzymes are involved in the formation of both erythrohydrobupropion and threohydrobupropion [5, 10, 11]. However, since GA might inhibit other enzymes, the relative contribution of 11β-HSD enzymes remained unclear. In the present study, we used liver microsomes and the highly selective 11β-HSD1 inhibitor T0504 (also known as Merck-544, [30, 38]), as well as recombinant 11β-HSD1 to characterize the carbonyl reduction of bupropion.

The comparison of human, rat and mouse liver microsomes revealed clearly highest activity of human liver microsomes to catalyze the carbonyl reduction of bupropion, and threohydrobupropion was the preferred metabolite formed (Fig. 2). These findings provide an explanation for the observations by Welch et al. who found only low levels of these metabolites in plasma of mice and rats [39]. Furthermore, these authors reported that hydroxybupropion was a major urinary metabolite in human, mouse and dog, whereas rats predominantly excreted side chain cleavage products of bupropion such as m-chlorobenzoic acid. It was proposed that the distinct metabolism of bupropion may account for the species-specific pharmacological response of bupropion. Thus, our findings further support earlier studies indicating that rodents are not adequate models for the prediction of bupropion metabolism in humans.

The specific 11β-HSD1 inhibitor completely abolished the formation of threohydrobupropion by liver microsomes from all three species, without affecting the formation of erythrohydrobupropion. Importantly, microsomes from liver-specific knock-out mice were unable to generate threohydrobupropion but the formation of erythrohydrobupropion was comparable to that by wild-type mouse liver microsomes. These results indicate that 11β-HSD1 is the major if not the only enzyme responsible for the formation of threohydrobupropion and emphasize the existence of another carbonyl reductase responsible for the formation of erythrohydrobupropion. The fact that erythrohydrobupropion is formed in the presence of G6P indicates that the unknown enzyme is localized within the ER and is dependent on H6PDH activity.

Using the recombinant enzyme, we showed that human 11β-HSD1 irreversibly catalyzes the carbonyl reduction of bupropion to threohydrobupropion. Analysis of the binding of bupropion and its metabolites to 11β-HSD1 by molecular modeling indicates that *R*-bupropion adopts a favorable binding position in the substrate pocket of 11β-HSD1, allowing the electron transfer

from the cofactor to form threohydrobupropion. In contrast, steric hindrance prevents optimal binding of *S*-bupropion and erythrohydrobupropion, suggesting that electron transfer cannot occur.

To start to understand whether administration of bupropion might interfere with 11β-HSD1-dependent glucocorticoid activation, we determined IC_{50} for cortisone reduction. Regarding the rapid metabolism of bupropion *in vivo* [39] and the high IC_{50} of 165 ± 51 μM, it is unlikely that exposure to bupropion will significantly inhibit the 11β-HSD1-dependent conversion of endogenous cortisone to cortisol. On the other hand, cortisone and prednisone efficiently inhibited the carbonyl reduction of bupropion. The low IC_{50} values of cortisone and prednisone to inhibit bupropion reduction suggest that pharmacological use of these glucocorticoids as well as elevated endogenous cortisone levels during stress may abolish the concomitant carbonyl reduction of bupropion.

Bupropion and its metabolites show different potency regarding the inhibition of biogenic amine uptake, different half-life and AUC [4, 6, 40-43]. It has been described earlier that hydroxybupropion, the metabolite generated by CYP2B6 has the highest potency [6, 7]. Pharmacological administration of cortisone and prednisone, high endogenous cortisone during stress, or the use of 11β-HSD1 inhibitors (currently in development to treat metabolic disease [15, 18]) are likely to result in higher hydroxybupropion levels, which will need a readjustment of the therapeutic dose of bupropion. Subjects receiving hormone replacement therapy, which leads to inhibition of CYP2B6 had diminished hydroxybupropion levels and increased erythro- and threohydrobupropion levels [44].

It has been shown that the glucuronides of erythro- and threohydrobupropion account for 13% of the urinary excretion of bupropion in man after a single 200 mg dose of bupropion [39]. An

impaired 11β-HSD1-mediated metabolism of bupropion is expected to result in a delayed excretion, which may enhance the pharmacological effect of bupropion and hydroxybupropion.

In conclusion, our results demonstrate that 11β-HSD1 exclusively catalyzes the carbonyl reduction of *R*-bupropion to threohydrobupropion and that another ER luminal enzyme is responsible for the formation of erythrohydrobupropion (Fig. 1). Bupropion reduction by human 11β-HSD1 is about 10 and 80 times more efficient than that by the rat and mouse enzymes. Whereas bupropion unlikely impairs 11β-HSD1-dependent glucocorticoid activation, the metabolism of bupropion is expected to be inhibited by high endogenous cortisone or pharmacological cortisone or prednisone, and dose adjustments of bupropion might be necessary to achieve optimal therapeutic effects. Further studies are needed to identify the ER luminal enzyme responsible for erythrohydrobupropion formation and to examine the consequences of 11β-HSD1 inhibition on bupropion metabolism in humans.

Footnotes

This work was supported by the Swiss National Science Foundation (PDFMP3_127330) to Alex Odermatt and a BBSRC David Philips fellowship (BB/G023468/1) to Gareth Lavery. Alex Odermatt has a Chair for Molecular and Systems Toxicology by the Novartis Research Foundation. Anna Vuorinen is supported by a PhD grant from the Austrian Academy of Sciences (ÖAW) and thanks the University of Innsbruck, Young Talents Grants (Nachwuchsförderung) for financial support. Daniela Schuster is financed by an Erika Cremer Habilitation Program from the University of Innsbruck.

Figure Legends

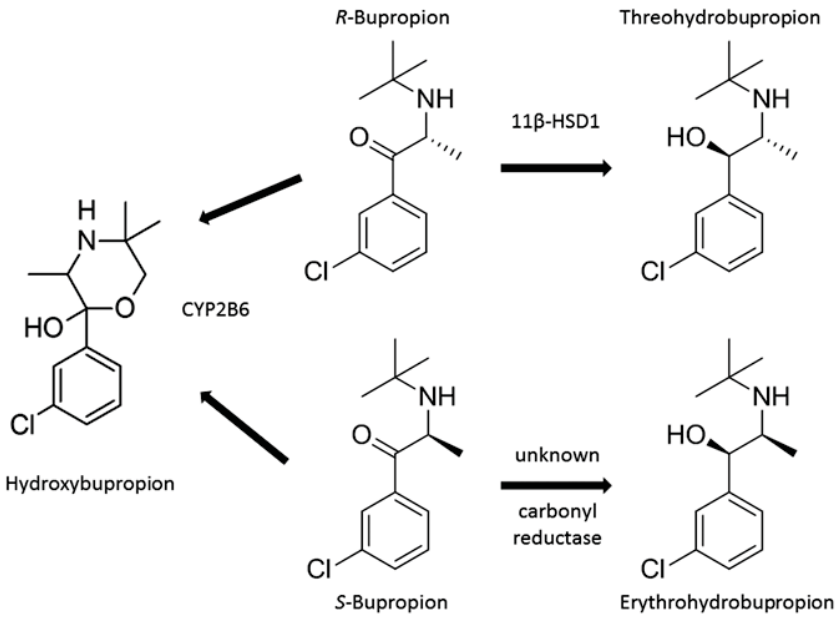

Fig. 1. Structures of bupropion and its major metabolites.

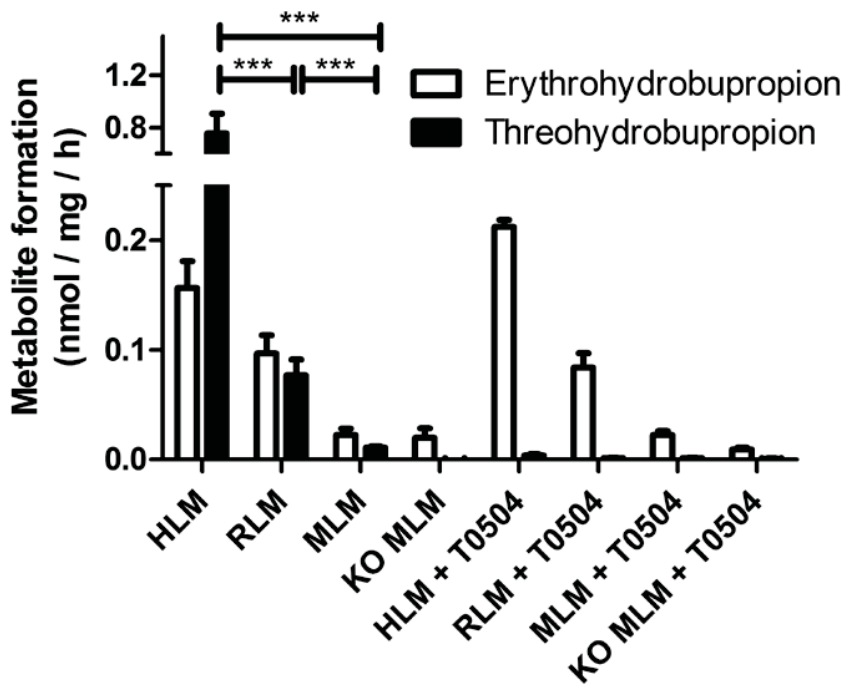

Fig. 2. Species-specific oxoreduction of bupropion by liver microsomes. Human liver microsomes (HLM, final concentration (f.c.) 0.4 mg/mL), rat liver microsomes (RLM, f.c. 1 mg/mL), mouse liver microsomes (MLM, f.c. 1 mg/mL) and microsomes from livers of liver-specific 11β-HSD1-deficient mice (LKO, f.c. 1 mg/mL) were incubated for 1 h at 37°C with 1 μM bupropion and 1 mM glucose-6-phosphate (G6P), in the absence or presence of 20 μM of the 11β-HSD1 inhibitor T0504. Data (mean ± SD) were obtained from at least three independent experiments using pooled microsomes. *** $p < 0.001$, multiple measures ANOVA found significant species differences in bupropion reduction ($p < 0.0001$), post hoc analysis by Tukey test was used for multiple comparison.

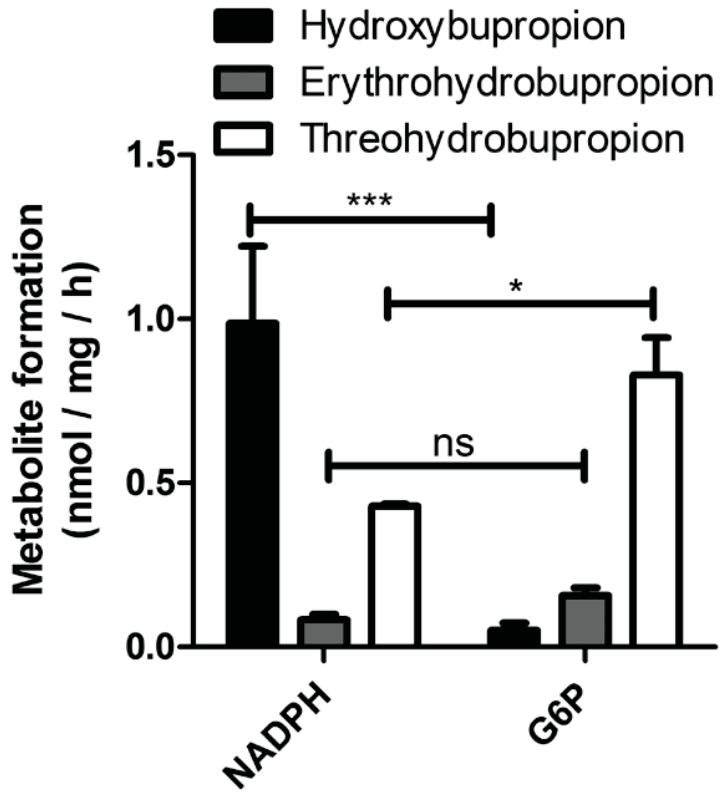

Fig. 3. Impact of cofactor on the metabolism of bupropion by human liver microsomes. Human liver microsomes (f.c. 0.4 mg/mL) were incubated for 1 h at 37°C in the presence of 1 µM bupropion and either 1 mM NADPH or 1 mM glucose-6-phosphate (G6P). Data represent mean ± SD from at least three independent experiments using pooled microsomes. ns = not significant, * $p < 0.05$, *** $p < 0.001$, multiple measures ANOVA found significant differences in the groups ($p < 0.0001$), post hoc analysis by Tukey test was used for multiple comparison.

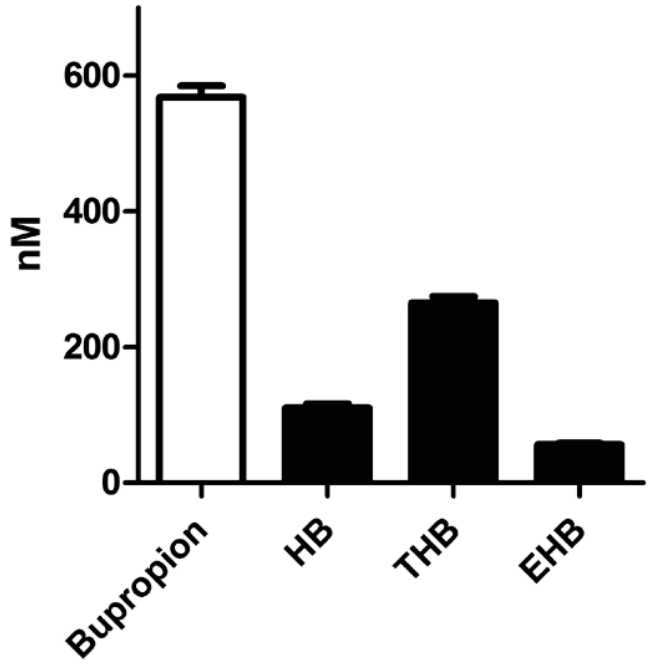

Fig. 4. Bupropion and its major metabolites after incubation of human liver microsomes with NADPH and G6P. Human liver microsomes (f.c. 0.2 mg/mL) were incubated for 1 h at 37°C in the presence of 1 μM bupropion, 1 mM NADPH and 1 mM G6P. Data represent mean ± SD from at least three independent experiments with pooled microsomes.

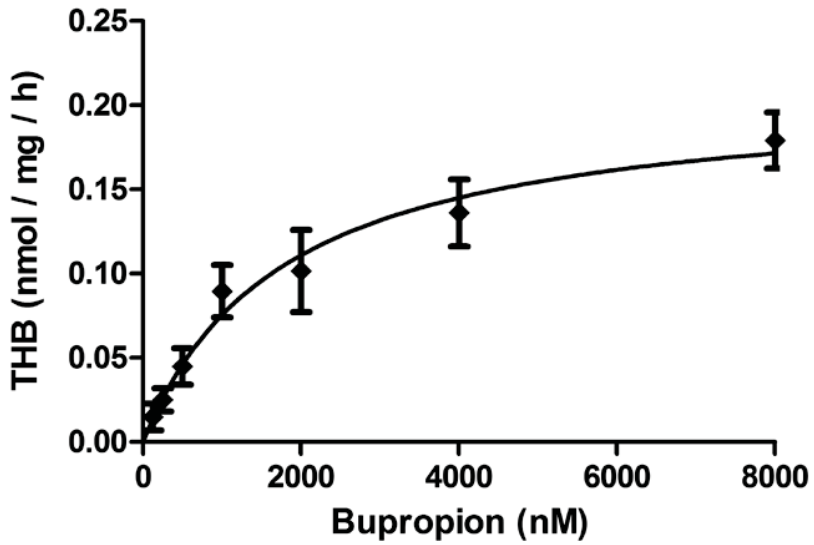

Fig. 5. Concentration-dependent reduction of bupropion to threohydrobupropion. HEK-293 cells transiently transfected with plasmid for human 11β-HSD1 were sonicated to obtain mixed vesicles, followed by incubation for 1 h at 37°C in the presence of 1 mM NADPH and different concentrations of bupropion as given in Materials and Methods. Apparent K_M (2.1 μM ± 0.9 μM) and apparent V_{max} (0.22 ± 0.03 nmol/mg/h) values were calculated. Data represent mean ± SD from at least three independent experiments.

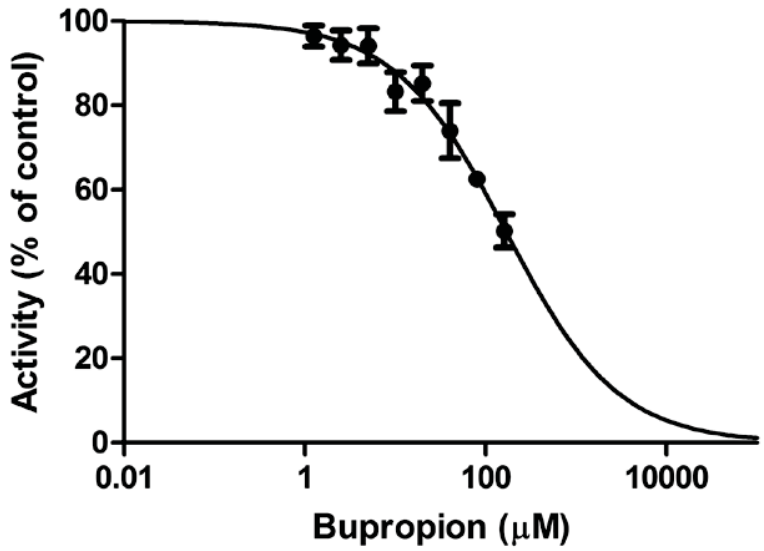

Fig. 6. Inhibition of 11β-HSD1-dependent reduction of cortisone by bupropion. Lysates of HEK-293 cells transiently transfected with human 11β-HSD1 were incubated with 1 μM cortisone, 1 mM NADPH and different concentrations of bupropion for 15 min at 37°C. Data were normalized to vehicle control (0.05% DMSO) and represent mean ± SD from three independent experiments.

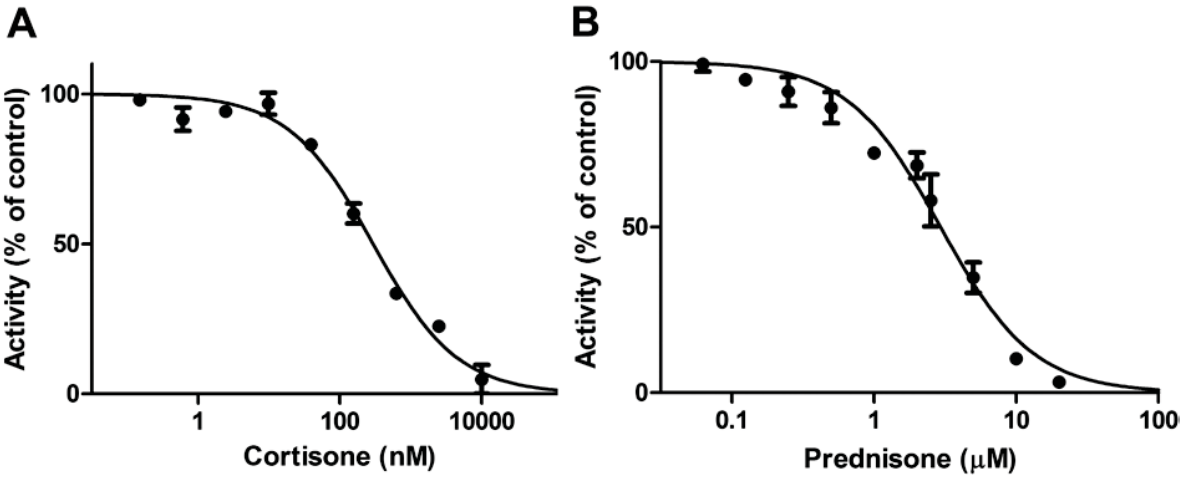

Fig. 7. Inhibition of 11β-HSD1-dependent threohydrobupropion reduction by cortisone and prednisone. Lysates of HEK-293 cells transiently transfected with human 11β-HSD1 were incubated with 1 μM bupropion, 1 mM NADPH and different concentrations of cortisone (A) or prednisone (B) for 60 min at 37°C. Data were normalized to activity of vehicle control (0.05% DMSO) and represent mean ± SD from three independent experiments.

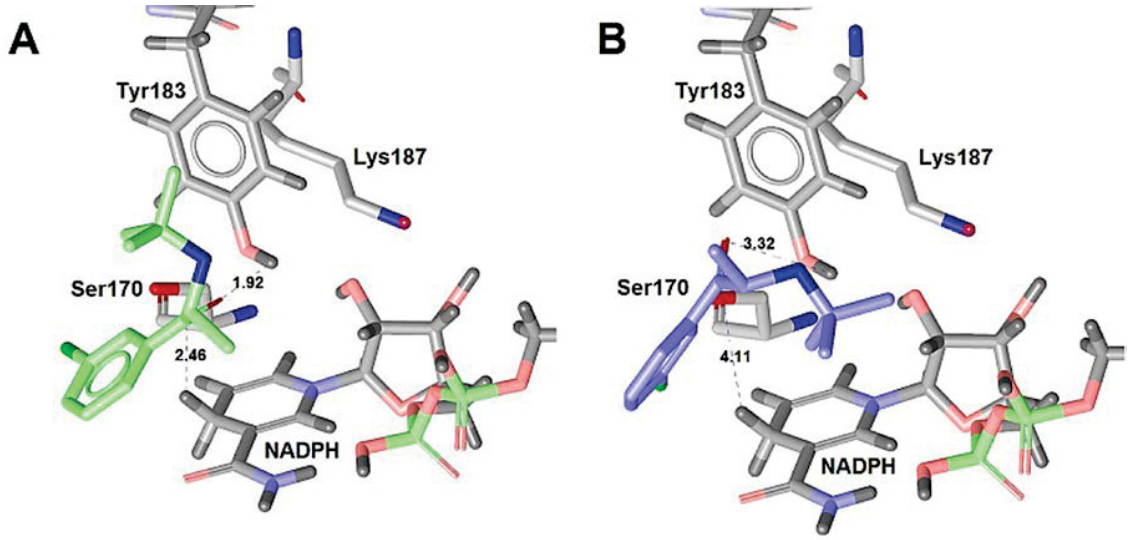

Fig. 8. Proposed binding modes of *R*-bupropion and *S*-bupropion in the ligand binding pocket of human 11β-HSD1. *R*-bupropion (A) is colored in green and *S*-bupropion (B) in blue. The catalytic triad and the cofactor are colored in grey. The distances between the substrate and the protein are given in Å.

References

[1] Holm KJ, Spencer CM. Bupropion: A Review of its Use in the Management of Smoking Cessation. Drugs 2000;59:1007-24.

[2] Jafarinia M, Mohammadi M-R, Modabbernia A, Ashrafi M, Khajavi D, Tabrizi M, et al. Bupropion versus methylphenidate in the treatment of children with attention-deficit/hyperactivity disorder: randomized double-blind study. Hum Psychopharm Clin 2012;27:411-8.

[3] Fava M, Rush AJ, Thase ME, Clayton A, Stahl SM, Pradko JF, et al. 15 years of clinical experience with bupropion HCl: from bupropion to bupropion SR to bupropion XL. Prim Care Companion J Clin Psychiatry 2005;7:106-13.

[4] Laizure SC, DeVane CL, Stewart JT, Dommisse CS, Lai AA. Pharmacokinetics of bupropion and its major basic metabolites in normal subjects after a single dose. Clin Pharmacol Ther 1985;38:586-9.

[5] Wang X, Abdelrahman DR, Zharikova OL, Patrikeeva SL, Hankins GDV, Ahmed MS, et al. Bupropion metabolism by human placenta. Biochem Pharmacol 2010;79:1684-90.

[6] Martin P, Massol J, Colin JN, Lacomblez L, Puech AJ. Antidepressant profile of bupropion and three metabolites in mice. Pharmacopsychiatry 1990;23:187-94.

[7] Schroeder DH. Metabolism and kinetics of bupropion. J Clin Psychiatry 1983;44:79-81.

[8] Faucette SR, Hawke RL, Lecluyse EL, Shord SS, Yan B, Laethem RM, et al. Validation of Bupropion Hydroxylation as a Selective Marker of Human Cytochrome P450 2B6 Catalytic Activity. Drug Metab Dispos 2000;28:1222-30.

[9] Hesse LM, Venkatakrishnan K, Court MH, von Moltke LL, Duan SX, Shader RI, et al. CYP2B6 Mediates the In Vitro Hydroxylation of Bupropion: Potential Drug Interactions with Other Antidepressants. Drug Metab Dispos 2000;28:1176-83.

[10] Wang X, Abdelrahman DR, Fokina VM, Hankins GD, Ahmed MS, Nanovskaya TN. Metabolism of bupropion by baboon hepatic and placental microsomes. Biochem Pharmacol 2011;82:295-303.

[11] Molnari JC, Myers AL. Carbonyl reduction of bupropion in human liver. Xenobiotica 2012;42:550-61.

[12] White PC, Mune T, Agarwal AK. 11β-Hydroxysteroid Dehydrogenase and the Syndrome of Apparent Mineralocorticoid Excess. Endocr Rev 1997;18:135-56.

[13] Odermatt A, Kratschmar DV. Tissue-specific modulation of mineralocorticoid receptor function by 11beta-hydroxysteroid dehydrogenases: An overview. Mol Cell Endocrinol 2012;350:168-86.

[14] Rebuffat AG, Tam S, Nawrocki AR, Baker ME, Frey BM, Frey FJ, et al. The 11-ketosteroid 11-ketodexamethasone is a glucocorticoid receptor agonist. Mol Cell Endocrinol 2004;214:27-37.

[15] Atanasov AG, Odermatt A. Readjusting the glucocorticoid balance: an opportunity for modulators of 11beta-hydroxysteroid dehydrogenase type 1 activity? Endocr Metab Immune Disord Drug Targets 2007;7:125-40.

[16] Hult M, Jornvall H, Oppermann UC. Selective inhibition of human type 1 11beta-hydroxysteroid dehydrogenase by synthetic steroids and xenobiotics. FEBS Lett 1998;441:25-8.

[17] Masuzaki H, Flier JS. Tissue-specific glucocorticoid reactivating enzyme, 11 beta-hydroxysteroid dehydrogenase type 1 (11 beta-HSD1)--a promising drug target for the treatment of metabolic syndrome. Curr Drug Targets Immune Endocr Metabol Disord 2003;3:255-62.

[18] Hughes KA, Webster SP, Walker BR. 11-Beta-hydroxysteroid dehydrogenase type 1 (11beta-HSD1) inhibitors in type 2 diabetes mellitus and obesity. Expert Opin Investig Drugs 2008;17:481-96.

[19] Sun D, Wang M, Wang Z. Small molecule 11beta-hydroxysteroid dehydrogenase type 1 inhibitors. Curr Top Med Chem 2011;11:1464-75.

[20] Odermatt A, Nashev LG. The glucocorticoid-activating enzyme 11[beta]-hydroxysteroid dehydrogenase type 1 has broad substrate specificity: Physiological and toxicological considerations. J Steroid Biochem Mol Biol 2010;119:1-13.

[21] Hult M, Elleby B, Shafqat N, Svensson S, Rane A, Jornvall H, et al. Human and rodent type 1 11beta-hydroxysteroid dehydrogenases are 7beta-hydroxycholesterol dehydrogenases involved in oxysterol metabolism. Cell Mol Life Sci 2004;61:992-9.

[22] Schweizer RA, Zurcher M, Balazs Z, Dick B, Odermatt A. Rapid hepatic metabolism of 7-ketocholesterol by 11beta-hydroxysteroid dehydrogenase type 1: species-specific differences between the rat, human, and hamster enzyme. J Biol Chem 2004;279:18415-24.

[23] Odermatt A, Da Cunha T, Penno CA, Chandsawangbhuwana C, Reichert C, Wolf A, et al. Hepatic reduction of the secondary bile acid 7-oxolithocholic acid is mediated by 11beta-hydroxysteroid dehydrogenase 1. Biochem J 2011;436:621-9.

[24] Nashev LG, Chandsawangbhuwana C, Balazs Z, Atanasov AG, Dick B, Frey FJ, et al. Hexose-6-phosphate dehydrogenase modulates 11beta-hydroxysteroid dehydrogenase type 1-dependent metabolism of 7-keto- and 7beta-hydroxy-neurosteroids. PLoS One 2007;2:e561.

[25] Meyer A, Vuorinen A, Zielinska AE, Da Cunha T, Strajhar P, Lavery GG, et al. Carbonyl reduction of triadimefon by human and rodent 11beta-hydroxysteroid dehydrogenase 1. Biochem Pharmacol 2013.

[26] Maser E, Friebertshauser J, Volker B. Purification, characterization and NNK carbonyl reductase activities of 11beta-hydroxysteroid dehydrogenase type 1 from human liver: enzyme cooperativity and significance in the detoxification of a tobacco-derived carcinogen. Chem Biol Interact 2003;143-144:435-48.

[27] Wsol V, Szotakova B, Skalova L, Maser E. Stereochemical aspects of carbonyl reduction of the original anticancer drug oracin by mouse liver microsomes and purified 11beta-hydroxysteroid dehydrogenase type 1. Chem Biol Interact 2003;143-144:459-68.

[28] Maser E, Bannenberg G. 11 beta-hydroxysteroid dehydrogenase mediates reductive metabolism of xenobiotic carbonyl compounds. Biochem Pharmacol 1994;47:1805-12.

[29] Hult M, Nobel CS, Abrahmsen L, Nicoll-Griffith DA, Jornvall H, Oppermann UC. Novel enzymological profiles of human 11beta-hydroxysteroid dehydrogenase type 1. Chem Biol Interact 2001;130-132:805-14.

[30] Arampatzis S, Kadereit B, Schuster D, Balazs Z, Schweizer RA, Frey FJ, et al. Comparative enzymology of 11beta-hydroxysteroid dehydrogenase type 1 from six species. J Mol Endocrinol 2005;35:89-101.

[31] Lavery GG, Zielinska AE, Gathercole LL, Hughes B, Semjonous N, Guest P, et al. Lack of significant metabolic abnormalities in mice with liver-specific disruption of 11beta-hydroxysteroid dehydrogenase type 1. Endocrinology 2012;153:3236-48.

[32] Verdonk ML, Cole JC, Hartshorn MJ, Murray CW, Taylor RD. Improved protein-ligand docking using GOLD. Proteins 2003;52:609-23.

[33] Jones G, Willett P, Glen RC, Leach AR, Taylor R. Development and validation of a genetic algorithm for flexible docking. J Mol Biol 1997;267:727-48.

[34] Berman HM, Westbrook J, Feng Z, Gililand G, Bhat TN, Weissig H, et al. The Protein Data Bank. Nucleic Acids Res 2000;28:235-42.

[35] Wu x, et al. The High Resolution Structures of Human, Murine and Guinea Pig 11-Beta-Hydroxysteroid Dehydrogenase Type 1 Reveal Critical Differences in Active Site Architecture. DOI:102210/pdb2bel/pdb

[36] Oppermann UC, Filling C, Berndt KD, Persson B, Benach J, Ladenstein R, et al. Active site directed mutagenesis of 3 beta/17 beta-hydroxysteroid dehydrogenase establishes differential effects on short-chain dehydrogenase/reductase reactions. Biochemistry 1997;36:34-40.

[37] Kavanagh KL, Jornvall H, Persson B, Oppermann U. Medium- and short-chain dehydrogenase/reductase gene and protein families : the SDR superfamily: functional and structural diversity within a family of metabolic and regulatory enzymes. Cell Mol Life Sci 2008;65:3895-906.

[38] Hermanowski-Vosatka A, Balkovec JM, Cheng K, Chen HY, Hernandez M, Koo GC, et al. 11beta-HSD1 inhibition ameliorates metabolic syndrome and prevents progression of atherosclerosis in mice. J Exp Med 2005;202:517-27.

[39] Welch RM, Lai AA, Schroeder DH. Pharmacological significance of the species differences in bupropion metabolism. Xenobiotica; the fate of foreign compounds in biological systems 1987;17:287-98.

[40] Horst WD, Preskorn SH. Mechanisms of action and clinical characteristics of three atypical antidepressants: venlafaxine, nefazodone, bupropion. J Affect Disord 1998;51:237-54.

[41] Jefferson JW, Pradko JF, Muir KT. Bupropion for major depressive disorder: Pharmacokinetic and formulation considerations. Clin Therapeut 2005;27:1685-95.

[42] Hsyu P-H, Singh A, Giargiari TD, Dunn JA, Ascher JA, Johnston JA. Pharmacokinetics of Bupropion and its Metabolites in Cigarette Smokers versus Nonsmokers. J Clin Pharmacol 1997;37:737-43.

[43] Golden Rn, DeVane C, Laizure S, Rudorfer MV, Sherer MA, Potter WZ. Bupropion in depression: Ii. the role of metabolites in clinical outcome. Arch Gen Psychiat 1988;45:145-9.

[44] Palovaara S, Pelkonen O, Uusitalo J, Lundgren S, Laine K. Inhibition of cytochrome P450 2B6 activity by hormone replacement therapy and oral contraceptive as measured by bupropion hydroxylation. Clin Pharmacol Ther 2003;74:326-33.

Chapter 3: Steroid metabolism of zebrafish enzymes

Introduction

In the course of my PhD thesis several projects focused on enzymes of the zebrafish (*danio rerio* (*dr*)) in order to address species-specific differences. The zebrafish is widely used as an aquatic model organism in research.

We tested inhibitory effects of organotins and of the dithiocarbamate thiram on zebrafish 11β-hydroxysteroid dehydrogenase type 2 (11β-HSD2). We reported earlier that these compounds inhibit the human enzyme [26, 27]. In humans, 11β-HSD2 is responsible for the conversion of cortisol to cortisone. Fish 11β-HSD2 has a dual role by converting cortisol to cortisone and 11β-hydroxytestosterone to 11-ketotestosterone [28-30], which is the main androgen in fish [31]. Thiram is a widely used pesticide and likely to enter the aquatic ecosystem. Organotins, even after being banned worldwide, are still found in aquatic ecosystems [32] and are found to accumulate in sediments and various species of fish [33, 34]. We investigated the effects of these chemicals on zebrafish 11β-HSD2, because inhibition of this enzyme may enhance glucocorticoid and diminish androgen effects in fish. The results of this project are included as the publication "Species-specific differences in the inhibition of human and zebrafish 11β-hydroxysteroid dehydrogenase 2 by thiram and organotins" at the end of this chapter.

Another enzyme involved in sex steroid metabolism in fish is 17β-hydroxysteroid dehydrogenase type 3 (17β-HSD3). The *dr*17β-HSD3 enzyme is a NADPH-dependent reductive enzyme, catalyzing the conversion of Δ^4-androstenedione to testosterone as well as the reaction of 11-ketoandrostenedione to the main androgen 11-ketotestosterone in fish [35]. It has been described earlier that a wide range of UV filters (benzophenone-1 (BP-1), benzophenone-2 (BP-2), benzophenone-6 (BP-6), 3-benzylidene camphor (3-BC) and 4-methyl-bezylidene camphor (4-MBC)) can potently inhibit the *hs*17β-HSD3 [36]. Together with the students Dominik Vogt, Céline Murer and Petra Strajhar I performed several experiments with *dr*11β-HSD2 and *dr*17β-HSD3.

We have successfully shown that the function of *dr*11β-HSD2 is to inactivate cortisol and that it is further responsible for the generation of 11-ketotestosterone. In humans 11β-HSD1 is known to convert cortisone to cortisol. Both enzymes together by interplay offer a sophisticated system to

control the ratio of active and inactive glucocorticoids. It can be regarded as a recycling system, as the amount of active glucocorticoids can be easily and rapidly adapted and *de novo* synthesis is not required for fast acting responses. Interestingly, in teleost species the gene encoding 11β-HSD1 is absent. It was assumed that an ancestor of 11β-HSD1 would take over that function. Two ancestors of 11β-HSD1 have been described in zebrafish, *dr*11β-hydroxysteroid dehydrogenase type 3a (11β-HSD3a) and *dr*11β-hydroxysteroid dehydrogenase type 3b (11β-HSD3b), also known as *dr*11β-HSD1-like-protein-like. It is widely assumed that either *dr*11β-HSD3a or *dr*11β-HSD3b take over the function to reduce cortisone to cortisol [37, 38]. We tested if one of the two ancestors is responsible for cortisone reduction. In addition, we incubated zebrafish microsomes under several conditions to check for 11-oxosteroid reductase activity. More information on this project can be found in the draft paper at the end of this chapter.

Results & Discussion

With the help of Dominik Vogt and Céline Murer, some UV filters were screened at a concentration of 20 µM on zebrafish homogenate and on *dr*17β-HSD3 expressed in *zf*4 cells. Fig. 6 shows the activity of Δ^4-androstenedione (AD) reduction in % compared to the vehicle control. Black bars show the % activity upon incubation with UV filters on *hs*17β-HSD3 expressed in HEK-293 cells as published by Nashev *et al*. [36]. We incubated the full body homogenate of a male zebrafish with UV filters and *dr*17β-HSD3 transiently transfected in *zf*4 cells. Important species-differences were found for BP-2 and BP-3. These two UV filters seem to have a higher inhibition on the zebrafish enzyme compared to the human enzyme. BP-6 shows a comparable inhibition, whereas 4-MBC and 3-BC show less inhibition upon incubation with the zebrafish enzyme compared to the human enzyme. Incubations with BP-1, BP-2 and BP-3 show less inhibition in the homogenate, pointing out that these compounds may be metabolized by full body zebrafish homogenate.

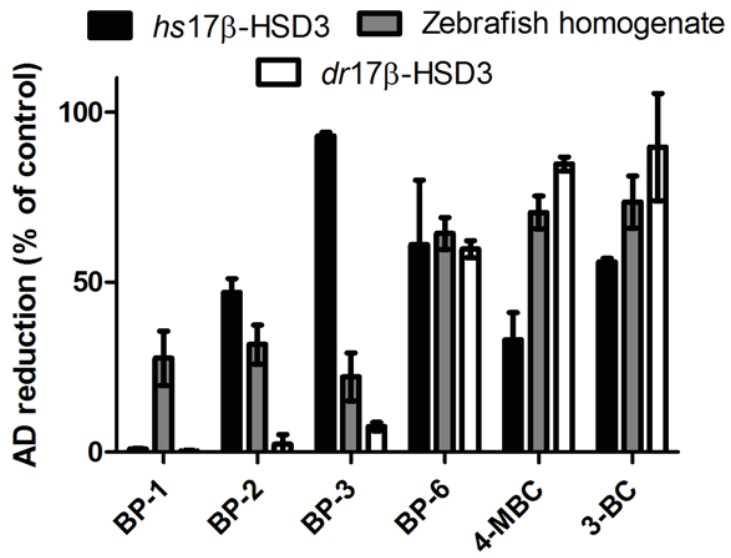

Figure 6: Δ^4-androstenedione (AD) reduction (% of control) of UV filters (benzophenone-1 (BP-1), benzophenone-2 (BP-2), benzophenone-3 (BP-3), benzophenone-6 (BP-6), 4-methyl-bezylidene camphor (4-MBC) and 3-benzylidene camphor (3-BC)) at a concentration of 20 µM, on human 17β-hydroxysteroid dehydrogenase type 3 (*hs*17β-HSD3) (data published by Nashev *et al.* [36]), zebrafish homogenate (final concentration 1.5 mg/ml) and intact *zf*4 cells transiently transfected with zebrafish 17β-hydroxysteroid dehydrogenase type 3 (*dr*17β-HSD3). Conversions were kept under 30%, AD (200 nM) NADPH (1 mM).

As BP-1, BP-2 and BP-3 showed a strong inhibition at 20 µM, we decided to determine IC_{50} values of these three UV-filters on the zebrafish enzyme. These determinations were performed by Céline Murer (Fig. 7).

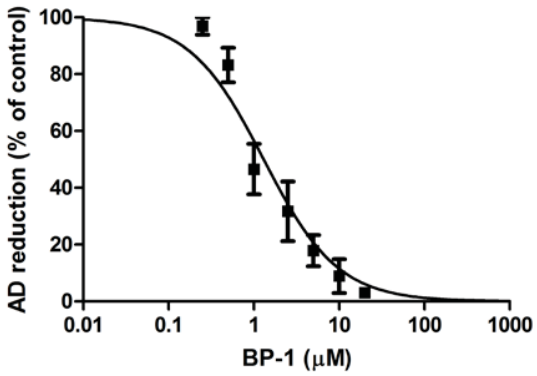

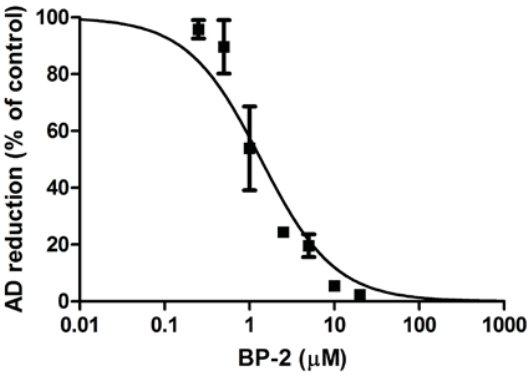

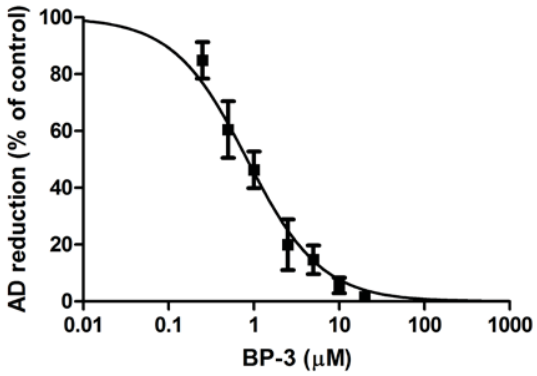

UV filter	IC_{50} value
BP-1	1.4 µM ± 0.8 µM
BP-2	1.4 µM ± 0.5 µM
BP-3	0.9 µM ± 0.4 µM

Figure 7: IC_{50} curves and table of inhibition of zebrafish 17β-HSD3 by the UV filters (benzophenone-1 (BP-1), benzophenone-2 (BP-2), benzophenone-3 (BP-3)). Inhibition of 17β-HSD3-dependent Δ^4-androstenedione (AD) reduction to testosterone by various concentrations of UV filters was measured in intact, transiently transfected *zf*4 cells. Incubation with AD (200 nM) and UV filters for 60 min at 37°C. Data were normalized to vehicle control (0.05% DMSO) and represent mean ± SD from three independent experiments.

Moreover, experiments by Petra Strajhar suggested that the UV filters have additive effects and that they bioaccumulate *in vitro* (Fig. 8). These experiments have been performed using the human enzyme.

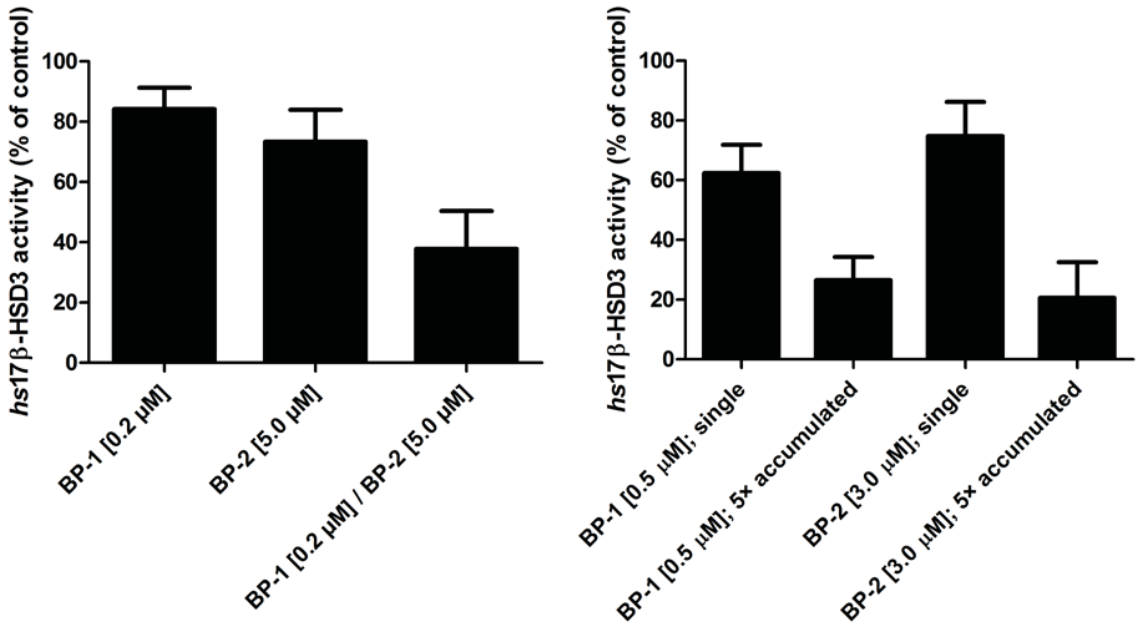

Figure 8: Additive effects by mixtures (left) and bioaccumulation (right) of UV filters (benzophenone-1 (BP-1), benzophenone-2 (BP-2)) on human 17β-hydroxysteroid dehydrogenase (*hs*17βHSD3) activity. Incubations have been performed as described in the Master thesis of Petra Strajhar.

We provide evidence that the UV filters BP-1, BP-2 and BP-3 might have stronger endocrine disrupting effects on the zebrafish compared to the human enzyme, because all three UV filters potently inhibited the zebrafish enzyme. Moreover, stronger effects can be assumed due to bioaccumulation and additive effects of mixtures.

This project should be continued, as the findings are relevant. To provide further evidence an *in vivo* assay should be performed with zebrafish. I would incubate zebrafish over different time periods and study exposure to mixtures of the three benzophenones. It would be interesting to measure concentrations of steroid hormones in zebrafish plasma by LC-MS/MS in order to detect potential changes in steroid hormone concentrations. I hypothesize that the additive effects of mixtures and the bioaccumulation effects can be seen *in vivo* as well.

Paper: Species-specific differences in the inhibition of human and zebrafish 11β-hydroxysteroid dehydrogenase 2 by thiram and organotins

Toxicology 301 (2012) 72–78

Contents lists available at SciVerse ScienceDirect

Toxicology

journal homepage: www.elsevier.com/locate/toxicol

Species-specific differences in the inhibition of human and zebrafish 11β-hydroxysteroid dehydrogenase 2 by thiram and organotins

Arne Meyer, Petra Strajhar, Céline Murer, Thierry Da Cunha, Alex Odermatt*

Swiss Center for Applied Human Toxicology and Division of Molecular and Systems Toxicology, Department of Pharmaceutical Sciences, University of Basel, Klingelbergstrasse 50, CH-4056 Basel, Switzerland

ARTICLE INFO

Article history:
Received 3 April 2012
Received in revised form 30 June 2012
Accepted 4 July 2012
Available online 11 July 2012

Keywords:
Dithiocarbamate
Thiram
Organotin
Cadmium
11β-Hydroxysteroid dehydrogenase
Glucocorticoid

ABSTRACT

Dithiocarbamates and organotins can inhibit enzymes by interacting with functionally essential sulfhydryl groups. Both classes of chemicals were shown to inhibit human 11β-hydroxysteroid dehydrogenase 2 (11β-HSD2), which converts active cortisol into inactive cortisone and has a role in renal and intestinal electrolyte regulation and in the feto-placental barrier to maternal glucocorticoids. In fish, 11β-HSD2 has a dual role by inactivating glucocorticoids and generating the major androgen 11-ketotestosterone. Inhibition of this enzyme may enhance glucocorticoid and diminish androgen effects in fish. Here, we characterized 11β-HSD2 activity of the model species zebrafish. A comparison with human and mouse 11β-HSD2 revealed species-specific substrate preference. Unexpectedly, assessment of the effects of thiram and several organotins on the activity of zebrafish 11β-HSD2 showed weak inhibition by thiram and no inhibition by any of the organotins tested. Sequence comparison revealed the presence of an alanine at position 253 on zebrafish 11β-HSD2, corresponding to cysteine-264 in the substrate-binding pocket of the human enzyme. Substitution of alanine-253 by cysteine resulted in a more than 10-fold increased sensitivity of zebrafish 11β-HSD2 to thiram. Mutating cysteine-264 on human 11β-HSD2 to serine resulted in 100-fold lower inhibitory activity. Our results demonstrate significant species differences in the sensitivity of human and zebrafish 11β-HSD2 to inhibition by thiram and organotins. Site-directed mutagenesis revealed a key role of cysteine-264 in the substrate-binding pocket of human 11β-HSD2 for sensitivity to sulfhydryl modifying agents.

1. Introduction

In humans, 11β-hydroxysteroid dehydrogenase type 2 (11β-HSD2) essentially catalyzes the conversion of the active glucocorticoid cortisol (corticosterone in rodents) to its inactive form cortisone (11-dehydrocorticosterone in rodents), thereby regulating the access of glucocorticoids to glucocorticoid receptors (GR) and mineralocorticoid receptors (MR), and rendering specificity of MR for aldosterone (Odermatt and Kratschmar, 2012). The consequences of impaired 11β-HSD2 activity on electrolyte balance and blood pressure are manifested in patients with genetic defects and suffering from apparent mineralocorticoid excess, and upon ingestion of large amounts of licorice, which contains the inhibitor glycyrrhetinic acid (Ferrari, 2010). Moreover, in the placenta 11β-HSD2 acts as a protective barrier for the fetus from high maternal cortisol concentrations, and studies in rodents indicated that 11β-HSD2 inhibition during pregnancy causes irreversible changes in fetal development that lead to a higher risk for cardiovascular and metabolic disease (Murphy et al., 2002; Seckl and Holmes, 2007; Shams et al., 1998; Welberg et al., 2005). Thus, besides genetic susceptibility, environmental factors, including the exposure to xenobiotics, need to be considered (Ma et al., 2011; Odermatt and Gumy, 2008; Odermatt et al., 2006).

In contrast to human and other mammalian species, studies addressing the inhibition of 11β-HSD2 by xenobiotics in fish and other aquatic species are missing. Studies on rainbow trout (Kusakabe et al., 2003), Japanese eel (Jiang et al., 2003; Miura et al., 1991) and Nile tilapia (Miura et al., 1991) revealed an important role of 11β-HSD2 in the formation of the main fish androgen 11-ketotestosterone from 11β-hydroxytestosterone. In fish, 11β-HSD2 is highly expressed in the gonads, supporting its role in androgen metabolism. Thus, xenobiotics inhibiting 11β-HSD2 are expected to enhance glucocorticoid effects and suppress androgen action in fish.

Abbreviations: 11β-HSD2, 11β-hydroxysteroid dehydrogenase 2; DBT, dibutyltin; DMSO, dimethylsulfoxide; DMT, dimethyltin; DOT, dioctyltin; DPT, diphenyltin; GR, glucocorticoid receptor; LC–MS, liquid chromatography–mass spectrometry; MR, mineralocorticoid receptor; MRM, multiple-reaction monitoring; NEM, N-ethylmaleimide; TBT, tributyltin; TMT, trimethyltin; TPT, triphenyltin.

* Corresponding author. Tel.: +41 61 267 1530; fax: +41 61 267 1515.
E-mail address: alex.odermatt@unibas.ch (A. Odermatt).

0300-483X/$ – see front matter © 2012 Elsevier Ireland Ltd. All rights reserved.
http://dx.doi.org/10.1016/j.tox.2012.07.001

We reported earlier that dithiocarbamates (Atanasov et al., 2003) and organotins (Atanasov et al., 2005), chemicals known to interfere with functionally important sulfhydryl groups, inhibit human 11β-HSD2. Several dithiocarbamates inhibit human 11β-HSD2 in the nanomolar range, i.e. thiram, disulfiram and maneb, and some in the micromolar range, i.e. pyrrolidine dithiocarbamate, diethyldithiocarbamate and zineb. These chemicals are expected to exert additive inhibitory effects on 11β-HSD2 (Atanasov et al., 2003).

Dithiocarbamates, including thiram (tetramethylthiuram disulfide), are widely used as fungicides on seeds and as foliar fungicides on turf, vegetables and fruits (Vettorazzi et al., 1995). The pesticides ferbam and ziram are environmentally degraded to thiram. Furthermore, thiram is used as an accelerator and vulcanization agent in the rubber industry. Gupta et al. have shown that the half-life of thiram under controlled laboratory conditions is longer than that of other carbamates and ranges from 5 to 12 days in water, depending on multiple parameters (Gupta et al., 2012). The extensive use of thiram, the fact that thiram is a degradation product of other pesticides, the possible persistence in the environment, and additive inhibitory effects of mixtures of dithiocarbamates, led us to investigate whether thiram might inhibit 11β-HSD2 of the aquatic model organism zebrafish (*danio rerio*).

Cadmium, that also may affect the function of sulfhydryl groups on proteins, has been found to decrease 11β-HSD2 activity in cultured primary human trophoblast cells and in cultured human choriocarcinoma JEG-3 cells, whereby it remained unclear whether the reduced activity was due to direct inhibition of 11β-HSD2 or reduced expression (Ronco et al., 2010; Yang et al., 2006). A very high environmental enrichment factor has been reported for cadmium (Shi et al., 2012).

Moreover, we tested whether organotins might inhibit zebrafish 11β-HSD2. Organotins are, even after the worldwide ban of TBT, readily detected in water ecosystems (Castro et al., 2012). They accumulate in sediments and show high bioaccumulation in various aquatic species with concentrations up to 53 μg/g in Cobia (Rachycentron canadum) (Jadhav et al., 2011; Kannan et al., 1995; Liu et al., 2006). Previously, we found that the organotins dibutyltin (DBT), tributyltin (TBT), diphenyltin (DPT) and triphenyltin (TPT) inhibit human 11β-HSD2, that they show additive inhibitory effects, and that mutant C264S was less sensitive to inhibition by TBT (Atanasov et al., 2005), suggesting reversible sulfhydryl modification as inhibitory mechanism.

In the present study, we assessed the effects of organotins, thiram, cadmium and the sulfhydryl modifying reference compound N-ethylmaleimide (NEM) on zebrafish 11β-HSD2 activity and compared the effects with those on the human enzyme. Finally, we performed site-directed mutagenesis to explain differential effects on human and zebrafish 11β-HSD2 by the xenobiotics investigated.

2. Materials and methods

2.1. Materials

Cadmium chloride was purchased from Merck KGaA (Darmstadt, Germany), [1,2,6,7-^{3}H]-cortisol from Amersham Pharmacia (Piscataway, NJ, USA), unlabeled steroids from Steraloids (Newport, RI), and all other chemicals and cell culture medium from Sigma–Aldrich Chemie GmbH (Buchs, Switzerland). The solvents were of analytical and high performance liquid chromatography grade and the reagents of the highest grade available. Cadmium chloride, thiram and organotins were dissolved in dimethyl sulfoxide (DMSO) and stored as 20 mM stock solution at −20 °C. N-ethylmaleimide (NEM) was dissolved in ethanol and stored as 20 mM stock solution at −20 °C.

2.2. Construction of expression plasmids and site-directed mutagenesis

Expression plasmids for human wild-type 11β-HSD2 and mutant C264S have been described earlier (Atanasov et al., 2005; Odermatt et al., 1999). A full length zebrafish (*danio rerio*) cDNA clone was purchased from ImaGenes GmbH, RZPD, Berlin, Germany. The cDNA was amplified by PCR using an oligonucleotide at the start codon to introduce a BamHI endonuclease restriction site and a Kozak consensus sequence (5′-CATAAGCTTCCGCCATGTCTATTTTTGTTGGTGGAGCAG-3′) and an oligonucleotide at the stop codon either to add an XbaI endonuclease restriction site (5′-ACCTCGAGCTAATCAATACACTTTGTGAAGTTGC-3′) or to attach a FLAG-epitope followed by the stop codon and an XbaI endonuclease restriction site (5′-ACCTCGAGTCACTTGTCATCGTCGTCCTTGTAGTCCATAGAACCATCAATACACTTTGTGA-AGTTGCTG-3′). The PCR product was inserted into the BamHI–XbaI sites of the pcDNA3.1 vector. Site-directed mutagenesis to construct mutant A253C was performed as described earlier (Atanasov et al., 2005). The selected clones used in this study were sequence verified. Protein expression and enzyme activity was assessed in transiently transfected HEK-293 cells. Protein expression of zebrafish wild-type 11β-HSD2 and mutant A253C was verified by Western blotting (Fig. S1), as described for human 11β-HSD2 wild-type and mutant C264S (Atanasov et al., 2005). Briefly, proteins were separated by sodium dodecyl sulfate gel electrophoresis and transferred on a polyvinyl difluoride membrane. The FLAG-tagged 11β-HSD2 was detected by mouse M2 antibody from Sigma–Aldrich Chemie GmbH. Actin was detected by rabbit anti-actin IgG from Santa Cruz Biotechnology Inc. (Santa Cruz, CA, USA). Horseradish peroxidase-conjugated secondary antibodies were used to visualize the bands with Immobilon Western Chemiluminescent HRP substrate from Millipore Corporation (Billerica, MA, USA). Untagged and C-terminally FLAG-epitope tagged proteins showed comparable activities as seen before for human 11β-HSD2 expression constructs (Odermatt et al., 1999).

2.3. Cell culture

Human embryonic kidney cells (HEK-293) were cultivated in Dulbecco's modified Eagle's medium (DMEM) containing 4.5 g/L glucose (D5796 Sigma–Aldrich), 10% fetal bovine serum, 100 U/mL penicillin, 0.1 mg/mL streptomycin, 1× MEM non-essential amino acids and 10 mM HEPES buffer, pH 7.4. Cells were incubated at 37 °C in a humidified 5% CO_2 atmosphere.

Zebrafish embryonic fibroblast cells ZF-4 (kindly provided by Dr. Jerzy Adamski, Helmholtz Zentrum, Munich, Germany) were cultivated in DMEM:F12 (D8437 Sigma–Aldrich), supplemented with 10% fetal bovine serum, 100 U/mL penicillin and 0.1 mg/mL streptomycin. These cells were maintained at 28 °C in a humidified 5% CO_2 atmosphere.

2.4. Transient transfection and harvesting of cells

HEK-293 cells were transiently transfected with plasmids for human wild-type 11β-HSD2 (Odermatt et al., 1999) or mutant C264S (Atanasov et al., 2005) using the calcium phosphate precipitation method. Transfection efficiency was approximately 20%. Zebrafish wild-type 11β-HSD2 and mutant A253C were transfected into ZF-4 cells using Fugene HD according to the manufacturer's protocol (Roche Applied Science, Rotkreuz, Switzerland). Transfection efficiency was approximately 25%. After 48 h transfected cells were detached, centrifuged and cell pellets (5 pellets/10 cm^2 dish) shock frozen on dry ice and stored at −80 °C until further use.

2.5. Determination of recombinant human, mouse and zebrafish 11β-HSD2 activities by liquid chromatography–tandem mass spectrometry (LC–MS)

Reactions were performed for 10 min at 37 °C in a total volume of 500 μL containing lysates of HEK-293 cells expressing human, mouse or zebrafish 11β-HSD2 in buffer TS2 (100 mM NaCl, 1 mM EGTA, 1 mM EDTA, 1 mM $MgCl_2$, 250 mM sucrose, 20 mM Tris–HCl, pH 7.4), supplemented with 500 μM NAD^+ and the corresponding substrate (2 nM–2 μM final concentration). Internal standard (100 nM deuterized d8-corticosterone) was added, followed by extraction with 1 mL ethyl acetate. The organic phase was transferred to a new tube, evaporated to dryness and reconstituted in 100 μL of methanol containing 0.1% formic acid.

Steroids were resolved on an Atlantis T3 (3 μm, 2.1 mm × 150 mm) column (Waters, Milford, MA) at 30 °C using an Agilent model 1200 Infinity Series chromatograph (Agilent Technologies, Basel, Switzerland). The mobile phase consisted of water and acetonitrile (95:5) containing 0.1% formic acid (solvent A), and water and acetonitrile (5:95) containing 0.1% formic acid (solvent B) at a total flow rate of 0.4 mL/min. A linear gradient was used starting from 30% solvent B to 70% solvent B from 0 to 13 min, followed by 95% solvent B for 2 min, and re-equilibration with 30% solvent B. A built-in switching valve was used to direct the LC flow to an Agilent 6410 triple quadrupole MS (controlled by Mass Hunter workstation software version B.01.04). The injection volume of each sample was 5 μL. The MS was operated in atmospheric pressure electrospray positive ionization mode, with nebulizer pressure and nebulizer gas flow rate of 45 psi and 10 L/min, respectively, a source temperature of 350 °C and capillary and cone voltage of 4000 V and 190 V, respectively.

The six steroids were analyzed using multiple-reaction monitoring (MRM). Metabolites were identified by comparing their retention time and mass to charge ratio (m/z) with those of authentic standards. The transitions, collision energy and retention time were m/z 363/121, 25 V, 11.4 min for cortisol; m/z 361/163, 20 V, 11.6 min for cortisone; m/z 347/121, 40 V, 13.4 min for corticosterone; m/z 355/125, 28 V, 13.4 min for d8-corticosterone; m/z 345/121, 40 V, 12.9 min for

Table 1
Comparison of substrate preference of human, mouse and zebrafish 11β-HSD2 activities.

	$_{app}K_m$	SEM	$_{app}V_{max}$	SEM	V_{max}/K_m
Human					
Cortisol	84	23	4.2	0.8	0.050
Corticosterone	5.7	1.7	1.2	0.3	0.211
11β-OH-Testo	37	12	3.8	1	0.103
Mouse					
Cortisol	44	4	0.41	0.03	0.0093
Corticosterone	24	3	0.17	0.01	0.0071
11β-OH-Testo	33	3	0.19	0.02	0.0058
Zebrafish					
Cortisol	72	18	0.040	0.003	0.00056
Corticosterone	147	25	0.17	0.02	0.00116
11β-OH-Testo	206	19	0.45	0.02	0.00218

Enzymatic activities of lysates from HEK-293 cells transiently transfected with either human, mouse or zebrafish 11β-HSD2 were determined by measuring the oxidation of cortisol, corticosterone or 11β-hydroxytestosterone in the presence of NAD^+ as described in Section 2. The $_{app}V_{max}$ values were expressed relative to total protein concentration in the lysates and allow comparison within a species but not between different species. Data represent mean ± SEM of inhibition curves from combined experiments calculated by non-linear regression using four parametric logistic curve fitting (GraphPad Prism).
11β-OH-Testo, 11β-hydroxytestosterone.

11-dehydrocorticosterone; *m/z* 305/121, 20 V, 12.3 min for 11β-hydroxytestosterone; and *m/z* 303/121, 24 V, 12.5 min for 11-ketotestosterone.

2.6. Determination of inhibition of human and zebrafish 11β-HSD2

Enzyme activity was measured using cell lysates as described previously (Kratschmar et al., 2011). Briefly, cell pellets were resuspended in TS2 buffer and sonicated using a Branson sonicator (5 pulses, output 2, duty cycles 20, performed at 4 °C). Lysates were incubated for 10 min at 37 °C in a total volume of 22 μL containing 10 nM [1,2,6,7-^{3}H]-cortisol, 40 nM unlabeled cortisol, 500 μM NAD^+ and either vehicle or inhibitor. To assess the inhibition by Cd^{2+}, TS2 buffer without EGTA and EDTA was applied. Reactions were stopped by adding an excess of cortisone and cortisol (2 mM) in methanol. Separation of the steroids was performed by thin layer chromatography (TLC) and product formation was determined by scintillation counting. In all experiments conversion of cortisol to cortisone was kept below 30%. IC_{50} values were calculated by non-linear regression using four parametric logistic curve fitting (GraphPad Prism). Data (mean ± SD) were obtained from at least three independent experiments.

3. Results

3.1. Substrate preference of human, mouse and zebrafish 11β-HSD2

The main physiological substrates of human, mouse and zebrafish 11β-HSD2 are cortisol, corticosterone and 11β-hydroxytestosterone, respectively. Therefore, we first compared 11β-HSD2-dependent oxidation of these three substrates in order to identify species-specific substrate preference (Table 1). Because radiolabeled 11β-hydroxytestosterone was not available, and to measure activities for the three substrates under comparable conditions, an LC-MS based method for quantification of these steroids was established. Due to higher protein expression of the human enzyme compared with mouse and zebrafish 11β-HSD2, as determined by immune-detection using antibody against the C-terminal FLAG-tag (data not shown), an approximately 10-fold higher apparent V_{max} (activity per total protein in the lysate) was obtained. Thus, the $_{app}V_{max}$ values only allow comparisons within a given species. A more than 10-fold higher affinity of human 11β-HSD2 for corticosterone compared with cortisol was obtained, with 3–4 times higher $_{app}V_{max}$ for the latter. The affinity for 11β-hydroxytestosterone was about two times higher than that for cortisol with comparable $_{app}V_{max}$. The differences between cortisol and corticosterone were less pronounced for the mouse enzyme, despite the fact that mice do not synthesize cortisol.

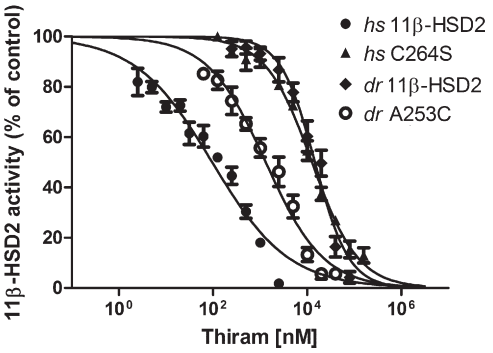

Fig. 1. Inhibition of human and zebrafish 11β-HSD2 activity by thiram. Inhibition of 11β-HSD2-dependent conversion of cortisol to cortisone by various concentrations of thiram was measured in lysates of HEK-293 cells transfected with wild-type and mutant human or zebrafish enzymes as described in Section 2. Lysates were simultaneously incubated with cortisol (50 nM) and thiram for 10 min at 37 °C. Data were normalized to vehicle control (0.05% DMSO) and represent mean ± SD from three independent experiments.

The affinities of zebrafish and human 11β-HSD2 for cortisol were comparable; however, the zebrafish enzyme had a more than ten times higher $_{app}V_{max}$ for 11β-hydroxytestosterone compared with cortisol, in line with a major role in 11-ketotestosterone formation.

3.2. The role of cysteine in the inhibition of human and zebrafish 11β-HSD2 by thiram

Because aquatic species may be potentially exposed to the pesticide thiram, we determined the inhibition of 11β-HSD2 from the model organism zebrafish by thiram and compared its effect with that on the human enzyme. Whereas human wild-type 11β-HSD2 was potently inhibited by thiram (IC_{50} 96 ± 17 nM, mean ± SD), zebrafish wild-type 11β-HSD2 was relatively resistant toward thiram inhibition with an IC_{50} of 18.3 ± 6.0 μM (Fig. 1).

A sequence comparison of human and zebrafish 11β-HSD2 (Fig. S2) revealed important differences in the presence of cysteine residues. The zebrafish enzyme has an alanine residue at position 253, which corresponds to cysteine-264 in the human enzyme. Molecular modeling suggested that cysteine-264 on human 11β-HSD2 has stabilizing interactions with the 3-carbonyl on cortisol (see Fig. 6 in Furstenberger et al., 2012), which may explain the inhibitory effect upon carbamoylation of this residue by dithiocarbamates. To investigate the role of this cysteine, we substituted alanine-253 on zebrafish 11β-HSD2 by a cysteine. Mutant A253C was well expressed and functionally intact despite approximately twofold lower $_{app}V_{max}$ than wild-type 11β-HSD2. We then compared the thiram-dependent inhibition of 11β-HSD2 zebrafish wild-type and mutant A253C with human wild-type and mutant C264S. Insertion of the cysteine in the zebrafish enzyme led to a ten times higher sensitivity toward thiram (IC_{50} 1.3 ± 0.1 μM). In contrast, substitution of cysteine-264 by serine rendered the human enzyme relatively resistant to thiram, with an over 100 times higher IC_{50} of 12.6 ± 1.9 μM.

3.3. Confirmation of the role of cysteine-264 by N-ethylmaleimide inhibition

The effect of the sulfhydryl modifying agent N-ethylmaleimide (NEM) on human 11β-HSD2 wild-type and mutant C264S was studied (Fig. 2). Estimated IC_{50} values of 1 μM and 10 μM, respectively, were obtained for the wild-type and mutant enzyme. As observed for dithiocarbamates (Atanasov et al., 2003), pre-incubation of 11β-HSD2 with NEM enhanced the inhibitory effect (not shown), in line

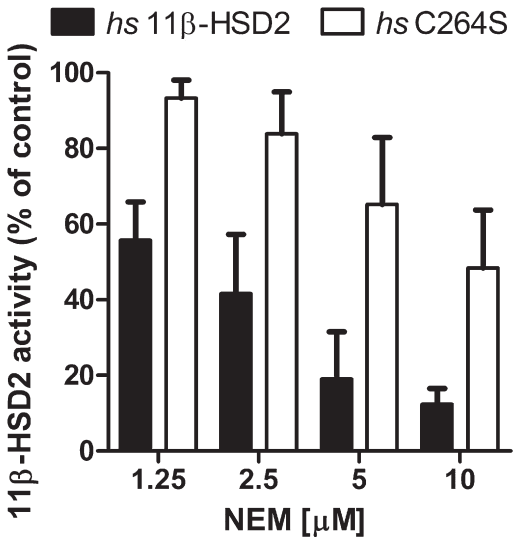

Fig. 2. Inhibition of human 11β-HSD2 wild-type and mutant C264S by N-ethylmaleimide. Lysates of cells expressing human 11β-HSD2 wild-type (black bars) or mutant C264S (white bars) were simultaneously incubated with cortisol (50 nM) and N-ethylmaleimide (NEM), followed by determination of cortisone formation. Data were normalized to vehicle control (0.05% DMSO) and represent mean ± SD from four independent experiments.

with the proposed covalent modification of catalytically relevant sulfhydryl groups by this chemical.

3.4. Effect of various organotins on human and zebrafish 11β-HSD2

Organotins can interfere with enzyme function by reversible interactions with sulfhydryl groups, and we previously reported the inhibition of 11β-HSD2 by some organotins (Atanasov et al., 2005). Therefore, we compared the effects of organotins on cortisol oxidation by human and zebrafish 11β-HSD2 (Fig. 3). The organotins DBT, TBT, DPT and TPT completely abolished the activity of human

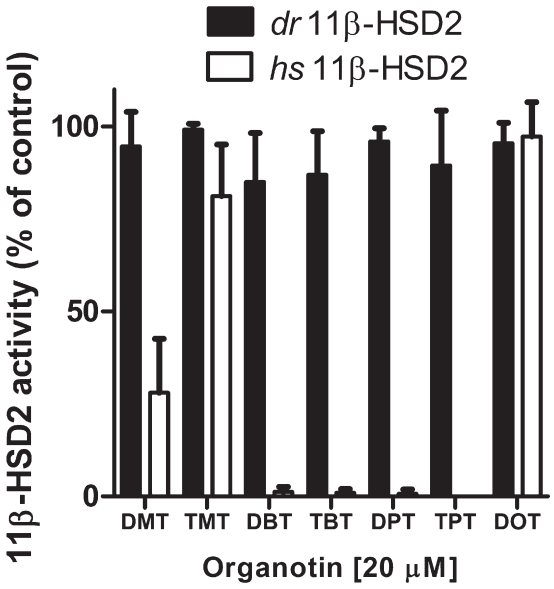

Fig. 3. Effect of various organotins on human and zebrafish 11β-HSD2 activity. Human (white bars) and zebrafish 11β-HSD2 (black bars) activity was measured with 50 nM cortisol as substrate in the presence of vehicle (0.05% DMSO) or 20 μM of the corresponding organotin for 10 min at 37 °C using cell lysates. Data were normalized to vehicle control and represent mean ± SD from three independent experiments.

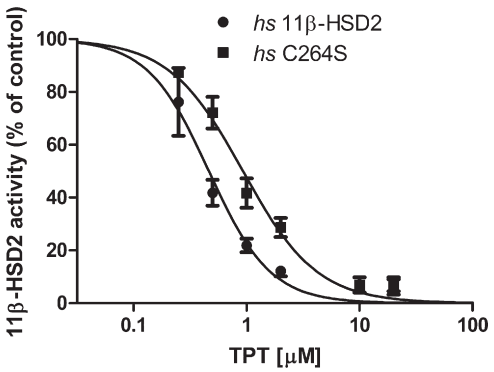

Fig. 4. Inhibition of human 11β-HSD2 wild-type and mutant C264S activity by TPT. The concentration-dependent inhibition of human 11β-HSD2 wild-type and mutant C264S was determined in cell lysates that were simultaneously incubated with 50 nM cortisol and the concentration of TPT indicated. Data were normalized to vehicle control (0.05% DMSO) and represent mean ± SD from three independent experiments.

11β-HSD2 at 20 μM, in line with our earlier study. While DMT was a weak inhibitor with 25% remaining activity at 20 μM, TMT and DOT did not affect the activity of human 11β-HSD2. Interestingly, the zebrafish enzyme was not affected by any of the organotins tested at concentrations up to 20 μM, demonstrating the lower sensitivity of the zebrafish compared with the human enzyme toward organotins.

In our earlier study, we observed an approximately twofold weaker inhibition by TBT of mutant C264S compared with human 11β-HSD2 wild-type enzyme (Atanasov et al., 2005). Here, we assessed whether other organotins also show this effect. Surprisingly, substitution of C264S did not affect inhibition of human 11β-HSD2 by DBT and DPT (not shown). We observed only for TPT a two times weaker inhibition of the mutant C264S (IC_{50} 0.95 ± 0.25 μM) compared with the wild-type enzyme (IC_{50} 0.38 ± 0.12 μM) (Fig. 4).

3.5. Inhibition of human 11β-HSD2 wild-type and mutant C264S by cadmium

Recent reports suggested that cadmium might inhibit 11β-HSD2 expression and/or activity (Ronco et al., 2010; Yang et al., 2006); however, the direct effect of cadmium on 11β-HSD2 activity has not been determined. Here, we incubated lysates expressing human 11β-HSD2 wild-type or mutant C264S with increasing concentrations of cadmium and observed an almost complete inhibition at 5 μM (Fig. 5). Only weak inhibition was seen at 2 μM. The fraction of bound and unbound cadmium was not determined because there was no obvious difference in the inhibition of wild-type and mutant enzymes. Cadmium-dependent inhibition was therefore not further studied.

4. Discussion

In a previous study, we reported on the inhibition of human 11β-HSD2 by dithiocarbamates, with thiram as the most potent inhibitor (Atanasov et al., 2003). Because mutation of cysteine-90 in the cofactor binding pocket resulted in a complete loss of enzyme activity, we postulated that dithiocarbamates might inhibit 11β-HSD2 by carbamoylation of cysteine-90, thereby preventing NAD^+ to bind. Zebrafish 11β-HSD2 also has a cysteine at the analogous position in the cofactor binding site (cysteine-79, see Fig. S2); therefore, we hypothesized that zebrafish 11β-HSD2 would exhibit a similarly high sensitivity to inhibition by dithiocarbamates and other chemicals interacting with sulfhydryl groups. However, as shown in the present study, the dithiocarbamate

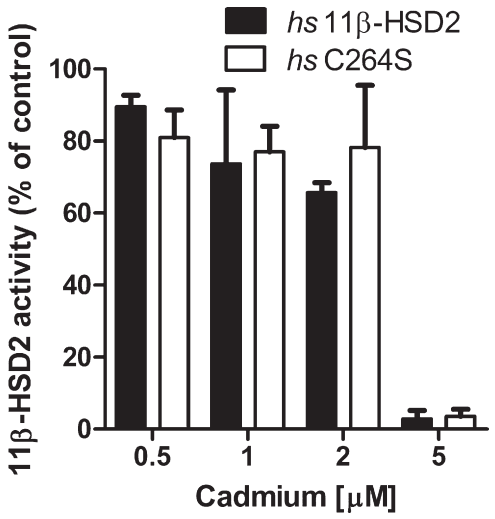

Fig. 5. Inhibition of human 11β-HSD2 wild-type and mutant C264S activity by cadmium. Lysates expressing human 11β-HSD2 wild-type and mutant C264S were simultaneously incubated for 10 min at 37 °C with 50 nM cortisol and various concentrations of cadmium chloride, followed by determination of cortisone formation. Data were normalized to vehicle control (0.05% DMSO) and represent mean ± SD from three independent experiments.

thiram exerts only a weak inhibitory effect on zebrafish 11β-HSD2. Thus, we conclude that the cysteine residue in the cofactor binding site seems to be essential for proper folding and enzyme activity but plays a minor role in the sensitivity to sulfhydryl modifying agents.

The lack of a cysteine in the substrate binding pocket of zebrafish 11β-HSD2, which can form stabilizing interactions with the 3-carbonyl on the steroid substrate, provides an explanation for the loss of inhibition by thiram. The increased sensitivity to thiram of the zebrafish mutant A253C emphasizes the importance of a cysteine residue in the substrate binding pocket of 11β-HSD2. Based on the observed weak inhibition of zebrafish 11β-HSD2 by thiram, it is unlikely that impaired glucocorticoid inactivation or 11-ketotestosterone formation contributes significantly to thiram-induced disturbances during zebrafish development such as notochord distortions (Teraoka et al., 2006) or craniofacial abnormalities (van Boxtel et al., 2010).

Covalent carbamoylation of cysteine-264 on human 11β-HSD2 upon incubation with thiram is expected to cause steric hindrance that prevents substrate binding. The dramatic loss of inhibition by thiram of mutant C264S suggests that cysteine-264 is the major site on human 11β-HSD2 for inhibition by dithiocarbamates.

The decreased inhibitory effects on human 11β-HSD2 mutant C264S by the tri-organotins TBT and TPT but not the di-organotins DMT, DBT and DPT suggest that the sulfhydryl group on cysteine-264 forms stabilizing interactions with tri- but not di-organotins, and that cysteine-264 plays a minor role in the inhibition of human 11β-HSD2 by di-organotins.

The major fish androgen 11-ketotestosterone activates androgen receptor transcriptional activity with comparable potency as testosterone, whereas 11β-hydroxytestosterone is far less potent (Yazawa et al., 2008). Therefore, in fish, inhibition of 11β-HSD2 is expected to show anti-androgenic effects. Our findings that none of the organotins tested inhibited the zebrafish enzyme are in line with reports on the association of the organotins TBT and TPT with androgenic effects and the cause of imposex in marine species (Birchenough et al., 2002; Castro et al., 2012; Matthiessen and Gibbs, 1998; Stange et al., 2012). TBT- and TPT-induced imposex, developmental disturbances and impaired cell differentiation may be caused, at least in part, by activation of retinoid X receptors (RXR) and peroxisome-proliferation activated receptors (PPARs) (Grun and Blumberg, 2006; Grun et al., 2006; Nakanishi et al., 2005; Stange et al., 2012).

Our results reveal significant species-specific differences of 11β-HSD2 in the substrate preference and sensitivity to environmental xenobiotics. Whereas the zebrafish enzyme is not inhibited by organotins and is relatively resistant to sulfhydryl modifying agents, human 11β-HSD2 is inhibited by several organotins and is highly sensitive to dithiocarbamates. Thus, 11β-HSD2 inhibition by these chemicals may be toxicologically relevant for humans but not fish.

Prenatal and perinatal exposure to elevated glucocorticoid concentrations has been associated with reduced birth weights and an increased susceptibility to metabolic and cardiovascular diseases later in life (Benediktsson et al., 1993; Reinisch et al., 1978; Seckl and Holmes, 2007). 11β-HSD2 is highly expressed in the syncythiotrophoblast at the site of the maternal-fetal exchange (Krozowski et al., 1995) and has a pivotal role throughout pregnancy to decrease fetal cortisol exposure (Edwards et al., 1993). Importantly, prenatal treatment with the 11β-HSD2 inhibitor carbenoxolone resulted in reduced birth weights, increased anxious behavior and enhanced secretion of corticotrophin-releasing hormone (Welberg et al., 2000). Evidence from 11β-HSD2-deficient mice indicated an association of reduced placental weight with a restricted increase in fetal vessel density in the final period of pregnancy (Wyrwoll et al., 2009). The diminished placental vascularization and the resulting impaired placental transport of nutrients were proposed to be causal for the observed restricted fetal growth. Organotins and dithiocarbamates were reported to efficiently penetrate the fetal-placental barrier (Adeeko et al., 2003; Cooke et al., 2004; Guven et al., 1998). Importantly, lower birth weights and edema formation were reported in the litter of pregnant rats that were treated with dithiocarbamates (Guven et al., 1998) and organotins (Adeeko et al., 2003; Cooke et al., 2004; Grote et al., 2007), suggesting elevated glucocorticoids due to 11β-HSD2 inhibition as a potential mode of action.

Reduced birth weights were also observed in the off-spring of pregnant rats treated with cadmium (Ronco et al., 2009). These rats had reduced serum testosterone levels (Ji et al., 2011). It was proposed that high levels of glucocorticoids, as a result of 11β-HSD2 inhibition, lower testosterone levels (Ge et al., 2005; Ma et al., 2011). Previous studies in humans indicated that newborns delivered from mothers who smoked during pregnancy had reduced birth weight, which was highly correlated with placental levels of cadmium, one of the toxic compounds of tobacco smoke (Ronco et al., 2005). These observations suggest 11β-HSD2 inhibition as a potential mechanism for the fetal developmental toxicity of dithiocarbamates, organotins and cadmium.

There is a lack of studies on concentrations of thiram and other dithiocarbamate pesticides in a larger human population. Although environmental concentrations of thiram are lower than the concentrations used in the present study, the additive inhibitory effects of dithiocarbamates and their suicide inhibition of 11β-HSD2 need to be taken into account. Thiram-induced toxicity is especially relevant for agricultural workers who are exposed to high concentrations.

Despite low concentrations of organotins in water, significant bioaccumulation has been observed in several marine species (Liu et al., 2006; López-Serrano Oliver et al., 2011; Wang et al., 2010), and it was shown that organotins enter the human food chain (Rantakokko et al., 2008). In addition to consumption of seafood, humans can be exposed to organotins from leaching of polyvinyl chloride water pipes and food packing material (Atanasov et al., 2005; Okoro et al., 2011; Sadiki and Williams, 1999). In human and wildlife, organotin concentrations in serum ranging from 10 to 400 nM were measured (Kannan et al., 1999; Nielsen and Strand,

2002; Takahashi et al., 1999). In lipid-rich tissues even higher concentrations may be reached.

Thus, inhibition of placental 11β-HSD2 by the compounds investigated in the present work should be considered for risk assessment since several animal studies indicate that 11β-HSD2 inhibition during pregnancy causes irreversible changes in fetal development that lead to a higher risk for cardiovascular and metabolic disease later in life (Murphy et al., 2002; Seckl and Holmes, 2007; Shams et al., 1998; Welberg et al., 2005). Further studies in vivo will need to address the impact of sulfhydryl modifying agents on 11β-HSD2 activity, especially under conditions of oxidative stress and glutathione depletion.

Conflict of interest statement

The authors declare that there are no conflicts of interest.

Acknowledgements

This work was supported by the Swiss National Science Foundation (PDFMP3_127330). A.O. has a Chair for Molecular and Systems Toxicology by the Novartis Research Foundation. We thank Dr. Jerzy Adamski, Helmholtz Zentrum Munich, Germany, for providing the ZF-4 cell line.

Appendix A. Supplementary data

Supplementary data associated with this article can be found, in the online version, at http://dx.doi.org/10.1016/j.tox.2012.07.001.

References

Adeeko, A., Li, D., Forsyth, D.S., Casey, V., Cooke, G.M., Barthelemy, J., Cyr, D.G., Trasler, J.M., Robaire, B., Hales, B.F., 2003. Effects of in utero tributyltin chloride exposure in the rat on pregnancy outcome. Toxicol. Sci. 74, 407–415.

Atanasov, A.G., Tam, S., Rocken, J.M., Baker, M.E., Odermatt, A., 2003. Inhibition of 11β-hydroxysteroid dehydrogenase type 2 by dithiocarbamates. Biochem. Biophys. Res. Commun. 308, 257–262.

Atanasov, A.G., Nashev, L.G., Tam, S., Baker, M.E., Odermatt, A., 2005. Organotins disrupt the 11β-hydroxysteroid dehydrogenase type 2-dependent local inactivation of glucocorticoids. Environ. Health Perspect. 113, 1600–1606.

Benediktsson, R., Lindsay, R.S., Noble, J., Seckl, J.R., Edwards, C.R., 1993. Glucocorticoid exposure in utero: new model for adult hypertension. Lancet 341, 339–341.

Birchenough, A.C., Barnes, N., Evans, S.M., Hinz, H., Kronke, I., Moss, C., 2002. A review and assessment of tributyltin contamination in the North Sea, based on surveys of butyltin tissue burdens and imposex/intersex in four species of neogastropods. Mar. Pollut. Bull. 44, 534–543.

Castro, I.B., Rossato, M., Fillmann, G., 2012. Imposex reduction and residual butyltin contamination in southern Brazilian harbors. Environ. Toxicol. Chem. 31, 947–954.

Cooke, G.M., Tryphonas, H., Pulido, O., Caldwell, D., Bondy, G.S., Forsyth, D., 2004. Oral (gavage), in utero and postnatal exposure of Sprague-Dawley rats to low doses of tributyltin chloride. Part 1: toxicology, histopathology and clinical chemistry. Food Chem. Toxicol. 42, 211–220.

Edwards, C.R., Benediktsson, R., Lindsay, R.S., Seckl, J.R., 1993. Dysfunction of placental glucocorticoid barrier: link between fetal environment and adult hypertension? Lancet 341, 355–357.

Ferrari, P., 2010. The role of 11β-hydroxysteroid dehydrogenase type 2 in human hypertension. Biochim. Biophys. Acta 1802, 1178–1187.

Furstenberger, C., Vuorinen, A., Da Cunha, T., Kratschmar, D.V., Saugy, M., Schuster, D., Odermatt, A., 2012. The anabolic androgenic steroid fluoxymesterone inhibits 11β-hydroxysteroid dehydrogenase 2-dependent glucocorticoid inactivation. Toxicol. Sci. 126, 353–361.

Ge, R.S., Dong, Q., Niu, E.M., Sottas, C.M., Hardy, D.O., Catterall, J.F., Latif, S.A., Morris, D.J., Hardy, M.P., 2005. 11β-Hydroxysteroid dehydrogenase 2 in rat leydig cells: its role in blunting glucocorticoid action at physiological levels of substrate. Endocrinology 146, 2657–2664.

Grote, K., Hobler, C., Andrade, A.J., Grande, S.W., Gericke, C., Talsness, C.E., Appel, K.E., Chahoud, I., 2007. Effects of in utero and lactational exposure to triphenyltin chloride on pregnancy outcome and postnatal development in rat offspring. Toxicology 238, 177–185.

Grun, F., Blumberg, B., 2006. Environmental obesogens: organotins and endocrine disruption via nuclear receptor signaling. Endocrinology 147, s50–s55.

Grun, F., Watanabe, H., Zamanian, Z., Maeda, L., Arima, K., Chubacha, R., Gardiner, D.M., Kanno, J., Iguchi, T., Blumberg, B., 2006. Endocrine disrupting organotin compounds are potent inducers of adipogenesis in vertebrates. Mol. Endocrinol. 20, 2141–2155.

Gupta, B., Rani, M., Kumar, R., 2012. Degradation of thiram in water, soil and plants: a study by high-performance liquid chromatography. Biomed. Chromatogr. 26, 69–75.

Guven, K., Deveci, E., Akba, O., Onen, A., de Pomerai, D., 1998. The accumulation and histological effects of organometallic fungicides Propineb and Maneb in the kidneys of fetus and female rats during pregnancy. Toxicol. Lett. 99, 91–98.

Jadhav, S., Bhosale, D., Bhosle, N., 2011. Baseline of organotin pollution in fishes, clams, shrimps, squids and crabs collected from the west coast of India. Mar. Pollut. Bull. 62, 2213–2219.

Ji, Y.-L., Wang, H., Liu, P., Zhao, X.-F., Zhang, Y., Wang, Q., Zhang, H., Zhang, C., Duan, Z.-H., Meng, C., Xu, D.-X., 2011. Effects of maternal cadmium exposure during late pregnant period on testicular steroidogenesis in male offspring. Toxicol. Lett. 205, 69–78.

Jiang, J.Q., Wang, D.S., Senthilkumaran, B., Kobayashi, T., Kobayashi, H.K., Yamaguchi, A., Ge, W., Young, G., Nagahama, Y., 2003. Isolation, characterization and expression of 11β-hydroxysteroid dehydrogenase type 2 cDNAs from the testes of Japanese eel (*Anguilla japonica*) and Nile tilapia (*Oreochromis niloticus*). J. Mol. Endocrinol. 31, 305–315.

Kannan, K., Tanabe, S., Iwata, H., Tatsukawa, R., 1995. Butyltins in muscle and liver of fish collected from certain Asian and Oceanian countries. Environ. Pollut. 90, 279–290.

Kannan, K., Grove, R.A., Senthilkumar, K., Henny, C.J., Giesy, J.P., 1999. Butyltin compounds in river otters (*Lutra canadensis*) from the northwestern United States. Arch. Environ. Contam. Toxicol. 36, 462–468.

Kratschmar, D.V., Vuorinen, A., Da Cunha, T., Wolber, G., Classen-Houben, D., Doblhoff, O., Schuster, D., Odermatt, A., 2011. Characterization of activity and binding mode of glycyrrhetinic acid derivatives inhibiting 11β-hydroxysteroid dehydrogenase type 2. J. Steroid Biochem. Mol. Biol. 125, 129–142.

Krozowski, Z., Albiston, A.L., Obeyesekere, V.R., Andrews, R.K., Smith, R.E., 1995. The human 11β-hydroxysteroid dehydrogenase type II enzyme: comparisons with other species and localization to the distal nephron. J. Steroid Biochem. Mol. Biol. 55, 457–464.

Kusakabe, M., Nakamura, I., Young, G., 2003. 11β-Hydroxysteroid dehydrogenase complementary deoxyribonucleic acid in rainbow trout: cloning, sites of expression, and seasonal changes in gonads. Endocrinology 144, 2534–2545.

Liu, S.-M., Hsia, M.-P., Huang, C.-M., 2006. Accumulation of butyltin compounds in cobia *Rachycentron canadum* raised in offshore aquaculture sites. Sci. Total Environ. 355, 167–175.

López-Serrano Oliver, A., Sanz-Landaluze, J., Muñoz-Olivas, R., Guinea, J., Cámara, C., 2011. Zebrafish larvae as a model for the evaluation of inorganic arsenic and tributyltin bioconcentration. Water Res. 45, 6515–6524.

Ma, X., Lian, Q.Q., Dong, Q., Ge, R.S., 2011. Environmental inhibitors of 11β-hydroxysteroid dehydrogenase type 2. Toxicology 285, 83–89.

Matthiessen, P., Gibbs, P.E., 1998. Critical appraisal of the evidence for tributyltin-mediated endocrine disruption in mollusks. Environ. Toxicol. Chem. 17, 37–43.

Miura, T., Yamauchi, K., Takahashi, H., Nagahama, Y., 1991. Hormonal induction of all stages of spermatogenesis in vitro in the male Japanese eel (*Anguilla japonica*). Proc. Natl. Acad. Sci. U.S.A. 88, 5774–5778.

Murphy, V.E., Zakar, T., Smith, R., Giles, W.B., Gibson, P.G., Clifton, V.L., 2002. Reduced 11β-hydroxysteroid dehydrogenase type 2 activity is associated with decreased birth weight centile in pregnancies complicated by asthma. J. Clin. Endocrinol. Metab. 87, 1660–1668.

Nakanishi, T., Nishikawa, J., Hiromori, Y., Yokoyama, H., Koyanagi, M., Takasuga, S., Ishizaki, J., Watanabe, M., Isa, S., Utoguchi, N., Itoh, N., Kohno, Y., Nishihara, T., Tanaka, K., 2005. Trialkyltin compounds bind retinoid X receptor to alter human placental endocrine functions. Mol. Endocrinol. 19, 2502–2516.

Nielsen, J.B., Strand, J., 2002. Butyltin compounds in human liver. Environ. Res. 88, 129–133.

Odermatt, A., Gumy, C., 2008. Glucocorticoid and mineralocorticoid action: why should we consider influences by environmental chemicals? Biochem. Pharmacol. 76, 1184–1193.

Odermatt, A., Kratschmar, D.V., 2012. Tissue-specific modulation of mineralocorticoid receptor function by 11β-hydroxysteroid dehydrogenases: an overview. Mol. Cell. Endocrinol. 350, 168–186.

Odermatt, A., Arnold, P., Stauffer, A., Frey, B.M., Frey, F.J., 1999. The N-terminal anchor sequences of 11β-hydroxysteroid dehydrogenases determine their orientation in the endoplasmic reticulum membrane. J. Biol. Chem. 274, 28762–28770.

Odermatt, A., Gumy, C., Atanasov, A.G., Dzyakanchuk, A.A., 2006. Disruption of glucocorticoid action by environmental chemicals: potential mechanisms and relevance. J. Steroid Biochem. Mol. Biol. 102, 222–231.

Okoro, H.K., Fatoki, O.S., Adekola, F.A., Ximba, B.J., Snyman, R.G., Opeolu, B., 2011. Human exposure, biomarkers, and fate of organotins in the environment. Rev. Environ. Contam. Toxicol. 213, 27–54.

Rantakokko, P., Turunen, A., Verkasalo, P.K., Kiviranta, H., Männistö, S., Vartiainen, T., 2008. Blood levels of organotin compounds and their relation to fish consumption in Finland. Sci. Total Environ. 399, 90–95.

Reinisch, J.M., Simon, N.G., Karow, W.G., Gandelman, R., 1978. Prenatal exposure to prednisone in humans and animals retards intrauterine growth. Science 202, 436–438.

Ronco, A.M., Arguello, G., Munoz, L., Gras, N., Llanos, M., 2005. Metals content in placentas from moderate cigarette consumers: correlation with newborn birth weight. Biometals 18, 233–241.

Ronco, A.M., Urrutia, M., Montenegro, M., Llanos, M.N., 2009. Cadmium exposure during pregnancy reduces birth weight and increases maternal and foetal glucocorticoids. Toxicol. Lett. 188, 186–191.
Ronco, A.M., Llaguno, E., Epunan, M.J., Llanos, M.N., 2010. Effect of cadmium on cortisol production and 11β-hydroxysteroid dehydrogenase 2 expression by cultured human choriocarcinoma cells (JEG-3). Toxicol. In Vitro 24, 1532–1537.
Sadiki, A.-D., Williams, D.T., 1999. A study on organotin levels in Canadian drinking water distributed through PVC pipesa. Chemosphere 38, 1541–1548.
Seckl, J.R., Holmes, M.C., 2007. Mechanisms of disease: glucocorticoids, their placental metabolism and fetal 'programming' of adult pathophysiology. Nat. Clin. Pract. Endocrinol. Metab. 3, 479–488.
Shams, M., Kilby, M.D., Somerset, D.A., Howie, A.J., Gupta, A., Wood, P.J., Afnan, M., Stewart, P.M., 1998. 11Beta-hydroxysteroid dehydrogenase type 2 in human pregnancy and reduced expression in intrauterine growth restriction. Hum. Reprod. 13, 799–804.
Shi, G., Chen, Z., Teng, J., Bi, C., Zhou, D., Sun, C., Li, Y., Xu, S., 2012. Fluxes, variability and sources of cadmium, lead, arsenic and mercury in dry atmospheric depositions in urban, suburban and rural areas. Environ. Res. 113, 28–32.
Stange, D., Sieratowicz, A., Oehlmann, J., 2012. Imposex development in *Nucella lapillus*—evidence for the involvement of retinoid X receptor and androgen signalling pathways in vivo. Aquat. Toxicol. 106–107, 20–24.
Takahashi, S., Mukai, H., Tanabe, S., Sakayama, K., Miyazaki, T., Masuno, H., 1999. Butyltin residues in livers of humans and wild terrestrial mammals and in plastic products. Environ. Pollut. 106, 213–218.
Teraoka, H., Urakawa, S., Nanba, S., Nagai, Y., Dong, W., Imagawa, T., Tanguay, R.L., Svoboda, K., Handley-Goldstone, H.M., Stegeman, J.J., Hiraga, T., 2006. Muscular contractions in the zebrafish embryo are necessary to reveal thiuram-induced notochord distortions. Toxicol. Appl. Pharmacol. 212, 24–34.
van Boxtel, A.L., Pieterse, B., Cenijn, P., Kamstra, J.H., Brouwer, A., van Wieringen, W., de Boer, J., Legler, J., 2010. Dithiocarbamates induce craniofacial abnormalities and downregulate sox9a during zebrafish development. Toxicol. Sci. 117, 209–217.
Vettorazzi, G., Almeida, W.F., Burin, G.J., Jaeger, R.B., Puga, F.R., Rahde, A.F., Reyes, F.G., Schvartsman, S., 1995. International safety assessment of pesticides: dithiocarbamate pesticides, ETU, and PTU—a review and update. Teratog. Carcinog. Mutagen. 15, 313–337.
Wang, X., Fang, C., Hong, H., Wang, W.-X., 2010. Gender differences in TBT accumulation and transformation in *Thais clavigera* after aqueous and dietary exposure. Aquat. Toxicol. 99, 413–422.
Welberg, L.A., Seckl, J.R., Holmes, M.C., 2000. Inhibition of 11β-hydroxysteroid dehydrogenase, the foeto-placental barrier to maternal glucocorticoids, permanently programs amygdala GR mRNA expression and anxiety-like behaviour in the offspring. Eur. J. Neurosci. 12, 1047–1054.
Welberg, L.A., Thrivikraman, K.V., Plotsky, P.M., 2005. Chronic maternal stress inhibits the capacity to up-regulate placental 11β-hydroxysteroid dehydrogenase type 2 activity. J. Endocrinol. 186, R7–R12.
Wyrwoll, C.S., Seckl, J.R., Holmes, M.C., 2009. Altered placental function of 11β-hydroxysteroid dehydrogenase 2 knockout mice. Endocrinology 150, 1287–1293.
Yang, K., Julan, L., Rubio, F., Sharma, A., Guan, H., 2006. Cadmium reduces 11β-hydroxysteroid dehydrogenase type 2 activity and expression in human placental trophoblast cells. Am. J. Physiol. Endocrinol. Metab. 290, E135–E142.
Yazawa, T., Uesaka, M., Inaoka, Y., Mizutani, T., Sekiguchi, T., Kajitani, T., Kitano, T., Umezawa, A., Miyamoto, K., 2008. Cyp11b1 is induced in the murine gonad by luteinizing hormone/human chorionic gonadotropin and involved in the production of 11-ketotestosterone, a major fish androgen: conservation and evolution of the androgen metabolic pathway. Endocrinology 149, 1786–1792.

Paper Draft: Absence of 11-oxosteroid reductase activity in the model organism zebrafish

Absence of 11-oxosteroid reductase activity in the model organism zebrafish

Arne Meyer[1], Benjamin Weger[2], Janina Tokarz[3], Thierry Da Cunha[1], Jerzy Adamski[3], Thomas Dickmeis[2] and Alex Odermatt[1]

[1]Swiss Center for Applied Human Toxicology and Division of Molecular and Systems Toxicology, Department of Pharmaceutical Sciences, University of Basel, Klingelbergstrasse 50, 4056 Basel, Switzerland

[2]Karlsruhe Institute of Technology (KIT), Institute of Toxicology and Genetics, Hermann-von-Helmholtz-Platz 1, Bau 439, 76344 Eggenstein-Leopoldshafen, Germany

[3]Helmholtz Zentrum München, German Research Center for Environmental Health, Institute of Experimental Genetics, Genome Analysis Center, Ingolstaedter Landstrasse 1, 85764 Neuherberg, Germany

Correspondence to:

Dr. Alex Odermatt, Division of Molecular and Systems Toxicology, Department of Pharmaceutical Sciences, University of Basel, Klingelbergstrasse 50, CH-4056 Basel, Switzerland

Phone: +41 61 267 1530, Fax: +41 61 267 1515, E-mail: alex.odermatt@unibas.ch

Abstract

The zebrafish is a widely used model organism in various research fields, with increasing use in the field of endocrinology. In humans, 11β-hydroxysteroid dehydrogenase type 1 (11β-HSD1) plays an important role in glucocorticoid activation by converting inactive cortisone to active cortisol and the synthetic prednisone to its active metabolite prednisolone. Activated glucocorticoids are able to transactivate the glucocorticoid receptor (GR) which results in the transcription of GR target genes. 11β-hydroxysteroid dehydrogenase type 2 (11β-HSD2) can be seen as a counterpart to 11β-HSD1 as it inactivates the 11-hydroxylated glucocorticoids and prevents GR activation. Interestingly, although cortisol is an important stress hormone in zebrafish, the zebrafish has no gene encoding 11β-HSD1. We have previously shown that zebrafish 11β-HSD2 is responsible for the conversion of cortisol to cortisone and 11β-hydroxytestosterone to 11-ketotestosterone, the main androgen in fish. A phylogenetic analysis identified two possible ancestors of 11β-HSD1 in zebrafish, 11β-HSD3a and 11β-HSD3b. We tested whether these two enzymes possess the ability to reduce cortisone to cortisol. Furthermore, the metabolism of cortisone in zebrafish microsomes was analysed. We found no conversion of cortisone to cortisol either by the two possible ancestors of 11β-HSD1, nor by zebrafish microsomes. Furthermore, zebrafish microsomes did not reduce 11-ketotestosterone. Our results suggest the absence of 11-oxosteroid reductase activity in zebrafish, which must be taken into account when studying the metabolism and/or effects of glucocorticoids and androgens in zebrafish.

1. Introduction

The increasing use of the zebrafish (*danio rerio*) as a model organism in various applications has been highlighted in a series of recent reviews [1-8]. The zebrafish is a small tropical fresh water fish, which is currently, with the help of advanced genetic techniques, being used to establish new models for neurodegeneration, depression and cancer. Furthermore, it is used to study embryonic development, angiogenesis, toxicity of nanomaterials, to assess drug-induced toxicity by high-throughput screening and, as proposed by Dickmeis *et al*., to screen for compounds that might impair glucocorticoid stress hormone signaling [1-9]. The advantages of using zebrafish as an *in vivo* model include their relatively low maintenance costs, high fecundity, and optical transparency during the development of the embryo and larvae, which allows unrestricted visualization of these processes [1]. Furthermore, the zebrafish genome has a high degree of homology with the human genome, and both species have a similar number of chromosomes [10].

A plethora of physiological processes are controlled by corticosteroids. Corticosteroids can be divided into the mineralocorticoids and the glucocorticoids, which are able to transactivate the mineralocorticoid receptor (MR) and glucocorticoid receptor (GR) respectively, and regulate their transcriptional activities [11]. It is believed that these receptors evolved from a common ancestor, the corticosteroid receptor, by a whole genome duplication event in the chondrichthyes. It is hypothesized that a second whole genome duplication event occurred in the teleost lineage, resulting in two genes encoding GR and two genes encoding MR, whereby the second gene coding for the MR was lost in the evolutionary process [12-15]. The fish MR has been shown to play a role in electrolyte balance [16], and can be activated by cortisol, aldosterone and deoxycorticosterone [12, 17-19], although aldosterone is absent in teleost fish [14]. It has been

shown that the fish MR, like the human MR, is activated by cortisol at lower concentrations than needed for GR transactivation [17, 19, 20]. It has been shown that 11β-hydroxysteroid dehydrogenase type 2 (11β-HSD2) is responsible for converting cortisol into cortisone and therefore prevents MR activation by cortisol [21]. We have shown recently that zebrafish 11β-HSD2 converts cortisol to cortisone, so it can be assumed that *dr*11β-HSD2 also protects the MR from transactivation by cortisol [22]. Additionally, 11β-HSD2 in fish is essential for the conversion of 11β-hydroxytestosterone to 11-ketotestosterone, the main androgen in fish [22-25].

The zebrafish has been proposed as a good model to study glucocorticoid-mediated endocrine disorders [7, 8, 26, 27], because the zebrafish has only one GR gene [27] as seen in mammals, compared to other teleost species where multiple GR genes are found [12-14, 19]. For the zebrafish as in mammals there are two splice-variants described, GRα and GRβ [28]. It has been shown that the GR together with cortisol regulates a multitude of physiological processes and plays a key role in the regulation of inflammation, insulin resistance, obesity, hypertension and hyperglycemia [29]. In fish it has been demonstrated that cortisol is the major stress hormone and plays a role in the regulation of metabolic processes and inflammation [27, 30] as well as in circadian cell cycle rhythm [31].

Crucial for GR activation is 11β-hydroxysteroid dehydrogenase type 1 (11β-HSD1), an enzyme converting the inactive glucocorticoid cortisone to the active glucocorticoid cortisol, which binds to the GR and leads to its translocation into the nucleus and transcription of GR target genes [32, 33]. In humans 11β-HSD1 together with 11β-HSD2 plays an important role in controlling the ratio of the inactive cortisone and the active glucocorticoid cortisol. Furthermore, 11β-HSD1 is essential for the activation of the synthetic glucocorticoid prednisone to its active metabolite prednisolone.

It is known that cortisol is the main glucocorticoid acting on teleost fish GR [12, 13, 34]. Interestingly, the zebrafish has no gene coding for 11β-HSD1, but it is has been speculated through phylogenetic analysis that 11β-HSD3a is the ancestor of 11β-HSD1 [35, 36] and may therefore reduce cortisone [36] and consecutively activate the GR and plays a role to maintain the balance between active and inactive glucocorticoids. On the other hand, it was shown by Huang *et al*. that human 11β-HSD3 (SCDR10B) can oxidize cortisol; however, only at very high substrate concentrations [37]. Recently, a novel isoform of 11β-HSD3a has been identified, called 11β-HSD3b, also known as 11β-HSD1-like-protein-like. It is widely assumed that either 11β-HSD3a or 11β-HSD3b could mimic the function of 11β-HSD1 to reduce cortisone to cortisol [35, 36], although this has never been shown. Nevertheless, based on the results of the phylogenetic analysis and the observation by Huang *et al*., it is generally accepted that a cortisone reductase activity exists in fish [37].

The increasing use of zebrafish as a model organism for endocrine studies [38] and the lack of knowledge on cortisone reduction in zebrafish, led us to investigate the role of the two ancestors of 11β-HSD1. Therefore, we tested whether cortisone is reduced to cortisol by *dr*11β-HSD3a and/or *dr*11β-HSD3b. We also employed zebrafish microsomes and homogenates to examine cortisone metabolism in zebrafish. Furthermore, we tested whether cortisone is activated to cortisol *in vivo* with the help of the GRIZLY assay (**G**lucocorticoid **R**esponsive ***I****n vivo* **Z**ebrafish **L**uciferase activit**Y**) [9].

2. Results

In a first experiment the two proposed ancestors of 11β-HSD1, *dr*11bHSD3a and *dr*11bHSD3b were tested in intact HEK-293 cells at 37°C (data not shown). We could not detect any cortisone reductase activity and therefore we repeated this experiment at 28°C. We could not detect any cortisone reductase activity (data not shown) and therefore, *dr*11bHSD3a and *dr*11bHSD3b were transiently transfected in *zf*4 cells at 28°C. Both enzymes showed no 11-oxosteroid reductase activity with cortisone. These experiments were performed in both intact cells and cell lysates (Table 1).

Since 11β-HSD1 did not show a reductase activity we wanted to test if *dr*11β-HSD2 had 11-oxosteroid reductase activity in zebrafish. We tested the cell lysates of transiently transfected *zf*4 cells, whether *dr*11β-HSD2 might be responsible for the reduction of cortisone by supplying NADH as a cofactor (Table 1). We did not observe any reduction of cortisone.

The results led us to investigate whether any 11-oxosteroid reductase activity can be observed in zebrafish microsomes. We were able to demonstrate that zebrafish microsomes are able to convert 11β-hydroxytestosterone to 11-ketotestosterone and cortisol to cortisone upon incubation with the cofactor NAD^+ (Table 1). We tested the reverse reaction with NADH and NADPH but could not observe any reduction of cortisone to cortisol or 11-ketotestosterone to 11β-hydroxytestosterone (Table 1). We observed that cortisone is not reduced to cortisol, but to 20β-hydroxycortisone as described recently by Tokarz *et al*. [39], using NADPH as cofactor (Figure 1). We stimulated the formation of 20β-hydroxycortisone upon incubation with NADPH and the detergent Brij®58. Additionally, we showed that 20β-hydroxycortisone was formed following the incubation of microsomes with glucose-6-phosphate (G6P) (Figure 1).

In order to translate our *in vitro* findings into an *in vivo* model, we performed the GRIZLY assay in 5 days post fertilization larvae to examine whether cortisone is metabolized to cortisol and can then activate the GR. Cortisol was able to activate the GR by glucocorticoid response elements (GRE) driven luciferase expression, whereas cortisone following a 24 h incubation at concentrations up to 80 μM did not show any effect on the GR-dependent reporter. These results indicate that 5 days post fertilization zebrafish larvae have no enzyme to reduce cortisone to cortisol, or any other steroid hormone that can activate the GR [9].

3. Discussion

The zebrafish does not have the gene encoding 11β-HSD1, and it was assumed that one of the ancestors of 11β-HSD1 would mimic its function and reduce cortisone to cortisol [35, 36]. Our results indicate that the ancestors of 11β-HSD1 are not able to reduce cortisone. We tested *dr*11β-HSD3a and *dr*11β-HSD3b in intact cells and cell lysates and could not detect any conversion of cortisone. Therefore, the role of these enzymes still remains unclear. Additionally, we tested whether *dr*11β-HSD2 might reduce cortisone. Similar observations have been made with *hs*11β-HSD1, a bidirectional enzyme, able to catalyze the cortisone reduction and cortisol oxidation the latter only under non-physiological conditions [40]. Our current results show that zebrafish 11β-HSD2 is not a bidirectional enzyme, comparable to the *hs*11β-HSD2, which also does not reduce cortisone.

Our results in zebrafish microsomes and our *in vivo* system show an important species-specific difference in cortisone metabolism. Cortisone is not metabolized to cortisol by zebrafish microsomes. Zebrafish larvae at 5 days post fertilization are not able to metabolize cortisone into cortisol or any other compound with GR activating properties, although it has been shown that these larvae already possess a functional hypothalamic pituitary adrenal (HPA) axis and respond to stress by increasing glucocorticoid production [8, 26, 30]. We conclude that there is a considerable difference between human and zebrafish in the regulation of the balance between inactive and active glucocorticoids. In humans the balance is controlled tightly by the interplay of 11β-HSD1 and 11β-HSD2 [41]. Cortisol can be locally inactivated in both species, but once cortisol is inactivated it cannot be regenerated in fish as we could not identify any 11-oxosteroid reductase activity. In contrast, in humans, cortisone can be reactivated by 11β-HSD1-dependent

conversion to cortisol. It remains unclear whether the teleost species possess another mechanism which involves different glucocorticoids and enzymes. Until now it was assumed that fish, like humans, control the balance of cortisone and cortisol through 11β-HSD1 and 11β-HSD2. We showed that our microsomal incubations with cortisone led solely to the formation of 20β-hydroxycortisone. This observation is in line with a novel pathway of cortisol catabolism in fish recently proposed by Tokarz *et al*., suggesting that cortisol is consecutively transformed by 11β-HSD2 and 20β-hydroxysteroid dehydrogenase type 2 (20β-HSD2) to 20β-hydroxycortisone. The authors suggest that a) the two enzymes act as a metabolic switch, since 20β-HSD2 irreversibly reduces the amount of available cortisone for the reverse reaction to cortisol by 11β-HSD3 and b) that 20β-hydroxycortisone can be excreted either directly or after glucuronidation or sulfatation [39]. Our results indicate that 20β-HSD type 2 will not act as a metabolic switch, since the reduction of cortisone to cortisol does not occur in zebrafish.

We were able to stimulate the formation of 20β-hydroxycortisone upon incubation with Brij®58. Moreover, we observed the conversion of cortisone to 20β-hydroxycortisone by sole incubation with G6P. These two finding suggest that the enzyme responsible for 20β-hydroxycortisone formation might face the lumen of the endoplasmic reticulum (ER). Detergents permeabilize the ER membrane allowing luminal enzymes greater access to cofactors and therefore enhance the activity of luminal enzymes. The formation of 20β-hydroxycortisone stimulated by G6P suggests the involvement of hexose-6-phosphate dehydrogenase (H6PDH). H6PDH is an ER luminal enzyme which converts $NADP^+$ to NADPH by using G6P, and has been described to stimulate 11β-HSD1, which is an ER luminal enzyme [42].

Our microsomal incubations show that 11-ketotestosterone, the main androgen in fish, is not converted to 11β-hydroxytestosterone, however we were able to measure the reaction of 11β-

hydroxytestosterone to 11-ketotestosterone. This provides a possible explanation why 11-oxosteroid reductase activity is absent in zebrafish, because the presence of an enzyme in zebrafish with 11-oxosteroid reductase activity might convert the main androgen 11-ketotestosterone to its inactive metabolite 11β-hydroxytestosterone.

To our knowledge this is the first study to show, that the ancestors of 11β-HSD1 in zebrafish, 11β-HSD3a and 11β-HSD3b do not reduce cortisone. We suggest that 11-oxoreductase activity is absent in teleost fish. We believe that the zebrafish is an interesting model for endocrinology, especially in glucocorticoid related research topics, because the zebrafish has only one GR gene [27]. However, it must be taken into account that 11-oxosteroid reductase activity is absent in zebrafish. There are clearly species-specific differences in cortisol metabolism, and it remains to be shown whether the zebrafish possesses a system to enzymatically modify the ratio of inactive to active glucocorticoids. Our results would suggest the absence of such a system. These findings must be taken into account when designing experiments and evaluating data obtained related to glucocorticoid research with the model organism zebrafish.

4. Materials and Methods

4.1. Materials

Steroids were purchased from Steraloids (Newport, RI), all other chemicals and cell culture medium from Sigma–Aldrich Chemie GmbH (Buchs, Switzerland). The solvents were of analytical and high performance liquid chromatography grade and the reagents of the highest grade available. Substrates were dissolved in methanol and stored as 10 mM stock solution at −20°C.

4.2. Construction of expression plasmids

The expression plasmid for zebrafish 11β-HSD3a was constructed by A. Odermatt and A. Dzyakonchuk and was described in the PhD thesis of A. Dzyakonchuk. For the construction of the zebrafish 11β-HSD3b expression plasmid, mRNA was isolated from a male whole zebrafish. The mRNA was transcribed to DNA using SuperScript® II from Invitrogen (Carlsbad, CA) according to the manufacturer's manual. The cDNA was amplified by PCR using an oligonucleotide at the start codon to introduce a BamHI endonuclease restriction site and a Kozak consensus sequence (5' - ATA GGA TCC GCC ATG AAG GTG CTT TTC GGG GTG-3') and an oligonucleotide at the stop codon either to add an XbaI endonuclease restriction site (5'- GAA TCT AGA TTA CGG CCC AGA CGA CAG TTT GC - 3') or to attach a FLAG-epitope followed by the stop codon and an XbaI endonuclease restriction site (5' - GAA TCT AGA TTA CTT GTC ATC GTC GTC CTT GTA GTC CAT AGA ACC CGG CCC AGA CGA CAG TTT

GC - 3'). The PCR product was inserted into the BamHI–XbaI sites of the pcDNA3.1 vector. The selected clones used in this study were sequence verified.

4.3. Cell culture, transfection and expression analysis

Human embryonic kidney cells (HEK-293) were cultivated in Dulbecco's modified Eagle medium (DMEM) containing 4.5 g/L glucose (D5796 Sigma-Aldrich), 10% fetal bovine serum, 100 U/ml penicillin, 0.1 mg/ml streptomycin, 1 × MEM non-essential amino acids and 10 mM HEPES buffer, pH 7.4. Cells were incubated at 37°C in a humidified 5% CO_2 atmosphere. Zebrafish embryonic fibroblast cells *zf*4 (kindly provided by Dr. Jerzy Adamski, Helmholtz Zentrum, Munich, Germany) were cultivated in DMEM:F12 (D8437 Sigma–Aldrich), supplemented with 10% fetal bovine serum, 100 U/mL penicillin and 0.1 mg/mL streptomycin. These cells were maintained at 28°C in a humidified 5% CO_2 atmosphere.

Cells were transiently transfected with *dr*11β-HSD3a, *dr*11β-HSD3b, *hs*11β-HSD1 [43] and *dr*11β-HSD2 [22]. HEK-293 cells were transfected using the calcium phosphate transfection method [44], transfection efficiency was approximately 20%. *Zf*4 cells were transfected using Fugene HD according to the manufacturer's protocol (Roche Applied Science, Rotkreuz, Switzerland). Transfection efficiency was approximately 25%.

Cells were trypsinized 48 h post transfection, and 5 pellets per 10 cm^2 dish were obtained after 4 min centrifugation at 900 g, the pellets were immediately shock frozen on dry ice and stored at -80°C. The protein concentration was measured with the Pierce BCA protein assay kit (Thermo Fisher Scientific Inc., Rockford, IL, USA) according to the manufacturer's manual. Protein expression was verified by western blot, loading 20 μg of the FLAG-tagged enzymes as described for *dr*11β-HSD2 enzyme [22], using mouse M2 antibody from Sigma-Aldrich Chemie

GmbH (Buchs, Switzerland). Actin was detected by rabbit anti-actin IgG from Santa Cruz Biotechnology Inc. (Santa Cruz, CA, USA). Horseradish peroxidase-conjugated secondary antibodies were used to visualize the bands with Immobilon Western Chemiluminescent HRP substrate from Millipore Corporation (Billerica, MA, USA).

4.4. Cell incubations

HEK-293 cells transiently transfected with *dr*11β-HSD3a, *dr*11β-HSD3b and with *hs*11β-HSD1 as a positive control, as well as *zf*4 cells transiently transfected with *dr*11β-HSD3a, *dr*11β-HSD3b and *dr*11β-HSD2 were incubated as described previously [45]. Briefly, 20'000 of the transfected cells were seeded on a 96 well plate. The medium was changed to charcoal-treated serum-free DMEM, followed by 24 h incubation with 1 µM cortisone or 1 µM cortisol at both 28°C and 37°C. The assay with cell lysates was performed as described previously [22]. Briefly, lysates were incubated at 28°C or 37°C in TS2 buffer (100 mM NaCl, 1 mM EGTA, 1 mM EDTA, 1 mM $MgCl_2$, 250 mM sucrose, 20 mM Tris–HCl, pH 7.4) with 1) 1 µM cortisone supplemented with either 500 µM NADPH or NADH or with 2) 1 µM cortisol supplemented with 500 µM NAD^+ or $NADP^+$. Cell lysates transfected with *dr*11β-HSD2 were incubated with 1) 1 µM cortisone supplemented with 500 µM NADH or with 2) 1 µM cortisol supplemented with 500 µM NAD^+.

Upon termination of the reactions the internal standard (100 nM deuterized d4-cortisol) was added, followed by extraction with 1 mL ethyl acetate. The organic phase was transferred to a new tube, evaporated to dryness and reconstituted in 100 µL methanol and stored at -20°C until analysis by liquid chromatography-tandem mass spectrometry (LC-MS/MS) (section 4.6).

4.5. Determination of microsomal activities

Zebrafish microsomes were prepared by ultracentrifugation as described previously [44]. Briefly, zebrafishes were homogenized using 2 ml of solution A (10 mM imidazole, 0.3 M sucrose, pH 7.0) per 100 mg, using 10 – 12 strokes with a Potter-Elvehjem with PTFE pestle while rotating (220 rpm). Debris and nuclei were removed by two centrifugation steps for 10 min at 1000 x g, the supernatant was centrifuged twice for 10 min at 12'000 x g to remove mitochondria, followed by ultracentrifugation for 1 h at 100'000 x g to obtain microsomes. The pellet was washed with 500 µL per 100 mg solution B (20 mM tris-maleate, 0.6 M potassium chloride, 0.3 M sucrose, pH 7.0) and the ultracentrifugation step was repeated. Afterwards, the pellet was resuspended in 200 µL per 100 mg solution C (10 mM tris-maleate, 0.15 M potassium chloride, 0.25 M sucrose, pH 7.0). The microsomes were then aliquoted and shock frozen on dry ice and stored at -80°C until further use. The concentration of the microsomes was measured with the Pierce BCA protein assay kit (Thermo Fisher Scientific Inc., Rockford, IL, USA) according to the manufacturer's manual.

To determine microsomal metabolism, the zebrafish microsomes (f.c. 1.5 mg/ml) were incubated for 1 h at 28°C in TS2 buffer with 1 µM cortisone or 1 µM 11-ketotestosterone in the presence of 1) 500 µM NADH, 2) 500 µM NADPH, 3) 500 µM NADPH and 0.05 % Brij®58, 4) 1 mM glucose-6-phosphate (G6P). Under the same experimental conditions, 1 µM cortisol or 1 µM 11β-hydroxytestosterone was incubated in the presence of 500 µM NAD^+.

Upon termination of the reactions the internal standard (100 nM deuterized d4-cortisol for cortisone and cortisol, 100 nM deuterized d2-testosterone for 11β-hydroxytestosterone and 11-ketotestosterone) was added, followed by extraction with 1 mL ethyl acetate. The organic phase

was transferred to a new tube, evaporated to dryness and reconstituted in 100 µL methanol and stored at -20°C until analysis by liquid chromatography-tandem mass spectrometry (LC-MS/MS) (section 4.6).

4.6. Liquid chromatography-tandem mass spectrometry settings

An Atlantis T3 column (3 µm, 2.1 × 150 mm, Waters) and an Agilent 1200 Infinity Series chromatograph (Agilent Technologies, Basel, Switzerland) were used for chromatographic separations (HPLC).

The mobile phase consisted of solvent A (95:5, H_2O:ACN (v/v), containing 0.1% formic acid) and solvent B (5:95, H_2O:ACN (v/v), containing 0.1% formic acid), at a total flow rate of 0.4 mL/min. 11β-hydroxytestosterone, 11-ketotestosterone and d2-testosterone were separated using 25% solvent B for 4 min, followed by a linear gradient from 4 to 6 min to reach 100% solvent B, and then 100% solvent B for 2 min. The column was then re-equilibrated with 25% solvent B.

20β-hydroxycortisone, cortisone, cortisol and d4-cortisol were separated using 30% solvent B for 4 min, followed by a linear gradient from 4 to 7 min to reach 40% solvent B, and then 100% solvent B from 7 to 7.5 min. The column was then re-equilibrated with 30% solvent B.

The LC was interfaced to an Agilent 6490 triple quadropole tandem mass spectrometer (MS/MS). The LC-MS/MS system was controlled by Mass Hunter workstation software (version B.01.05). The injection volume of each sample was 10 µL. The mass spectrometer was operated in electrospray ionization (ESI) positive ionization mode, with the source temperature of 350°C, with nebulizer pressure of 20 psi. The capillary voltage was set at 4000 V.

The compounds were analyzed using multiple-reaction monitoring (MRM) and identified by comparing their retention time and mass to charge ratio (*m/z*) with those of authentic standards. The transitions, collision energy and retention time were *m/z* 305.2/121, 20 V, 3.5 min for 11β-hydroxytestosterone; *m/z* 303.1/121, 24 V, 3.3 min for 11-ketotestosterone; and *m/z* 291.3/99, 28 V, 5.6 min for the internal standard d2-testosterone; *m/z* 363/121, 25 V, 3.35 min for 20β-hydroxycortisone; *m/z* 361/163, 25 V, 4.9 min for cortisone, *m/z* 363/121, 25 V, 4.6 min for cortisol; and *m/z* 367/121, 25 V, 4.6 min for the internal standard d4-cortisol.

4.7. GRIZLY assay

The GRIZLY assay was performed by Weger *et al*. as described previously [9].

Acknowledgement

This work was supported by the Swiss National Science Foundation (PDFMP3_127330). A.O. has a Chair for Molecular and Systems Toxicology by the Novartis Research Foundation.

Figure Legends

	cortisone to cortisol	cortisol to cortisone	11-KT to 11β-OHT	11β-OHT to 11-KT
Zebrafish microsomes	No activity	Conversion, qualitative measurement	No activity	Conversion, qualitative measurement
*dr*11β-HSD3a in *zf*4 at 28°C	No activity	No activity	ND	ND
*dr*11β-HSD3b in *zf*4 at 28°C	No activity	No activity	ND	ND
*dr*11β-HSD2 in *zf*4 at 28°C	No activity	0.12 ± 0.023 nmol/mg/h	ND	Conversion described in HEK-293 [22]

ND: not determined

Table 1: Overview of incubations. Incubations were performed as outlined in the Materials and Methods section. Briefly, zebrafish microsomes (f.c. 1.5 mg/ml) were incubated for 1 h at 28°C in TS2 buffer with 1 µM cortisone or 1 µM 11-ketotestosterone (11-KT) in the presence of 1) 500 µM NADH, 2) 500 µM NADPH, 3) 500 µM NADPH and 0.05 % Brij®58, 4) 1 mM glucose-6-phosphate (G6P). Under the same experimental conditions, 1 µM cortisol or 1 µM 11β-hydroxytestosterone (11β-OHT) was incubated in the presence of 500 µM NAD^+.

Cell lysates transiently transfected with *dr*11β-HSD3a or *dr*11β-HSD3b were incubated at 28°C in TS2 buffer with 1) 1 µM cortisone supplemented with either 500 µM NADH or NADPH or with 2) 1 µM cortisol supplemented with 500 µM NAD^+ or $NADP^+$.

Cell lysates transfected with *dr*11β-HSD2 were incubated with 1) 1 µM cortisone supplemented with 500 µM NADH or with 2) 1 µM cortisol supplemented with 500 µM NAD^+.

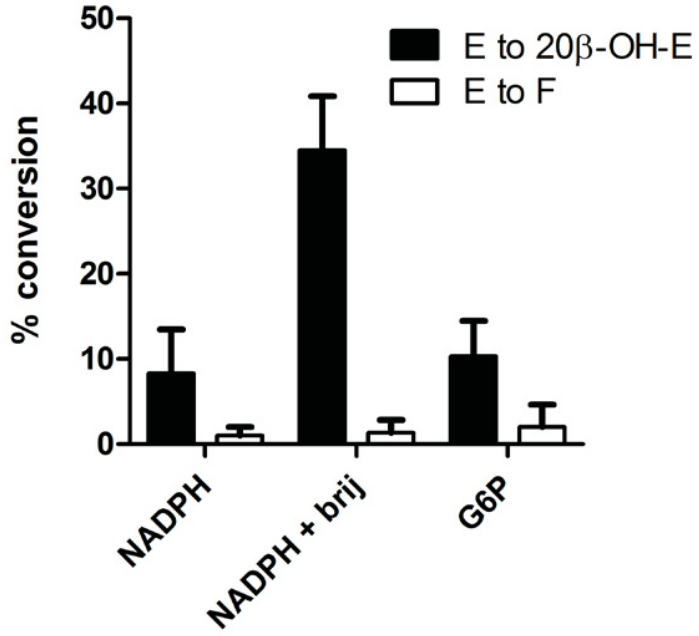

Figure 1: % conversion of 1 μM cortisone (E) in zebrafish microsomes (final concentration 1.5 mg/ml) to 20β-hydroxycortisone (20β-OH-E) (black bars) and cortisol (F) (white bars). Microsomes were incubated for 1 h at 28°C in the presence of 500 μM NADPH with or without 0.05% Brij®58 or 1 mM glucose-6-phosphate (G6P). Data (mean ± SD) were obtained from three independent experiments using pooled samples.

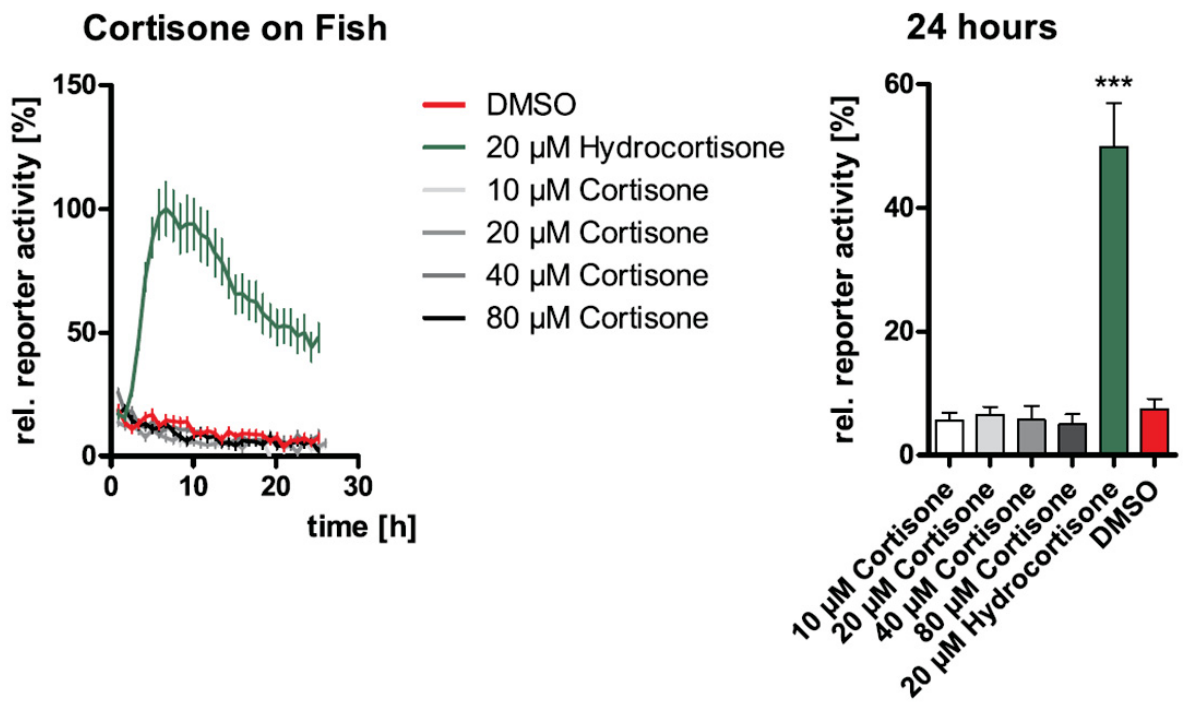

Figure 2: Measuring glucocorticoid signaling activity in a living animal via glucocorticoid response elements (GRE) driven luciferase expression in a transgenic zebrafish line (GRE:Luc). Bioluminescence from individual 5 days post fertilization transgenic larvae in 96-well microtiter plates was monitored on a luminescence plate reader. GRE:Luc larvae responded to a treatment with hydrocortisone with an increase in relative luciferase activity. No increase in relative luciferase activity was observed after treatment with cortisone.

References

[1] Pyati UJ, Look AT, Hammerschmidt M. Zebrafish as a powerful vertebrate model system for in vivo studies of cell death. Seminars in Cancer Biology 2007;17:154-65.

[2] Fako VE, Furgeson DY. Zebrafish as a correlative and predictive model for assessing biomaterial nanotoxicity. Advanced Drug Delivery Reviews 2009;61:478-86.

[3] Littleton RM, Hove JR. Zebrafish: A nontraditional model of traditional medicine. Journal of Ethnopharmacology.

[4] McGrath P, Li C-Q. Zebrafish: a predictive model for assessing drug-induced toxicity. Drug Discovery Today 2008;13:394-401.

[5] Teittinen KJ, Grönroos T, Parikka M, Rämet M, Lohi O. The zebrafish as a tool in leukemia research. Leukemia Research 2012;36:1082-8.

[6] Berton O, Hahn C-G, Thase ME. Are We Getting Closer to Valid Translational Models for Major Depression? Science 2012;338:75-9.

[7] Nesan D, Vijayan MM. Role of glucocorticoid in developmental programming: Evidence from zebrafish. General and Comparative Endocrinology.

[8] Schaaf MJM, Chatzopoulou A, Spaink HP. The zebrafish as a model system for glucocorticoid receptor research. Comparative Biochemistry and Physiology Part A: Molecular & Integrative Physiology 2009;153:75-82.

[9] Weger BD, Weger M, Nusser M, Brenner-Weiss G, Dickmeis T. A Chemical Screening System for Glucocorticoid Stress Hormone Signaling in an Intact Vertebrate. ACS Chemical Biology 2012;7:1178-83.

[10] Postlethwait JH, Woods IG, Ngo-Hazelett P, Yan Y-L, Kelly PD, Chu F, et al. Zebrafish Comparative Genomics and the Origins of Vertebrate Chromosomes. Genome Research 2000;10:1890-902.

[11] Mangelsdorf DJ, Thummel C, Beato M, Herrlich P, Schütz G, Umesono K, et al. The nuclear receptor superfamily: The second decade. Cell 1995;83:835-9.

[12] Bury NR, Sturm A, Le Rouzic P, Lethimonier C, Ducouret B, Guiguen Y, et al. Evidence for two distinct functional glucocorticoid receptors in teleost fish. J Mol Endocrinol 2003;31:141-56.

[13] Li Y, Sturm A, Cunningham P, Bury NR. Evidence for a divergence in function between two glucocorticoid receptors from a basal teleost. BMC Evol Biol 2012;12:137.

[14] Bridgham JT, Carroll SM, Thornton JW. Evolution of Hormone-Receptor Complexity by Molecular Exploitation. Science 2006;312:97-101.

[15] Hoegg S, Brinkmann H, Taylor J, Meyer A. Phylogenetic Timing of the Fish-Specific Genome Duplication Correlates with the Diversification of Teleost Fish. J Mol Evol 2004;59:190-203.

[16] Gilmour KM. Mineralocorticoid Receptors and Hormones: Fishing for Answers. Endocrinology 2005;146:44-6.

[17] Pippal JB, Cheung CMI, Yao Y-Z, Brennan FE, Fuller PJ. Characterization of the zebrafish (Danio rerio) mineralocorticoid receptor. Mol Cell Endocrinol 2011;332:58-66.

[18] Colombe L, Fostier A, Bury N, Pakdel F, Guiguen Y. A mineralocorticoid-like receptor in the rainbow trout, Oncorhynchus mykiss: cloning and characterization of its steroid binding domain. Steroids 2000;65:319-28.

[19] Greenwood AK, Butler PC, White RB, DeMarco U, Pearce D, Fernald RD. Multiple corticosteroid receptors in a teleost fish: distinct sequences, expression patterns, and transcriptional activities. Endocrinology 2003;144:4226-36.
[20] Sturm A, Bury N, Dengreville L, Fagart J, Flouriot G, Rafestin-Oblin ME, et al. 11-Deoxycorticosterone Is a Potent Agonist of the Rainbow Trout (Oncorhynchus mykiss) Mineralocorticoid Receptor. Endocrinology 2005;146:47-55.
[21] Odermatt A, Dick B, Arnold P, Zaehner T, Plueschke V, Deregibus MN, et al. A mutation in the cofactor-binding domain of 11beta-hydroxysteroid dehydrogenase type 2 associated with mineralocorticoid hypertension. J Clin Endocrinol Metab 2001;86:1247-52.
[22] Meyer A, Strajhar P, Murer C, Da Cunha T, Odermatt A. Species-specific differences in the inhibition of human and zebrafish 11beta-hydroxysteroid dehydrogenase 2 by thiram and organotins. Toxicology 2012;301:72-8.
[23] Kusakabe M, Nakamura I, Young G. 11β-Hydroxysteroid Dehydrogenase Complementary Deoxyribonucleic Acid in Rainbow Trout: Cloning, Sites of Expression, and Seasonal Changes in Gonads. Endocrinology 2003;144:2534-45.
[24] Jiang JQ, Wang DS, Senthilkumaran B, Kobayashi T, Kobayashi HK, Yamaguchi A, et al. Isolation, characterization and expression of 11beta-hydroxysteroid dehydrogenase type 2 cDNAs from the testes of Japanese eel (Anguilla japonica) and Nile tilapia (Oreochromis niloticus). J Mol Endocrinol 2003;31:305-15.
[25] Miura T, Yamauchi K, Takahashi H, Nagahama Y. Hormonal induction of all stages of spermatogenesis in vitro in the male Japanese eel (Anguilla japonica). Proceedings of the National Academy of Sciences of the United States of America 1991;88:5774-8.
[26] Schoonheim PJ, Chatzopoulou A, Schaaf MJ. The zebrafish as an in vivo model system for glucocorticoid resistance. Steroids 2010;75:918-25.
[27] Alsop D, Vijayan MM. Development of the corticosteroid stress axis and receptor expression in zebrafish. American Journal of Physiology - Regulatory, Integrative and Comparative Physiology 2008;294:R711-R9.
[28] Schaaf MJM, Champagne D, van Laanen IHC, van Wijk DCWA, Meijer AH, Meijer OC, et al. Discovery of a Functional Glucocorticoid Receptor β-Isoform in Zebrafish. Endocrinology 2008;149:1591-9.
[29] Odermatt A, Nashev LG. The glucocorticoid-activating enzyme 11[beta]-hydroxysteroid dehydrogenase type 1 has broad substrate specificity: Physiological and toxicological considerations. The Journal of Steroid Biochemistry and Molecular Biology 2010;119:1-13.
[30] Alsop D, Vijayan MM. Molecular programming of the corticosteroid stress axis during zebrafish development. Comparative Biochemistry and Physiology Part A: Molecular & Integrative Physiology 2009;153:49-54.
[31] Dickmeis T, Lahiri K, Nica G, Vallone D, Santoriello C, Neumann CJ, et al. Glucocorticoids Play a Key Role in Circadian Cell Cycle Rhythms. PLoS Biol 2007;5:e78.
[32] Staab CA, Maser E. 11β-Hydroxysteroid dehydrogenase type 1 is an important regulator at the interface of obesity and inflammation. The Journal of Steroid Biochemistry and Molecular Biology 2010;119:56-72.
[33] Seckl JR, Morton NM, Chapman KE, Walker BR. Glucocorticoids and 11beta-Hydroxysteroid Dehydrogenase in Adipose Tissue. Recent Prog Horm Res 2004;59:359-93.

[34] Wendelaar Bonga SE. The stress response in fish. Physiological Reviews 1997;77:591-625.
[35] Baker ME. Evolutionary analysis of 11[beta]-hydroxysteroid dehydrogenase-type 1, -type 2, -type 3 and 17[beta]-hydroxysteroid dehydrogenase-type 2 in fish. FEBS Letters 2004;574:167-70.
[36] Baker ME. Evolution of 11[beta]-hydroxysteroid dehydrogenase-type 1 and 11[beta]-hydroxysteroid dehydrogenase-type 3. FEBS Letters 2010;584:2279-84.
[37] Huang C, Wan B, Gao B, Hexige S, Yu L. Isolation and characterization of novel human short-chain dehydrogenase/reductase SCDR10B which is highly expressed in the brain and acts as hydroxysteroid dehydrogenase. Acta Biochim Pol 2009;56:279-89.
[38] Tokarz J, Möller G, Hrabě de Angelis M, Adamski J. Zebrafish and steroids: What do we know and what do we need to know? The Journal of Steroid Biochemistry and Molecular Biology.
[39] Tokarz J, Mindnich R, Norton W, Moller G, Hrabe de Angelis M, Adamski J. Discovery of a novel enzyme mediating glucocorticoid catabolism in fish: 20beta-hydroxysteroid dehydrogenase type 2. Mol Cell Endocrinol 2012;349:202-13.
[40] Tomlinson JW, Walker EA, Bujalska IJ, Draper N, Lavery GG, Cooper MS, et al. 11β-Hydroxysteroid Dehydrogenase Type 1: A Tissue-Specific Regulator of Glucocorticoid Response. Endocrine Reviews 2004;25:831-66.
[41] White PC, Mune T, Agarwal AK. 11β-Hydroxysteroid Dehydrogenase and the Syndrome of Apparent Mineralocorticoid Excess. Endocrine Reviews 1997;18:135-56.
[42] Nashev LG, Chandsawangbhuwana C, Balazs Z, Atanasov AG, Dick B, Frey FJ, et al. Hexose-6-phosphate dehydrogenase modulates 11beta-hydroxysteroid dehydrogenase type 1-dependent metabolism of 7-keto- and 7beta-hydroxy-neurosteroids. PLoS One 2007;2:e561.
[43] Odermatt A, Arnold P, Stauffer A, Frey BM, Frey FJ. The N-terminal anchor sequences of 11beta-hydroxysteroid dehydrogenases determine their orientation in the endoplasmic reticulum membrane. J Biol Chem 1999;274:28762-70.
[44] Meyer A, Vuorinen A, Zielinska AE, Da Cunha T, Strajhar P, Lavery GG, et al. Carbonyl reduction of triadimefon by human and rodent 11beta-hydroxysteroid dehydrogenase 1. Biochem Pharmacol 2013.
[45] Furstenberger C, Vuorinen A, Da Cunha T, Kratschmar DV, Saugy M, Schuster D, et al. The anabolic androgenic steroid fluoxymesterone inhibits 11beta-hydroxysteroid dehydrogenase 2-dependent glucocorticoid inactivation. Toxicol Sci 2012.

Chapter 4: 17β-HSD2 inhibitor testing

Introduction

The inhibition of 17β-hydroxysteroid dehydrogenase type 2 (17β-HSD2) has recently been suggested to be a potential drug target to treat osteoporosis [39]. We currently collaborate with two research groups aiming at the development of selective 17β-HSD2 inhibitors. 17β-HSD2 belongs to the SDR superfamily and has been shown to play an important role in estradiol metabolism. It can deactivate active estradiol into inactive estrone, but also testosterone and 5α-dihydrotestosterone (DHT) into their inactive forms Δ4-androstenedione, and 5α-androstanedione [40]. Active androgens and estrogens are described to play an important role in bone formation and resorption, therefore a local inhibition of 17β-HSD2 in bones might be a potential mechanism to treat osteoporosis [39, 41, 42]. 17β-HSD2 inhibitors have been proposed as a treatment for osteoporosis, a disease that is often caused by estrogen-deficiency, especially in post-menopausal women.

The group of Prof. Hartmann (Saarland University, Germany) has constructed potent 17β-HSD2 inhibitors. I tested their structurally optimized 2,5-thiophene amides for selectivity on *hs*11β-HSD1 and *hs*11β-HSD2. The publication can be found at the end of this chapter.

The group of Prof. Schuster (University Innsbruck, Austria) approached the search for new 17β-HSD2 inhibitors by employing ligand-based pharmacophore modeling and virtual screening. Published 17β-HSD2 inhibitors were identified from the literature, and pharmacophore models representing the common chemical and steric features of these inhibitors were constructed. These models were then employed to virtual screening of the commercial database SPECS. The hitlists of the models were compared with each other and 29 compounds were purchased for biological evaluation according to their drug-likeness, pharmacophore fit score, novelty, and availability.

With the same pharmacophore model the complete Sigma® catalogue was screened. Over 120 compounds were identified to potentially inhibit 17β-HSD2. Based on possible exposure, 16 of these chemicals are now being tested on *hs*17β-HSD2 by Fabio Bachmann.

Results & Discussion

Anna Vuorinen (University Innsbruck, Austria) performed the biological evaluation of selected compounds from her *in silico* screening and found that seven of these compounds inhibited at least 70% of the enzyme activity at concentration of 20 μM and that they showed acceptable selectivity over the other related SDR enzymes tested. These results validated their pharmacophore models and the newly discovered 17β-HSD2 inhibitors are suitable lead structures for further drug development.

The obtained results were then used to search for similar compounds to get further structure-activity relationship (SAR) information. The selection of these hits was not guided by the model. These compounds were then tested by Fabio Bachmann for inhibition of 17β-HSD2 and for selectivity toward 11β-HSD1/2 and 17β-HSD3. Only one compound showed strong inhibition at 20 μM. This compound is currently being analyzed further. The fact that the selected compounds are less active gives Anna Vuorinen valuable information for the model refinement and help also to understand how the binding pocket is built.

From the 16 chemicals tested of the virtual Sigma® catalogue library only two substances showed strong inhibition at 20 μM. These two compounds will be further analyzed by Fabio Bachmann.

In my opinion, screening with pharmacophore models is a very fast and low-cost approach to screen a huge quantity of compounds. But the data obtained must be carefully analyzed and it does not replace the biological evaluation. Another pitfall might be false-negative results. It is not known how many chemicals are missed by this approach.

Paper: Structural optimization of 2,5-thiophene amides as highly potent and selective 17β-hydroxysteroid dehydrogenase type 2 inhibitors for the treatment of osteoporosis

Journal of Medicinal Chemistry

Article

pubs.acs.org/jmc

Structural Optimization of 2,5-Thiophene Amides as Highly Potent and Selective 17β-Hydroxysteroid Dehydrogenase Type 2 Inhibitors for the Treatment of Osteoporosis

Sandrine Marchais-Oberwinkler,[†,#] Kuiying Xu,[†,#] Marie Wetzel,[†] Enrico Perspicace,[†] Matthias Negri,[‡] Arne Meyer,[§] Alex Odermatt,[§] Gabriele Möller,[∥] Jerzy Adamski,[∥,⊥] and Rolf W. Hartmann*[,†,‡]

[†]Pharmaceutical and Medicinal Chemistry, Saarland University, D-66041 Saarbrücken, Germany

[‡]Helmholtz Institute for Pharmaceutical Research Saarland (HIPS), Campus C2$_3$, D-66123 Saarbrücken, Germany

[§]Division of Molecular and Systems Toxicology, Department of Pharmaceutical Sciences, University of Basel, Klingelbergstraße 50, CH-4056 Basel, Switzerland

[∥]Genome Analysis Center, Institute of Experimental Genetic, Helmholtz Zentrum München, D-85764 Neuherberg, Germany

[⊥]Lehrstuhl für Experimentelle Genetik, Technische Universität München, D-85350 Freising-Weihenstephan, Germany

Supporting Information

ABSTRACT: Inhibition of 17β-HSD2 is an attractive mechanism for the treatment of osteoporosis. We report here the optimization of human 17β-HSD2 inhibitors in the 2,5-thiophene amide class by varying the size of the linker (*n* equals 0 and 2) between the amide moiety and the phenyl group. While none of the phenethylamides (*n* = 2) were active, most of the anilides (*n* = 0) turned out to moderately or strongly inhibit 17β-HSD2. The four most active compounds showed an IC$_{50}$ of around 60 nM and a very good selectivity toward 17β-HSD1, 17β-HSD4, 17β-HSD5, 11β-HSD1, 11β-HSD2 and the estrogen receptors α and β. The investigated compounds inhibited monkey 17β-HSD2 moderately, and one of them showed good inhibitory activity on mouse 17β-HSD2. SAR studies allowed a first characterization of the human 17β-HSD2 active site, which is predicted to be considerably larger than that of 17β-HSD1.

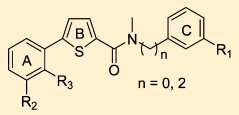

Cmpd	n	R2	R3	R1	Human 17β-HSD2 IC$_{50}$ (nM)	Selectivity Factor (17β-HSD1)
7	1	OMe	F	OH	61	73
31	0	OMe	F	OMe	62	>800
32	0	OMe	F	Me	62	132

INTRODUCTION

17β-Hydroxysteroid dehydrogenase type 2[1] (17β-HSD2) catalyzes the conversion of the highly active 17β-hydroxysteroids into the inactive 17-ketosteroids, i.e., the estrogen estradiol (E2), as well as the androgens testosterone (T) and 5α-dihydrotestosterone (DHT) into their inactive forms estrone (E1), Δ^4-androstene-3,17-dione (Δ^4-AD), and 5α-androstanedione, respectively (Chart 1). In addition, it has been described to exhibit a 20α-dehydrogenase activity,[1] transforming 20α-dihydroprogesterone in progesterone, and a 3β-dehydrogenase activity,[2] converting pregnenolone into progesterone and dehydroepiandrosterone (DHEA) in Δ^4-AD.

E2 is known to play an important role in the growth, development, and maintenance of a diverse range of tissues (e.g., reproductive tissues, brain). It is also involved in the maintenance of bone balance, inducing bone formation and repressing bone resorption by action on the osteoblasts.[3] There is also evidence that T has beneficial effects on bone formation.[4,5]

Osteoporosis[6] is a systemic disease where rigidity and mechanical stability of the bone decline. Balance between bone formation and bone resorption is disrupted, leading to an increased risk of fractures. High incidence of this disease is observed in women after menopause when the E2 levels drop or following treatment with aromatase inhibitors,[7] which block estrogen biosynthesis. Nowadays two first-line therapies are administered to osteoporotic patients: (1) Bisphosphonates (alendronate) are effective in both postmenopausal women[8] and men;[9,10] however, they lead to reduction of only 50% of fracture risk and are often associated to osteonecrosis of the jaw. (2) Selective estrogen receptor modulators,[11] also called SERMs (raloxifene), are efficient too but are often associated with an increased risk of venous thromboembolism. As the reduction of circulating estrogens induces accelerated bone loss, estrogen replacement therapy (ERT) was given to postmenopausal osteoporosis patients.[12,13] It reduced the risk of fractures but increased the incidence of cardiovascular diseases and breast cancer, which prevented the further use of this therapy.[13−15] All therapies currently available for the treatment of osteoporosis have limitations, and none of them offers a complete cure for the condition. Osteoporosis is an age-

Received: September 27, 2012
Published: November 12, 2012

Chart 1. 17β-HSD1, -2, -3, -4, and -5 in Sex Steroid Metabolism

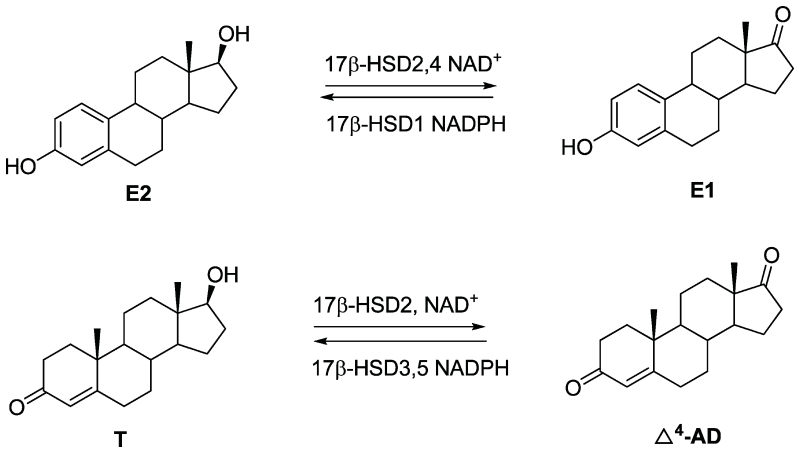

Chart 2. Structures of Known 17β-HSD2 Inhibitors

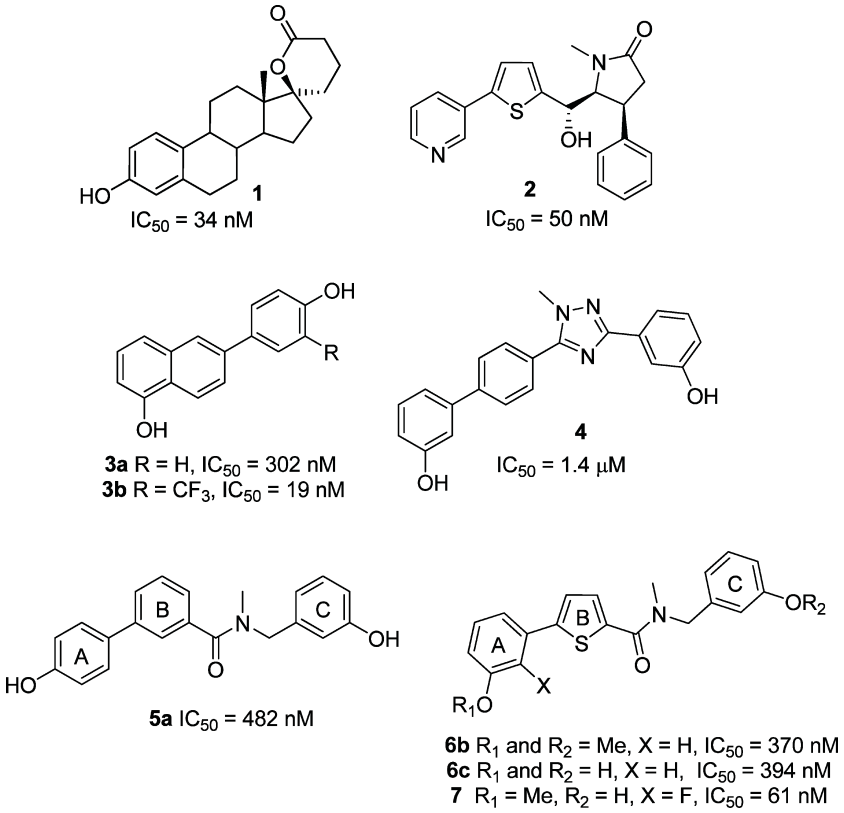

dependent disease, and because of the increasing life expectancy and aging population in the industrialized countries, there is a need for development of improved drugs to combat this disease. As 17β-HSD2 is expressed in osteoblastic cells,[16−18] inhibition of 17β-HSD2, which will lead to an increase in E2 and T levels locally in the bones, therefore offers the potential as a novel therapy for osteoporosis.

Ideally, 17β-HSD2 inhibitors should be highly potent and selective. They should not exhibit inhibitory activities on functionally related 17β-HSD subtypes like types 1, 3, 4, 5 (Chart 1). Inhibition of 17β-HSD type 4, which catalyzes the same reaction as type 2, is not desirable because it is ubiquitously expressed and its dysfunction leads to severe human disorders,[19] e.g., Zellweger syndrome like D-bifunctional protein deficiency. Activity suppression of 17β-HSD1, -3, or -5, which catalyze the reverse reaction (reduction of estrogens or androgens) will thus be counterproductive because it would decrease E2 and T levels in bone and might lead to systemic side effects.

17β-HSD2 inhibitors should not bind to the estrogen receptors (ER) α and β, as it is expected that the E2 effects are ER mediated. In addition, activation upon binding to these receptors might lead to proliferative or antiproliferative effects in steroidogenic tissues, which should be avoided.

Although 17β-HSD2 was already revealed in 1985 by Blomquist[20] and characterized by Wu in 1993,[1] very few 17β-

dx.doi.org/10.1021/jm3014053 | J. Med. Chem. 2013, 56, 167−181

HSD2 inhibitor classes have been reported to date. Among the steroidal inhibitors, Poirier and colleagues described a series of steroidal spirolactone derivatives;[21−24] the most potent compound is the C17-spiro-δ-lactone **1** (Chart 2, IC_{50} = 34 nM [22]). Wood et al.[25−27] reported about a novel class of *cis*-pyrrolidinones as active and selective nonsteroidal 17β-HSD2 inhibitors, with **2** (Chart 2) being one of the most potent compound (IC_{50} = 50 nM in a cell-free assay). Three further classes of nonsteroidal potent and selective 17β-HSD2 inhibitors were recently published by our group (Chart 2): the hydroxyphenylnaphth-1-ol **3a** and **3b**,[28,29] the hydroxyphenylmethanones[30] derived from the triazole **4**,[31] and the amides **5a**, **6b**, **6c**, and **7**.[32] These amide derivatives are all substituted by a benzyl group that is linked to a biphenylamide **5a** or a phenylthiophene **6b**, **6c**, **7** moiety.

At the time we started this work, a proof of concept for therapeutic efficacy of 17β-HSD2 inhibition had been described using compound **2** in vivo in a monkey model,[33] showing a decrease of bone resorption and maintenance of bone formation. Despite high variations and the moderate effects observed, this in vivo experiment validates this approach and underlines the need for new optimized 17β-HSD2 inhibitors.

In the current report, we describe the optimization of 17β-HSD2 inhibitors in the biphenylamide and phenylthiophene amide classes focusing on the suppression of the methylene from the benzyl group (anilide derivatives) or its replacement by an ethylene linker (phenethylamide derivatives). The synthesis of a small library of achiral derivatives, the biological evaluation, and the structure−activity relationship (SAR) of the new 17β-HSD2 inhibitors will be presented and compared to the benzyl analogues.[32] The selectivity toward further HSD enzymes and the cytotoxicity profile of the best candidates were investigated. Selectivity toward 17β-HSD1 was achieved based on the expertise from the group developing potent and selective inhibitors of 17β-HSD1.[34−45] In order to identify which species could be more suitable to perform a proof of concept in a preclinical model, the most potent and selective compounds (at the human enzymes) identified in this study were further tested for their ability to inhibit 17β-HSD2 from different species (rodents and monkey).

DESIGN

In a previous study, it was shown that, starting from the weakly active disubstituted triazole **4**,[31] opening of the triazole central moiety[32] led to the discovery of a new class of biphenylamide **5a** and phenylthiophene amides **6b**, **6c**, and **7** as 17β-HSD2 inhibitors (Chart 2). All the compounds discovered in this class share a methylated amide and two hydroxy/methoxyphenyl moieties differentiated in this study as rings A and C (Chart 2). In addition ring C is attached to the nitrogen of the amide via a methylene linker (n = 1, benzyl group). The compounds differ in their central ring B, which is either a 1,4-phenyl, 1,3-phenyl, or 2,5-thiophene group. Moderately active compounds were identified in the class of the 1,3-phenyl derivatives **5a**, showing an IC_{50} of around 500 nM. Moderate to good active molecules were discovered in the 2,5-thiophene class **6b** and **6c**, with IC_{50} of around 380 nM with the exception of **7**, the most active and promising 17β-HSD2 inhibitor (IC_{50} = 61 nM and selectivity factor of 73 toward 17β-HSD1).

With the hypothesis that the central core B and the hydroxy/methoxyphenyl A ring bind at the same position in the enzyme, variation of the linker size n (n = 0, 1, and 2) will bring ring C into different areas of the binding cavity as seen in Figure 1.

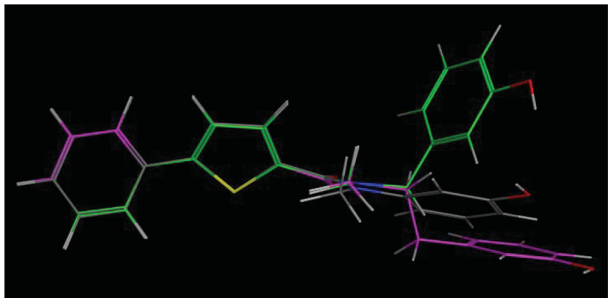

Figure 1. Superimposition of the designed compounds with n = 0 (gray), 1 (green), and 2 (violet). The picture was generated using Moe 2010.10.

Variation of the size of the linker will help the mapping of the enzyme's active site, which is unknown, providing information on the space available there and the global size of the inhibitor accepted by the enzyme as well as on inhibitor rigidity (n = 0)/flexibility (n = 2) tolerated by the enzyme.

In order to investigate more deeply the enzyme's active site and in an attempt to optimize this class of compounds, a small library of 17β-HSD2 inhibitors was synthesized keeping the phenyl C unchanged and varying the size of the linker (n = 0 and n = 2, to be compared with n = 1 previously described[32]) as well as the substituents at ring A in both biphenyl and phenylthiophene amides classes (Chart 3, compounds **8**−**41**).

Chart 3. Designed Structures

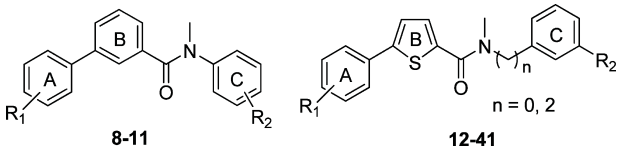

RESULTS

Chemistry. The synthesis of the 1,3-phenyl derivatives **8**−**11**, depicted in Scheme 1, and the synthesis of the 2,5-thiophene derivatives **12**−**41**, depicted in Scheme 2, were performed following a two- to three-step reaction pathway. First, amidation was carried out by reaction of the commercially

Scheme 1. Synthesis of 1,3-Phenyl Derivatives 8−11[a]

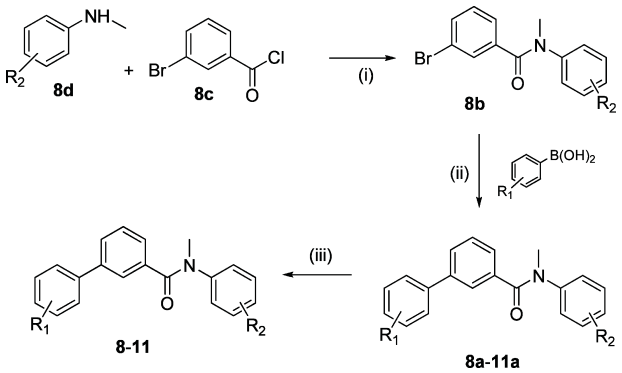

[a]Reagents and conditions: (i) NEt_3, CH_2Cl_2, 0 °C, 3 h, method A; (ii) DME/H_2O (1/1), Na_2CO_3, $Pd(PPh_3)_4$, 80 °C, 4−14 h, method B; (iii) $BF_3{\cdot}S(Me)_2$, CH_2Cl_2, rt, 6−14 h, method C.

dx.doi.org/10.1021/jm3014053 | J. Med. Chem. 2013, 56, 167−181

Scheme 2. Synthesis of 2,5-Thiophene Derivatives 12−41[a]

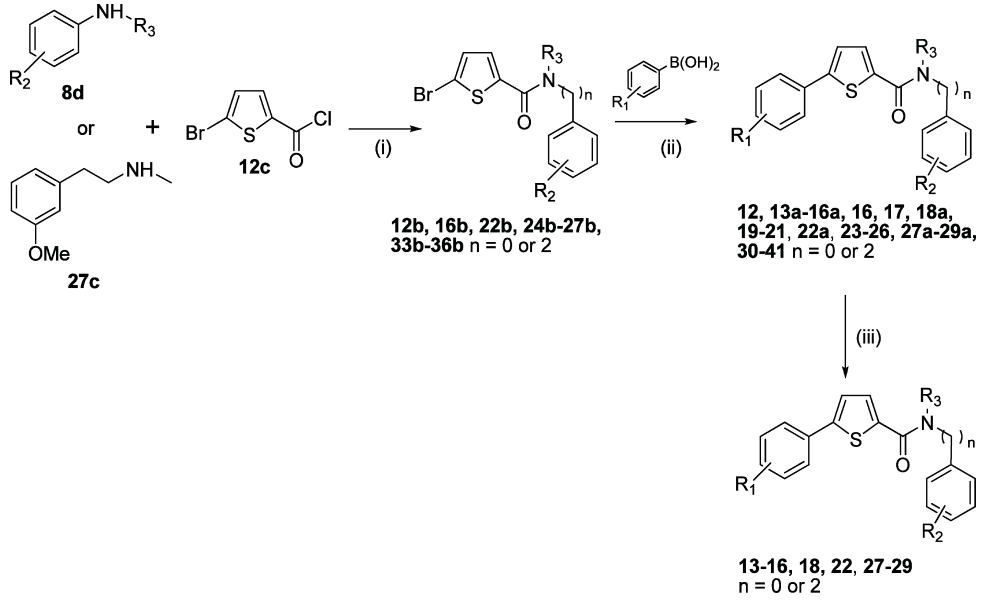

[a]Reagents and conditions: (i) NEt_3, CH_2Cl_2, 0 °C, 3 h, method A; (ii) DME/H_2O (1/1), Na_2CO_3, $Pd(PPh_3)_4$, 80 °C, 4−14 h, method B; (iii) $BF_3{\cdot}S(Me)_2$, CH_2Cl_2, rt, 6−14 h, method C.

Table 1. Inhibition of Human 17β-HSD2 and 17β-HSD1 by Diphenylamide Derivatives 8−11 in Cell-Free System

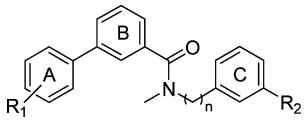

5a-d, 8-11

		n = 0			n = 1		
			% inhibition at 1 μM[a,d]			% inhibition at 1 μM[a,d]	
R_1	R_2	compd	17β-HSD2[b]	17β-HSD1[c]	compd	17β-HSD2[b]	17β-HSD1[c]
4-OH	OH	**8**	28	ni	**5a**	70	31
4-OMe	OMe	**8a**	53	ni	**5b**	13	ni
3-OH	OH	**9**	35	13	**5c**	60	10
3-OMe	OMe	**9a**	64	ni	**5d**	11	ni
2-OH	OH	**10**	18	ni			
2-OMe	OMe	**10a**	40	ni			
H	OH	**11**	28	ni			
H	OMe	**11a**	37	ni			

[a]Mean value of three determinations, standard deviation less than 10%. [b]Human placental, microsomal fraction, substrate E2, 500 nM, cofactor NAD^+, 1500 μM. [c]Human placental, cytosolic fraction, substrate E1, 500 nM, cofactor NADH, 500 μM. [d]ni: no inhibition (inhibition of <10%).

available 5-bromothiophene **12c** or the 3(4)-bromobenzoyl chloride **8c** with substituted anilines **8d** or with the 2-(3-methoxyphenyl)-*N*-methylethanamine **27c** under standard conditions (method A consisting of triethylamine, dichloromethane at 0 °C for 3 h) providing the brominated intermediates **8b**, **12b**, **16b**, **22b**, **24b−27b**, **33b−36b** in isolated yields between 57% and 99%. Subsequently, Suzuki coupling using tetrakis(triphenylphosphine)palladium and sodium carbonate in a mixture DME/water, 1:1 (method B), afforded the biphenylamides **8a−11a** or the phenylthiophene amides derivatives **12**, **13a−16a**, **16**, **17**, **18a**, **19−21**, **22a**, **23−26**, **27a−29a**, **30−41** with good yields. Methoxy compounds were submitted to ether cleavage using boron trifluoride−dimethyl sulfide complex and yielded the hydroxy molecules **8−11**, **13−16**, **18**, **22**, **27−29**.

Biological Results. *1. Inhibition of Human 17β-HSD2 in Cell-Free Assay and Cellular Assay.* 17β-HSD2 inhibitory activities of the synthesized compounds were first evaluated in a cell-free assay. Human placental enzyme was obtained and used according to described methods.[23,46,47] Briefly, incubations were run with the enzyme microsomal fraction, tritiated E2, cofactor, and inhibitor. The separation of substrate and product was accomplished by HPLC. The percent inhibition values of compounds **8−41** are shown in Tables 1−3. The IC_{50} values determined for selected compounds are reported in Table 4. Compounds showing less than 10% inhibition when tested at 1 μM were considered to be inactive. The spiro-δ-lactone **1**,

dx.doi.org/10.1021/jm3014053 | J. Med. Chem. 2013, 56, 167−181

Table 2. Inhibition of Human 17β-HSD2 and 17β-HSD1 by Phenylthiophene Amide Derivatives Monosubstituted on the A-Ring 12−29 in Cell-Free System

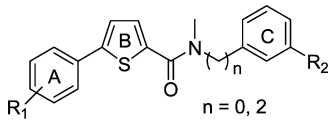

6a-l, 12-29

		$n = 0$			$n = 1$			$n = 2$		
			% inhibition at 1 μM[a,d]			% inhibition at 1 μM[a,d]			% inhibition at 1 μM[a,d]	
R_1	R_2	compd	17β-HSD2[b]	17β-HSD1[c]	compd	17β-HSD2[b]	17β-HSD1[c]	compd	17β-HSD2[b]	17β-HSD1[c]
4-OMe	3-OMe	**12**	89	15	**6a**	61	ni			
3-OMe	3-OMe	**13a**	90	11	**6b**	63	ni	**27a**	31	ni
3-OH	3-OH	**13**	34	33	**6c**	70	21	**27**	37	23
2-OMe	3-OMe	**14a**	66	ni	**6d**	48	ni			
2-OH	3-OH	**14**	69	47	**6e**	83	16			
H	3-OMe	**15a**	82	24	**6f**	49	ni	**28a**	18	11
H	3-OH	**15**	60	50	**6g**	81	15	**28**	11	ni
3-OMe	H	**16a**	67	ni	**6h**	68	ni			
3-OH	H	**16**	31	12	**6i**	42	ni			
H	H	**17**	48	14						
4-CN	3-OMe	**18a**	48	ni	**6j**	ni	ni			
4-CN	3-OH	**18**	28	ni	**6k**	54	7			
3-Me	3-OMe	**19**	95	26						
3-$N(Me)_2$	3-OMe	**20**	82	11						
3-SMe	3-OMe	**21**	88	28						
3-OMe	3-Me	**22a**	87	ni						
3-OH	3-Me	**22**	71	24						
3-F	3-OMe	**23**	67	23				**29a**	ni	ni
3-F	3-OH				**6l**	71	20	**29**	17	12
3-OMe	3-CF_3	**24**	75	13						
3-Me	2-F	**25**	68	ni						
3-OMe	3-Ph	**26**	83	50						

[a]Mean value of three determinations, standard deviation less than 10%. [b]Human placental, microsomal fraction, substrate E2, 500 nM, cofactor NAD^+, 1500 μM. [c]Human placental, cytosolic fraction, substrate E1, 500 nM, cofactor NADH, 500 μM. [d]ni: no inhibition (inhibition of <10%).

described by Poirier et al.,[22] was taken as external reference (68% at 1 μM in our test; 62−66% at 1 μM in their assay).

In the 1,3-phenyl class (Table 1), comparison of the biological results indicates that the best 17β-HSD2 inhibitory activities are obtained either when *n* is 0 and the substituents R1 and R2 are methoxy groups (compounds **8a**, **9a**, **10a**) or when *n* is 1 and R1 and R2 are hydroxy moieties (compounds **5a** and **5c**). Taking away R2 (R2 = H; **11** and **11a**) is detrimental for the activity, independent of the nature of R1. It indicates that R2 is important for the stabilization of the molecule in the active site. R1 and R2 therefore interact with amino acids from the binding cavity and behave as H-bond acceptors when *n* is 0 or H-bond donors when *n* is 1.

In the 2,5-thiophene class (Table 2), the highest inhibition data are observed with the compounds having the linker *n* = 0 and the substitutents R1 and R2 being methoxy (**13a**) or when the linker *n* is 1 and R1 and R2 are hydroxy (**6e**) as observed in the 1,3-phenyl class. The compounds with the linker *n* = 2 are either inactive (**28**, **29a**) or weakly active (**27a**, **27**), independent of the substituents at rings A and C. With the ethylene linker the compounds might be too long and/or too flexible to fit in the enzyme active site. They were not further investigated.

Focusing on compounds with *n* = 0, the influence of the central core can also be evaluated. By comparison of the 1,3-phenyl to the 2,5-thiophene derivatives (for **9a** compared to **13a**, 64% and 90% inh at 1 μM, respectively; for **10a** compared to **14a**, 40% and 66% inh at 1 μM, respectively; for **11a** compared to **15a**, 37% and 82% inh at 1 μM, respectively), it is obvious that the 2,5-thiophene is better than the 1,3-phenyl moiety. This preference is difficult to explain, as both aromatic moieties can establish a π-stacking interaction with aromatic amino acids from the active site. However the overall electronic density and the molecular electrostatic potential (MEP) differ depending on the nature of the central scaffold. It is likely that the MEP induced by the 2,5-thiophene leads to a better recognition with the corresponding region in the binding cavity. This property has already been evidence in the discovery of 17β-HSD1 inhibitors.[39,48] Thus, the 2,5-thiophene class only was further investigated in the rest of the study.

Furthermore, the influence of the A and C ring substituents on the activity can be deduced in the 2,5-thiophene class with the linker *n* = 0. Taking away the methoxy group on the A ring (R2 = H **15a**/R2 = OMe **13a**, 82%/90% inh at 1 μM, respectively) does not influence the potency of the compound, indicating that this group does not play a critical role in the stabilization of the inhibitor in the active site. Deleting the same group on the C ring (R1 = H **16a**/R1 = OMe **13a**, 67%/90% inh at 1 μM, respectively) leads to a more consistent decrease in activity, suggesting that this methoxy is involved in specific interactions that stabilize the inhibitor in the binding cavity or

dx.doi.org/10.1021/jm3014053 | J. Med. Chem. 2013, 56, 167−181

that it affects the electrostatic potential of the C ring which again favors the binding.

The importance of electronic effects is also indicated by the fact that replacement of the methoxy moiety at the A ring (**13a**, 90% inh at 1 μM) by other electron donating groups (3-Me **19**, 3-NMe_2 **20**, and 3-SMe **21** giving 95%, 82%, and 88% inh at 1 μM, respectively) is well accepted, whereas replacement by electron withdrawing groups (4-CN **18a** and 3-F **23** giving 48% and 67% inh at 1 μM, respectively) leads to a decrease in activity. The same is also valid for the C ring, where exchange of the methoxy moiety **13a** (90% inh at 1 μM) by electron withdrawing groups like 3-CF_3 **24** (75% inh at 1 μM) or 2-F **25** (68% at 1 μM) slightly reduces the 17β-HSD2 inhibitory activity, while in the presence of the electron donating 3-Me **22a** the percentage inhibition does not change. Introduction of the large 3-Ph **26** (83% inh at 1 μM) is also well tolerated by the enzyme, indicating that there is space in the area of the binding site for introduction of bulky substituents.

A fluorine has been introduced at the 3-methoxyphenyl A ring as second substituent in this ring (compounds **30**–**32**, **36**–**39**, Table 3) in the 2,5-thiophene class with the linker n = 0.

Table 3. Inhibition of Human 17β-HSD2 and 17β-HSD1 by Phenylthiophene Amide Derivatives Di- or Trisubstituted on the A-Ring 30–41 in Cell-Free System

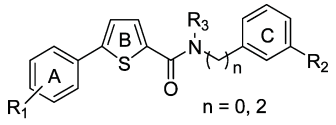

7, 30-41

					% inhibition at 1 μM[a,d]	
compd	n	R_1	R_2	R_3	17β-HSD2[b]	17β-HSD1[c]
7	1	2-F,3-OMe	3-OH	Me	89	ni
30	0	2-F,3-OMe	3-OH	Me	76	33
31	0	2-F,3-OMe	3-OMe	Me	93	17
32	0	2-F,3-OMe	3-Me	Me	85	20
33	0	2-F,3-OMe	3-OMe	H	ni	ni
34	0	2-F,3-OMe	3-OMe	Ph	ni	13
35	0	2-F,3-OMe	4-OMe	Me	49	18
36	0	2-F,3-Me	3-OMe	Me	77	ni
37	0	2-F,6-F,3-OMe	3-OMe	Me	94	28
38	0	3-F,4-OMe	3-OMe	Me	72	15
39	0	3-OMe,4-F	3-OMe	Me	66	17
40	0	3-F,4-F	3-OMe	Me	50	ni
41	0	2-OMe,4-OMe	3-OMe	Me	77	30

[a]Mean value of three determinations, standard deviation less than 8% except for **27** in HSD1, 23%. [b]Human placental, microsomal fraction, substrate E2, 500 nM, cofactor NAD^+, 1500 μM. [c]Human placental, cytosolic fraction, substrate E1, 500 nM, cofactor NADH, 500 μM. [d]ni: no inhibition (inhibition of <10%).

Introduction at the 2 position led to **31** and **32** (93% and 85% inh at 1 μM, respectively), which have similar activity as the corresponding compounds **13a** and **22a**. This substituent does not achieve any specific interaction with the active site but is also not disturbing the stabilization. Addition of the fluorine at position 4 induces a slight loss in activity, **39** (66% inh at 1 μM). This decrease in activity is consistent with the electronic effect described previously (replacement of a methoxy for an electron withdrawing group, compounds **18a** and **23**).

Addition of a third substituent on the A ring, a 6-F (**37** 94% inh at 1 μM), does not increase the potency of **31**.

Compound **31** (93% inh at 1 μM), differing from **35** (49% inh at 1 μM) in the displacement of the methoxy group on the C ring from the 3 to the 4 position, leads to a decrease in activity and reveals the importance of the interaction achieved by this group, which must have the right orientation.

It was then investigated if the methyl group on the amide function of **31** is necessary for activity: exchange with a hydrogen **33** or a phenyl **34** led to two inactive compounds. The methyl group might be located in a small lipophilic cavity and participate actively in the stabilization of the compound. Loss of this group prevents this interaction, and the phenyl group might be too big to fit into this lipophilic cavity.

For the most active compounds showing more than 70% inhibition at 1 μM, IC_{50} values were determined in the cell-free assay and are shown in Table 4. Four highly active compounds with the linker n = 0 (**13a**, **19**, **31**, and **32**) were identified displaying IC_{50} values of around 60 nM. They are equipotent to the previously described **7** carrying a methylene linker. Five other interesting compounds (**12**, **20**, **26**, **36**, and **37**) were discovered with IC_{50} between 100 and 200 nM.

The inhibitory activity of the most potent compounds on 17β-HSD2 was also evaluated in a cellular model system, using the MDA-MB-231 cell line. The compounds' efficiency is expressed as IC_{50} for the most potent compounds or as percentage of inhibition for the others (Table 4). The data obtained lie in the same range as the cell-free inhibition data, with IC_{50} values around 100 nM or below. The results indicate that the compounds can permeate the cell membrane, are stable in the cell, and are not quickly metabolized.

2. Selectivity Aspect. As 17β-HSD1 catalyzes the reduction of E1 to E2, the reversed 17β-HSD2 reaction, it should not be affected by 17β-HSD2 inhibitors. In the 1,3-phenyl class (compounds **8a**–**11**), the selectivity observed toward this enzyme (Table 1) is very good: no or a very weak inhibition of the 17β-HSD1 enzyme was measured at 1 μM. In the series of the 2,5-thiophenes, independent of the linker size (n = 0, 1, or 2; compounds **12**–**29**), the same results were observed except for the middle active 17β-HSD2 inhibitors **14**, **15**, and **30** (69%, 60%, and 67% 17β-HSD2 inh at 1 μM, respectively), which showed around 50% 17β-HSD1 inhibition at 1 μM. For the most potent 17β-HSD2 inhibitors (Table 4), the selectivity was expressed as selectivity factor (SF) calculated as the ratio of IC_{50} (17β-HSD2) over IC_{50} (17β-HSD1). For the compounds with an IC_{50} (17β-HSD2) below 200 nM, the SF varied between 26 and above 800 except for **26** with a SF of 8. The selectivity toward 17β-HSD1 is good to very good for most of the new 17β-HSD2 inhibitors described. It is even better for the compounds without linker (SF of 112, 116, above 800, and 132 for **13a**, **19**, **31**, and **32**) compared to the one with a methylene linker (SF of 73 for **7**).

Inhibitors of 17β-HSD2 should have no affinity for the estrogen receptors (ER) α and β, as it is expected that most E2 effects are ER mediated. All the compounds with an IC_{50} (17β-HSD2, cell-free assay) below 500 nM were evaluated for their relative binding affinity (RBA) to the ERα and ERβ in a competitive assay using a previously described assay[47,49] and taking E2 as internal reference. All of the tested compounds showed a RBA below 0.1%, compared to the affinity of E2, which was arbitrarily set to 100%.

17β-HSD4 catalyzes the oxidation of E2 into E1 as 17β-HSD2 (Chart 1) and is ubiquitously expressed. 17β-HSD5 is a

dx.doi.org/10.1021/jm3014053 | J. Med. Chem. 2013, 56, 167–181

Table 4. IC_{50} Values (17β-HSD2 and 17β-HSD1) and Selectivity Factor for Selected Compounds

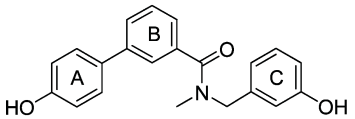

5a

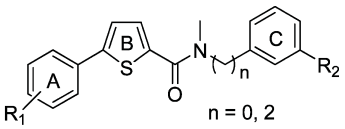

6c, 7, 12,13a,15a,19-22, 24, 26, 31, 32, 36-38, 41

				cell-free assay IC_{50} (nM)[a]			cell test[i]	
compd	n	R_1	R_2	17β-HSD2[b]	17β-HSD1[c]	selectivity factor[d]	IC_{50} (nM)[g] HSD2[e]	cLogP[f]
5a	1	3-OH	OH	482	3801	8	nd	4.04
6c	1	3-OH	OH	394	5449	14	nd	4.08
7	1	2-F,3-OMe	OH	61	4452	73	78	4.50
12	0	4-OMe	OMe	148	6217	42	81%[h]	4.54
13a	0	3-OMe	OMe	68	7593	112	119	4.54
15a	0	H	OMe	207	4337	21	nd	4.66
19	0	3-Me	OMe	58	6752	116	73	5.15
20	0	3-N(Me)$_2$	OMe	169	10573	63	71%[h]	4.95
21	0	3-SMe	OMe	242	5306	22	nd	5.10
22a	0	3-OMe	Me	207	11454	55	nd	5.15
22	0	3-OH	Me	645	6800	11	nd	4.89
24	0	3-OMe	CF_3	721	12259	17	nd	5.58
26	0	3-OMe	Ph	137	1109	8	nd	6.34
31	0	2-F,3-OMe	OMe	62	>50000	>800	105	4.69
32	0	2-F,3-OMe	Me	62	8209	132	80%[h]	5.31
36	0	2-F,3-Me	OMe	130	5426	42	83%[h]	5.79
37	0	2-F,6-F,3-OMe	OMe	184	4812	26	83%[h]	4.85
38	0	3-F,4-OMe	OMe	242	>40000	>165	nd	4.69
41	0	2-OMe,4-OMe	OMe	313	1927	6	nd	4.41

[a]Mean value of three determinations, standard deviation less than 15%. [b]Human placental, microsomal fraction, substrate E2, 500 nM, cofactor NAD^+, 1500 μM. [c]Human placental, cytosolic fraction, substrate E1, 500 nM, cofactor NADH, 500 μM. [d]IC_{50}(17β-HSD1)/IC_{50}(17β-HSD2). [e]MDA-MB-231 cell line, substrate E2, 200 nM. [f]Calculated data. [g]Mean value of two determinations, standard deviation less than 15%. [h]Inhibition measured at an inhibitor concentration of 1 μM. [i]nd: not determined.

reductive enzyme; it converts the inactive DHEA and 4-androstene-3,17-dione into the potent 5-androstene-3β,17β-diol and testosterone, respectively (Chart 1). In order to avoid systemic side effects and not to counteract the effect of 17β-HSD2 inhibition, inhibition of these enzymes should be avoided.

The five most potent compounds **7**, **13a**, **19**, **31**, and **32** were evaluated for their ability to inhibit these two enzymes, using recombinant human 17β-HSD4 and 17β-HSD5 expressed in *E. coli* following the described procedure.[50,51] The compounds did not show any inhibition of 17β-HSD4 when tested at 1 μM and inhibited 17β-HSD5 only weakly (inhibition between 17% and 33% at 1 μM, Table 5).

11β-HSDs are involved in the glucocorticoid biosynthesis. 11β-HSD1 catalyzes the transformation of the inactive cortisone into the potent cortisol, and 11β-HSD2 catalyzes the reverse reaction. Some inhibitors of 11β-HSD1[52] have a close structural analogy to the amides identified in this study. In addition, 17β-HSD2 has a relatively high sequence identity with 11β-HSD2 (45%).[53] Therefore, the selectivity profile of the five structurally most relevant compounds **7**, **13a**, **19**, **31**, and **32** was thus extended to these two enzymes using the recombinant enzymes 11β-HSD1 and 11β-HSD2 stably transfected in HEK-293 cells following the described procedure.[54] Absence or very low 11β-HSD1 and 11β-HSD2 inhibition was observed at 2 μM except for **7**, which showed an IC_{50} of 1 μM for 11β-HSD1. This activity is not negligible, but compared to the IC_{50} of 61 nM for 17β-HSD2, a selectivity factor of around 16 might be acceptable, especially regarding the fact that 11β-HSD1 activates glucocorticoids and elevated glucocorticoids have been associated with osteoporosis.[55]

Table 5. Selectivity toward 17β-HSD4, 17β-HSD5, 11β-HSD1, and 11β-HSD2 for Selected Compounds

compd	inhibition of 17β-HSD4, % at 1 μM[a,b,f]	inhibition of 17β-HSD5, % at 1 μM[a,c]	inhibition of 11β-HSD1, % at 2 μM (IC_{50})[a,d,f]	inhibition of 11β-HSD2, % at 2 μM[a,d,f]
7	ni	33	68 (1 μM)	10
13a	ni	17	ni	ni
19	ni	20	23	14
31	ni	26	9	8
32	ni	29	ni	ni
2–9[e]	ni	88	nd	nd

[a]Mean value of three determinations, standard deviation less than 19% for 17β-HSD5 and less than 9% for 17β-HSD4. [b]Enzyme expressed in bacteria (bacterial suspension), substrate [^{3}H]E2, 21 nM, cofactor NAD^+, 750 μM. [c]Enzyme expressed in bacteria (bacterial lysate), substrate [^{3}H]A-dione, 21 nM, cofactor NADPH, 600 μM. [d]Determined in lysate of HEK-293 cells expressing recombinant human enzymes. [e]External reference: compounds **2–9** described by Schuster et al.[50] [f]ni = no inhibition. nd = not determined.

3. Further Tests. The lipophilicity profiles of **7**, **13a**, **19**, **31**, and **32** were evaluated by calculation of log P (Table 4). For most of the compounds it is between 4 and 5 or slightly above

dx.doi.org/10.1021/jm3014053 | J. Med. Chem. 2013, 56, 167–181

5, which is still in a good range according to the Lipinski rule of five[56] and which should be correlated to a good permeability.

The cytotoxicity of **7**, **13a**, **19**, **31**, and **32** was evaluated in the MDA-MB-231 cell line based on MTT conversion following the procedure described by Denisot et al.[57] at three different concentrations: 2.5, 10, and 50 μM. No cytotoxicity could be observed even at the highest concentration after 3 h of incubation (data not shown).

In order to identify the appropriate species for demonstration of in vivo efficacy in a disease-oriented model, the five most potent compounds **7**, **13a**, **19**, **31**, and **32** were tested for their ability to inhibit the enzyme responsible for E2 into E1 transformation from three different animals: rat, mouse, and monkey *Callithrix jacchus*. The compounds were evaluated in a cell-free assay using the microsomal fraction of liver preparation from rat and mouse. In the case of the monkey, the microsomal enzyme was gained from placenta. The compounds showed middle activity on the monkey enzyme, between 45% and 53% inh at 1 μM (Table 6). They were inactive to very low active in the rat, the best one being **7** with 25% inh at 1 μM. In mouse compounds **13a**, **19**, and **31** were also barely active (between 26% and 30% inh at 1 μM) except for **32** and **7** which were middle to good active with 45% and 65% inh at 1 μM, respectively. It is striking that such a difference in activity is observed between the rat (*Rattus norvegicus*) and the mouse (*Mus musculus*) 17β-HSD2 inhibition data, as the protein sequence of both species is highly similar. However from this study, compound **7**, identified as a highly active and selective 17β-HSD2 inhibitor at the human enzyme, exhibits the highest 17β-HSD2 inhibition on the mouse enzyme. This result suggests that the mouse might be a promising species to perform an in vivo experiment using compound **7** and to verify that 17β-HSD2 inhibitors could be effective for the treatment of osteoporosis.

Table 6. Inhibition of E1 Formation by Rat, Mouse, and Monkey Enzymes Compared to Human Enzyme for Selected Compounds

compd	human 17β-HSD2[a] inh (%) at 1 μM	rat E1 formation[b] inh (%) at 1 μM	mouse E1 formation[c] inh (%) at 1 μM	monkey E1 formation[d] inh (%) at 1 μM
7	89	25	65	47
13a	90	14	29	45
19	95	ni	30	53
31	93	ni	26	45
32	85	ni	45	49

[a]Human placenta, microsomal fraction, substrate [^{3}H]E2 + E2 [500 nM], NAD$^+$ [1500 μM], mean value of three determinations, relative standard deviation of <10%. [b]Rat liver, microsomal fraction, substrate [^{3}H]E2 + E2 [500 nM], NAD$^+$ [1500 μM], mean value of three determinations, relative standard deviation of <10%. ni: no inhibition. [c]Mouse liver, microsomal fraction, substrate [^{3}H]E2 + E2 [500 nM], NAD$^+$ [1500 μM], mean value of three determinations, relative standard deviation of <10%. [d]Monkey placenta, microsomal fraction, substrate [^{3}H]E2 + E2 [500 nM], NAD$^+$ [1500 μM], mean value of three determinations, relative standard deviation of <10%.

DISCUSSION

The aim of this study was the optimization of 17β-HSD2 inhibitors from the amide class by variation of the size of the linker (n) located between the amide function and the C ring. Introduction of an ethylene linker (n = 2) is detrimental for the activity, independent of the central moiety 1,3-phenyl or 2,5-thiophene. The compounds might be too long or too flexible. Taking out these two carbons linker (n = 0) led to the identification of four promising compounds **13a**, **19**, **31**, and **32** with IC_{50} values of around 60 nM. Interestingly these compounds all bear a methoxy function on the C ring while the equally active **7** with a methylene linker (n = 1) is hydroxylated on this ring. High activity is only achieved when n = 1 and the C ring is hydroxylated (**7**) or n = 0 and the C ring is methoxylated (**13a**, **19**, **31**, and **32**). It is striking that there is no difference in activity between these two series of compounds. These requirements to achieve high activity are also intriguing. These data suggest that these two series of compounds may not interact with the same amino acids in the binding site. Thus, a different binding mode could be expected for these two groups of inhibitors.

From this study it is clear that the 2,5-thiophene central core is superior to the 1,3-phenyl independent of the size of the linker n = 0 or 1. This result was already observed developing 17β-HSD1 inhibitors. The molecular electrostatic potential

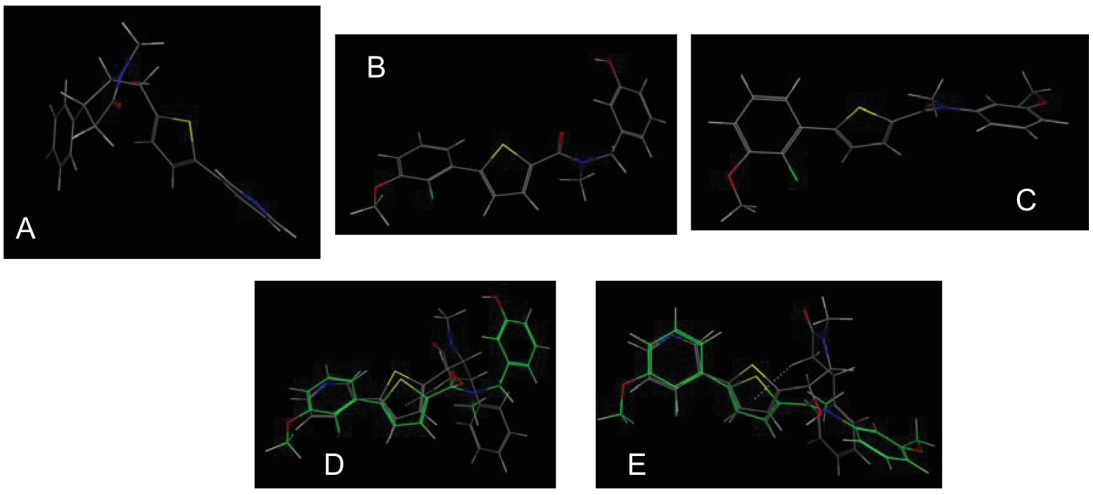

Figure 2. Mapping of 17β-HSD2 active site: (A) 3D-structure of **2**; (B) 3D-structure of **7**; (C) 3D-structure of **31**; (D) superimposition of **2** to **7** (n = 1); (E) superimposition of **2** to **31** (n = 0). **2** is colored gray, and **7** and **31** are green. The picture was generated using Moe 2010.10.

dx.doi.org/10.1021/jm3014053 | J. Med. Chem. 2013, 56, 167−181

induced by the thiophene on the whole molecule might lead to better interactions with the enzyme active site. Further, the thiophene differs from the phenyl ring in the presence of d-orbitals on the sulfur. They might allow the thiophene derivatives to undergo specific interactions compared to the phenyl one.

The human 17β-HSD2 accepts ligands with a high structural diversity: steroidal substrates E2, T, 20α-dihydroprogesterone, pregnenolone, and DHEA, steroidal inhibitor spirolactone **1**, nonsteroidal inhibitors *cis*-pyrrolidinone **2**, and amides **7** and **31**. These ligands differ in their shape and volume, but they are all very large. In order to map the enzyme active site, which is unknown, and having the hypothesis that all these compound bind in the enzyme active site, we compared the new nonsteroidal 17β-HSD2 inhibitors with two different linker sizes (**31** for n = 0 and **7** for n = 1) with the equipotent *cis*-pyrrolidinone **2** described by Wood et al.[25−27] Visualization of the 3D-structure of these three compounds, after energy minimization, highlights the folded shape of compound **2** with the thiophene ring almost parallel to the pyrrolidinone moiety (Figure 2). Thereby the two aromatic groups, phenyl and pyridine, are directed in opposite direction while for **7** and **31** they assume an elongated shape. Superimposition of **7** and **31** to **2** (Figure 2) may indicate that the area occupied by the different compounds varies and sustains the hypothesis that compound **2** may fit into the enzyme's active site with another binding mode compared to **7** and **31**. In addition, the fact that compound **2** does not require any hydroxy or methoxy groups to achieve high activity in contrast to **7** or **31** also suggests a different positioning of these compounds in the binding site. It could therefore be deduced that the 17β-HSD2 active site may be very large. This space could easily be used to achieve selectivity toward other enzymes by introduction of appropriate substituents. It is striking that compounds with a linker n = 2 were inactive, although they were expected to fit from the steric hindrance point of view. It might indicate that the flexibility induced by the ethylene linker is not appropriate.

The selectivity profile of the 17β-HSD2 inhibitor is an important issue. Not to counteract the therapeutic concept, the functionally related enzymes like 17β-HSD1, -4, -5 should not be inhibited and no binding affinity to the ERs should be identified. The most potent 17β-HSD2 inhibitors identified in this study, **13a**, **19**, **31**, **32**, **1**, **2**, and **7**, are all selective toward 17β-HSD1 and do not bind to the estrogen receptors. It might indicate that the 17β-HSD2 active site is larger than that of 17β-HSD1 and the binding domains of the ERs. The size difference of the binding sites of these proteins is an interesting property, as it could facilitate the gain in selectivity of the 17β-HSD2 inhibitor toward 17β-HSD1 and ERs. In addition it is notable that the most active compounds with a linker n = 0, i.e., **13a**, **19**, **31**, and **32**, have a much higher selectivity factor than the one compound with n = 1, i.e., compound **7**. In the case of n = 0, the C ring seems to adopt a conformation of higher steric hindrance in the 17β-HSD1 active site than in the case of n = 1.

11β-HSD1 and 11β-HSD2 catalyze the oxidoreduction at position 11 of cortisone in cortisol. These two enzymes have an important function in the glucocorticoid biosynthesis and should not be inhibited. On the basis of structural similarities identified between 11β-HSD1 inhibitors and our amides derivatives, it is also important to verify the selectivity of our inhibitors toward these enzymes. None of the new amides discovered in this study inhibit 11β-HSD1 or 11β-HSD2 to an appreciable extend except for compound **7** which shows an IC_{50} of 1 μM for 11β-HSD1 and an IC_{50} of 61 nM for 17β-HSD2, the ratio resulting in a selectivity factor (SF) of 16. On the basis of the fact that elevated glucocorticoids levels have been associated with osteoporosis, moderate 11β-HSD1 inhibition might be still of advantage for the therapeutic concept.

Inhibition of 17β-HSD2 is a completely new approach for the treatment of osteoporosis compared to the existing treatments. A therapeutic effect similar to the one observed with estrogen replacement therapy (ERT), which has already been proven to be efficient in the treatment of osteoporosis, is expected after treatment with 17β-HSD2 inhibitors. ERT is not recommended because of severe side effects caused by the systemic increase in E2 at the necessary high doses. Inhibition of 17β-HSD2 will allow an increase in E2 in lower doses and only in targeted organs where the enzyme is present, i.e., in organs like placenta, brain, bone, breast, and ovaries. In addition after menopause, the ovaries do not function anymore and there is atrophy of the breast and of the uterus connected to a reduction of the metabolism/catabolism of the tissues. The levels in androstenedione and estrone in these organs may be reduced and therefore the amount of E2 and testosterone as well. Consequently treatment with 17β-HSD2 inhibitors may be less susceptible to induce breast cancer compared to ERT. 17β-HSD2 inhibition is thus not expected to induce severe adverse effects. A targeted effect in the bones should result in a superior drug compared to SERMs or bisphosphonates.

The five most potent compounds **7**, **13a**, **19**, **31**, and **32** were investigated regarding their ability to inhibit 17β-HSD2 from other species in order to identify an appropriate species for conducting in vivo experiments. The compounds were tested on the rat, mouse, and monkey 17β-HSD2. Only inhibitor **7** showed a good inhibition on the mouse enzyme. At this stage, the mouse can be considered as potential species to perform the in vivo proof of concept. It has the advantage that it is easily accessible and is well described, as it is often used for the study of bone diseases.[58,59] Metabolic stability and the pharmacokinetic profile of compound **7** have to be evaluated in the mouse to validate this species as adequate model.

In this study, we described the optimization of 17β-HSD2 inhibitors in the 2,5-thiophene and 1,3-phenylamide class by variation of the linker size between the C ring and the amide moiety. It led to the discovery of four new highly active compounds with the C ring directly attached to the amides **13a**, **19**, **31**, and **32** with an IC_{50} of around 60 nM in a cell-free assay, a very good cellular activity in the same range as in the cell-free assay, and a very high selectivity factor toward 17β-HSD1 above 100 and even higher than 800 for **31**. Compounds **13a**, **19**, **31**, and **32** are equipotent to the compound with the methylene linker **7** but show higher selectivity toward 17β-HSD1. SAR studies allowed a first characterization of the 17β-HSD2 active site which must be quite large and certainly larger than the one of 17β-HSD1. The mouse was identified as a potential animal in order to perform an in vivo proof of concept for the demonstration of the efficacy of 17β-HSD2 inhibitors in osteoporosis.

EXPERIMENTAL SECTION

1. Chemical Methods. Chemical names follow IUPAC nomenclature.

Starting materials were purchased from Aldrich, Acros, Lancaster, Roth, Merck, Combi-Blocks, or Fluka and were used without purification.

dx.doi.org/10.1021/jm3014053 | J. Med. Chem. 2013, 56, 167−181

Flash column chromatography (FC) was performed on silica gel (70−200 μm), and reaction progress was monitored by TLC on Alugram SIL G/UV254 (Macherey-Nagel). Visualization was accomplished with UV light.

^{1}H NMR and ^{13}C NMR spectra were measured on a Bruker AM500 spectrometer (at 500 and 125 MHz, respectively) at 300 K in CD_3COCD_3. Chemical shifts are reported in δ (parts per million, ppm) by reference to the hydrogenated residues of deuterated solvent as internal standard: 2.05 ppm (^{1}H NMR) and 30.8 and 206.3 ppm (^{13}C NMR). Signals are described as br (broad), s (singlet), d (doublet), t (triplet), dd (doublet of doublets), ddd (doublet of doublet of doublets), dt (doublet of triplets), or m (multiplet). All coupling constants (J) are given in hertz (Hz).

MS measurements were executed using a TSQ Quantum equipped with an electrospray interface (ESI) or an atmospheric pressure chemical ionization source (APCI) (Thermo Fischer, Dreieich, Germany) instrument. GC/MS spectra were measured on a GCD series G1800A (Hewlett-Packard) instrument with an Optima-5-MS (0.25 μM, 30 m) column (Macherey Nagel).

IR spectra were recorded on a Spectrum 100 FT-IR spectrometer (PerkinElmer) as neat sample.

Melting points were measured in open capillaries on a Stuart Scientific SMP3 apparatus and are uncorrected.

The purity of the compounds was evaluated by LC/MS. The Surveyor-LC-system consisted of a pump, an autosampler, and a PDA detector. Mass spectrometry was performed on a TSQ Quantum (ThermoFisher, Dreieich, Germany). The triple quadrupole mass spectrometer was equipped with an electrospray interface (ESI) or an atmospheric pressure chemical ionization (APCI). The system was operated by the standard software Xcalibur. A RP C18 Nucleodur 100-5 (3 mm) column (Macherey-Nagel GmbH, Dühren, Germany) was used as stationary phase. All solvents were HPLC grade. In a gradient run, the percentage of acetonitrile (containing 0.1% trifluoroacetic acid) in 0.1% trifluoroacetic acid was increased from an initial concentration of 0% at 0 min to 100% at 15 min and kept at 100% for 5 min. The injection volume was 15 μL, and flow rate was set to 800 μL/min. MS analysis was carried out at a needle voltage of 3000 V and a capillary temperature of 350 °C. Mass spectra were acquired in positive mode from 100 to 1000 m/z, and UV spectra were recorded at a wavelength of 254 nm and in some cases at 360 nm. All tested compounds have ≥95% chemical purity except compounds **15a** and **21**, which have a purity of 94% and 90%, respectively.

Compounds **4**,[31] **5a−d**,[32] **6a−l**,[32] and **7**[32] were prepared according to previously described procedures.

General Procedure for Amidation. Method A. At 0 °C, a solution of 3(4)-bromobenzoyl chloride or 5-bromothiophene-2-carbonyl chloride (1 equiv) in CH_2Cl_2 (2 mL/equiv) was added dropwise to a solution of the corresponding amine (1 equiv) and triethylamine (1.15 equiv) in solution in CH_2Cl_2 (2 mL/equiv). The mixture was kept stirred at 0 °C for 3 h and evaporated under reduced pressure. The residue was purified by FC with *n*-hexane/ethyl acetate or dichloromethane as eluant.

General Procedure for Suzuki Coupling. Method B. A mixture of aryl bromide (1 equiv), substituted phenylboronic acid (1.2 equiv), sodium carbonate (2 equiv), and tetrakis(triphenylphosphine)-palladium (0.1 equiv) in an oxygen free DME/water (1:1) solution was stirred at 80 °C for 4−14 h under nitrogen. The reaction mixture was cooled to room temperature. The aqueous layer was extracted with dichloromethane. The combined organic layers were washed with brine, dried over sodium sulfate, filtered, and concentrated to dryness. The product was purified by FC with *n*-hexane/ethyl acetate, dichloromethane, or dichloromethane/methanol as eluant.

General Procedure for Ether Cleavage. Method C. To a solution of methoxyphenyl compounds (1 equiv) in dry dichloromethane (5 mL/mmol of reactant), boron trifluoride−dimethyl sulfide complex (6 equiv/methoxy function) was added dropwise at 0 °C and stirred for 6−14 h. After the reaction was finished, the reaction mixture was diluted with dichloromethane and 5% aqueous $NaHCO_3$ was added until neutral pH was obtained. The aqueous layer was extracted with dichloromethane. The combined organic layers were washed with brine, dried over sodium sulfate, evaporated to dryness under reduced pressure. The product was purified by FC, with dichloromethane/methanol as eluant.

Detailed Synthesis Procedures of the Most Interesting Compounds. *N*-(3-Methoxyphenyl)-5-(4-methoxyphenyl)-*N*-methylthiophene-2-carboxamide (12). The title compound was prepared by reaction of 5-bromo-*N*-(3-methoxyphenyl)-*N*-methylthiophene-2-carboxamide **12b** (40 mg, 0.12 mmol) and 4-methoxyphenylboronic acid (22 mg, 0.14 mmol) with tetrakis(triphenylphosphine) palladium (14 mg, 0.012 mmol) according to method B for 6 h. Purification by FC (CH_2Cl_2/CH_3OH, 200:1) afforded the desired compound as a brown solid (40 mg, yield 92%). $C_{20}H_{19}NO_3S$; MW 353; mp 119−120 °C; MS (ESI) 354 (M + H)$^+$; ^{1}H NMR (CD_3COCD_3) 3.37 (s, 3H), 3.81 (s, 3H), 3.82 (s, 3H), 6.55 (d, J = 4.1 Hz, 1H), 6.92−6.96 (m, 3H), 6.97−7.01 (m, 2H), 7.02 (d, J = 4.1 Hz, 1H), 7.37 (td, J = 7.9, 0.6 Hz, 1H), 7.51 (d, J = 9.1 Hz, 2H).

***N*,5-Bis(3-methoxyphenyl)-*N*-methylthiophene-2-carboxamide (13a).** The title compound was prepared by reaction of 5-bromo-*N*-(3-methoxyphenyl)-*N*-methylthiophene-2-carboxamide **12b** (75 mg, 0.23 mmol) and 3-methoxyphenylboronic acid (41 mg, 0.27 mmol) with tetrakis(triphenylphosphine)palladium (27 mg, 0.023 mmol) according to method B for 5 h. Purification by FC (CH_2Cl_2) afforded the desired compound as a yellow solid (80 mg, yield 98%). $C_{20}H_{19}NO_3S$; MW 353; mp 116−117 °C; MS (ESI) 354 (M + H)$^+$; ^{1}H NMR (CD_3COCD_3) 3.38 (s, 3H), 3.82 (s, 3H), 3.83 (s, 3H), 6.58 (d, J = 4.1 Hz, 1H), 6.90 (ddd, J = 8.2, 2.5, 0.9 Hz, 1H), 6.94 (ddd, J = 7.6, 1.6, 0.9 Hz, 1H), 6.98−7.01 (m, 2H), 7.12 (t, J = 2.0 Hz, 1H), 7.15 (ddd, J = 7.6, 1.6, 0.9 Hz, 1H), 7.15 (d, J = 4.1 Hz, 1H), 7.30 (t, J = 8.0 Hz, 1H), 7.38 (td, J = 8.0, 0.9 Hz, 1H).

***N*-(3-Methoxyphenyl)-*N*-methyl-5-phenylthiophene-2-carboxamide (15a).** The title compound was prepared by reaction of 5-bromo-*N*-(3-methoxyphenyl)-*N*-methylthiophene-2-carboxamide **12b** (75 mg, 0.23 mmol) and phenylboronic acid (33 mg, 0.27 mmol) with tetrakis(triphenylphosphine)palladium (27 mg, 0.023 mmol) according to method B for 4 h. Purification by FC (*n*-hexane/ethyl acetate, 10:1 → 6:1) afforded the desired compound as a beige solid (70 mg, yield 94%). $C_{19}H_{17}NO_2S$; MW 323; mp 126−127 °C; MS (ESI) 324 (M + H)$^+$; ^{1}H NMR (CD_3COCD_3) 3.38 (s, 3H), 3.82 (s, 3H), 6.60 (d, J = 4.0 Hz, 1H), 6.94 (ddd, J = 8.0, 2.1, 0.9 Hz, 1H), 6.99−7.01 (m, 2H), 7.16 (d, J = 4.0 Hz, 1H), 7.32 (ddt, J = 8.0, 6.3, 1.2 Hz, 1H), 7.36−7.41 (m, 3H), 7.59 (d, J = 8.0 Hz, 2H).

***N*-(3-Methoxyphenyl)-*N*-methyl-5-*m*-tolylthiophene-2-carboxamide (19).** The title compound was prepared by reaction of 5-bromo-*N*-(3-methoxyphenyl)-*N*-methylthiophene-2-carboxamide **12b** (33 mg, 0.1 mmol) and 3-methylphenylboronic acid (19 mg, 0.14 mmol) with tetrakis(triphenylphosphine)palladium (12 mg, 0.01 mmol) according to method B for 8 h. Purification by FC (*n*-hexane/ethyl acetate, 10:1 → 6:1) afforded the desired compound as a beige solid (26 mg, yield 77%). $C_{20}H_{19}NO_2S$; MW 337; mp 128−129 °C; MS (ESI) 338 (M + H)$^+$; ^{1}H NMR (CD_3COCD_3) 2.34 (s, 3H), 3.38 (s, 3H), 3.81 (s, 3H), 6.57 (d, J = 4.0 Hz, 1H), 6.94 (ddd, J = 7.9, 2.2, 0.9 Hz, 1H), 6.98−7.01 (m, 2H), 7.13 (d, J = 4.0 Hz, 1H), 7.14−7.16 (m, 1H), 7.27 (t, J = 7.9 Hz, 1H), 7.36−7.39 (m, 2H), 7.41−7.42 (m, 1H).

5-(3-(Dimethylamino)phenyl)-*N*-(3-methoxyphenyl)-*N*-methylthiophene-2-carboxamide (20). The title compound was prepared by reaction of 5-bromo-*N*-(3-methoxyphenyl)-*N*-methylthiophene-2-carboxamide **12b** (49 mg, 0.15 mmol) and 3-(dimethylamino)phenylboronic acid (30 mg, 0.18 mmol) with tetrakis(triphenylphosphine)palladium (17 mg, 0.015 mmol) according to method B for 14 h. Purification by FC (*n*-hexane/ethyl acetate, 10:1 → 6:1) afforded the desired compound as an orange solid (26 mg, yield 47%). $C_{21}H_{22}N_2O_2S$; MW 366; mp 121−122 °C; MS (ESI) 367 (M + H)$^+$; ^{1}H NMR (CD_3COCD_3) 2.96 (s, 6H), 3.38 (s, 3H), 3.82 (s, 3H), 6.56 (d, J = 4.0 Hz, 1H), 6.72 (dd, J = 8.2, 2.4 Hz, 1H), 6.86 (d, J = 7.6 Hz, 1H), 6.89 (t, J = 2.0 Hz, 1H), 6.94 (d, J = 7.6 Hz, 1H), 6.98−7.01 (m, 2H), 7.10 (d, J = 4.0 Hz, 1H), 7.19 (t, J = 7.9 Hz, 1H), 7.37 (t, J = 7.9 Hz, 1H).

***N*-(3-Methoxyphenyl)-*N*-methyl-5-(3-(methylthio)phenyl)-thiophene-2-carboxamide (21).** The title compound was prepared

by reaction of 5-bromo-*N*-(3-methoxyphenyl)-*N*-methylthiophene-2-carboxamide **12b** (33 mg, 0.1 mmol) and 3-(methylthio)-phenylboronic acid (23 mg, 0.14 mmol) with tetrakis-(triphenylphosphine)palladium (12 mg, 0.01 mmol) according to method B for 8 h. Purification by FC (*n*-hexane/ethyl acetate, 10:1 → 7:1) afforded the desired compound as a yellowish solid (22 mg, yield 59%). $C_{20}H_{19}NO_2S_2$; MW 369; mp 109−110 °C; MS (ESI) 370 (M + H)$^+$; ^{1}H NMR (CD_3COCD_3) 2.52 (s, 3H), 3.38 (s, 3H), 3.82 (s, 3H), 6.59 (d, *J* = 4.0 Hz, 1H), 6.94 (ddd, *J* = 8.0, 1.9, 0.9 Hz, 1H), 6.98−7.02 (m, 2H), 7.18 (d, *J* = 4.0 Hz, 1H), 7.23 (dt, *J* = 6.9, 1.9 Hz, 1H), 7.30−7.35 (m, 2H), 7.38 (td, *J* = 8.0, 0.9 Hz, 1H), 7.44−7.45 (m, 1H).

5-(2-Fluoro-3-methoxyphenyl)-*N*-(3-methoxyphenyl)-*N*-methylthiophene-2-carboxamide (31). The title compound was prepared by reaction of 5-bromo-*N*-(3-methoxyphenyl)-*N*-methylthiophene-2-carboxamide **12b** (40 mg, 0.12 mmol) and 2-fluoro-3-methoxyphenylboronic acid (25 mg, 0.14 mmol) with tetrakis-(triphenylphosphine)palladium (14 mg, 0.012 mmol) according to method B for 14 h. Purification by FC (*n*-hexane/ethyl acetate, 10:1 → 6:1) afforded the desired compound as a brown solid (30 mg, yield 66%). $C_{20}H_{18}FNO_3S$; MW 371; mp 159−160 °C; MS (ESI) 372 (M + H)$^+$; ^{1}H NMR (CD_3COCD_3) 3.38 (s, 3H), 3.82 (s, 3H), 3.90 (s, 3H), 6.65 (dd, *J* = 4.0, 1.0 Hz, 1H), 6.95 (ddd, *J* = 7.6, 1.8, 1.0 Hz, 1H), 6.99−7.01 (m, 2H), 7.09−7.20 (m, 3H), 7.23 (dd, *J* = 4.0, 1.0 Hz, 1H), 7.37 (dd, *J* = 9.1, 7.9 Hz, 1H).

5-(2-Fluoro-3-methylphenyl)-*N*-(3-methoxyphenyl)-*N*-methylthiophene-2-carboxamide (36). The title compound was prepared by reaction of 5-bromo-*N*-(3-methoxyphenyl)-*N*-methylthiophene-2-carboxamide **12b** (49 mg, 0.15 mmol) and 2-fluoro-3-methylphenylboronic acid (28 mg, 0.18 mmol) with tetrakis-(triphenylphosphine)palladium (17 mg, 0.015 mmol) according to method B for 14 h. Purification by FC (*n*-hexane/ethyl acetate, 10:1) afforded the desired compound as a colorless solid (50 mg, yield 94%). $C_{20}H_{18}FNO_2S$; MW 355; mp 142−143 °C; MS (APCI) 356 (M + H)$^+$; ^{1}H NMR (CD_3COCD_3) 2.29 (d, *J* = 2.5 Hz, 3H), 3.39 (s, 3H), 3.81 (s, 3H), 6.63 (dd, *J* = 4.1, 0.9 Hz, 1H), 6.94 (ddd, *J* = 7.9, 1.9, 0.9 Hz, 1H), 6.98−7.01 (m, 2H), 7.11 (t, *J* = 7.9 Hz, 1H), 7.22 (dd, *J* = 4.1, 0.9 Hz, 1H), 7.23−7.25 (m, 1H), 7.36−7.39 (m, 1H), 7.45−7.48 (m, 1H).

5-(2,6-Difluoro-3-methoxyphenyl)-*N*-(3-methoxyphenyl)-*N*-methylthiophene-2-carboxamide (37). The title compound was prepared by reaction of 5-bromo-*N*-(3-methoxyphenyl)-*N*-methylthiophene-2-carboxamide **12b** (33 mg, 0.1 mmol) and 2,6-difluoro-3-methoxyphenylboronic acid (26 mg, 0.14 mmol) with tetrakis-(triphenylphosphine)palladium (12 mg, 0.01 mmol) according to method B for 14 h. Purification by FC (*n*-hexane/ethyl acetate, 10:1) afforded the desired compound as an orange solid (10 mg, yield 26%). $C_{20}H_{17}F_2NO_3S$; MW 389; mp 147−148 °C; MS (ESI) 390 (M + H)$^+$; ^{1}H NMR (CD_3COCD_3) 3.40 (s, 3H), 3.82 (s, 3H), 3.90 (s, 3H), 6,71 (dt, *J* = 4.1, 0.9 Hz, 1H), 6.95 (ddd, *J* = 7.6, 1.9, 0.9 Hz, 1H), 6.99−7.01 (m, 2H), 7.05 (ddd, *J* = 11.4, 9.1, 2.2 Hz, 1H), 7.16 (td, *J* = 9.1, 5.0 Hz, 1H), 7.23 (dt, *J* = 4.1, 1.1 Hz, 1H), 7.36−7.39 (m, 1H).

5-(3-Fluoro-4-methoxyphenyl)-*N*-(3-methoxyphenyl)-*N*-methylthiophene-2-carboxamide (38). The title compound was prepared by reaction of 5-bromo-*N*-(3-methoxyphenyl)-*N*-methylthiophene-2-carboxamide **12b** (40 mg, 0.12 mmol) and 3-fluoro-4-methoxyphenylboronic acid (25 mg, 0.14 mmol) with tetrakis-(triphenylphosphine)palladium (14 mg, 0.015 mmol) according to method B for 6 h. Purification by FC (*n*-hexane/ethyl acetate, 10:1 → 6:1) afforded the desired compound as a yellow solid (40 mg, yield 72%). $C_{20}H_{18}FNO_3S$; MW 371; mp 157−158 °C; MS (ESI) 372 (M + H)$^+$; ^{1}H NMR (CD_3COCD_3) 3.38 (s, 3H), 3.82 (s, 3H), 3.91 (s, 3H), 6.55 (d, *J* = 4.0 Hz, 1H), 6.94 (ddd, *J* = 7.9, 1.9, 0.9 Hz, 1H), 6.99−7.01 (m, 2H), 7.08 (d, *J* = 4.0 Hz, 1H), 7.15 (t, *J* = 8.5 Hz, 1H), 7.33−7.39 (m, 3H).

5-(2,4-Dimethoxyphenyl)-*N*-(3-methoxyphenyl)-*N*-methylthiophene-2-carboxamide (41). The title compound was prepared by reaction of 5-bromo-*N*-(3-methoxyphenyl)-*N*-methylthiophene-2-carboxamide **12b** (40 mg, 0.12 mmol) and 2,4-dimethoxyphenylboronic acid (27 mg, 0.14 mmol) with tetrakis(triphenylphosphine) palladium (14 mg, 0.012 mmol) according to method B for 14 h. Purification by FC (*n*-hexane/ethyl acetate, 10:1 → 6:1) afforded the desired compound as a colorless solid (35 mg, yield 74%). $C_{21}H_{21}NO_4S$; MW 383; mp 117−118 °C; MS (ESI) 384 (M + H)$^+$; ^{1}H NMR (CD_3COCD_3) 3.37 (s, 3H), 3.82 (s, 3H), 3.83 (s, 3H), 3.89 (s, 3H), 6.57 (ddd, *J* = 8.5, 2.4, 0.9 Hz, 1H), 6.63−6.64 (m, 2H), 6.92 (ddd, *J* = 7.9, 2.1, 0.9 Hz, 1H), 6.97 (t, *J* = 2.1 Hz, 1H), 7.00 (ddd, *J* = 8.2, 2.7, 0.9 Hz, 1H), 7.15 (d, *J* = 4.3 Hz, 1H), 7.37 (t, *J* = 8.1 Hz, 1H), 7.55 (d, *J* = 8.5 Hz, 1H).

5-(3-Methoxyphenyl)-*N*-methyl-*N*-*m*-tolylthiophene-2-carboxamide (22a). The title compound was prepared by reaction of 5-bromo-*N*-methyl-*N*-*m*-tolylthiophene-2-carboxamide **22b** (78 mg, 0.25 mmol) and 3-methoxyphenylboronic acid (45 mg, 0.3 mmol) with tetrakis(triphenylphosphine)palladium (29 mg, 0.025 mmol) according to method B for 4 h. Purification by FC (*n*-hexane/ethyl acetate, 25:1 → 10:1) afforded the desired compound as a colorless solid (65 mg, yield 77%). $C_{20}H_{19}NO_2S$; MW 337; mp 97−98 °C; MS (ESI) 338 (M + H)$^+$; ^{1}H NMR (CD_3COCD_3) 2.36 (s, 3H), 3.37 (s, 3H), 3.83 (s, 3H), 6.51 (d, *J* = 4.1 Hz, 1H), 6.90 (ddd, *J* = 8.2, 2.5, 0.9 Hz, 1H), 7.10−7.11 (m, 1H), 7.13−7.17 (m, 3H), 7.23 (s, 1H), 7.26 (d, *J* = 7.6 Hz, 1H), 7.30 (t, *J* = 7.6 Hz, 1H), 7.36 (t, *J* = 7.7 Hz, 1H).

5-(3-Hydroxyphenyl)-*N*-methyl-*N*-*m*-tolylthiophene-2-carboxamide (22). The title compound was prepared by reaction of 5-(3-methoxyphenyl)-*N*-methyl-*N*-*m*-tolylthiophene-2-carboxamide **22a** (40 mg, 0.12 mmol) with boron trifluoride−dimethyl sulfide complex (0.08 mL, 0.72 mmol) according to method C for 14 h. Purification by FC (CH_2Cl_2/CH_3OH, 100:1 → 50:1) afforded the title compound as a beige solid (30 mg, yield 79%). $C_{19}H_{17}NO_2S$; MW 323; mp 157−158 °C; MS (ESI) 324 (M + H)$^+$; ^{1}H NMR (CD_3COCD_3) 2.36 (s, 3H), 3.37 (s, 3H), 6.52 (d, *J* = 4.1 Hz, 1H), 6.81 (ddd, *J* = 8.0, 2.5, 0.9 Hz, 1H), 7.03−7.06 (m, 2H), 7.08 (d, *J* = 4.1 Hz, 1H), 7.16 (d, *J* = 8.0 Hz, 1H), 7.20 (d, *J* = 7.6 Hz, 1H), 7.22 (s, 1H), 7.26 (d, *J* = 7.6 Hz, 1H), 7.36 (t, *J* = 8.0 Hz, 1H), 8.51 (s, 1H).

5-(2-Fluoro-3-methoxyphenyl)-*N*-methyl-*N*-(*m*-tolylthiophene)-2-carboxamide (32). The title compound was prepared by reaction of 5-bromo-*N*-methyl-*N*-*m*-tolylthiophene-2-carboxamide **22b** (46 mg, 0.15 mmol) and 2-fluoro-3-methoxyphenylboronic acid (31 mg, 0.18 mmol) with tetrakis(triphenylphosphine)palladium (17 mg, 0.015 mmol) according to method B for 14 h. Purification by FC (*n*-hexane/ethyl acetate, 10:1) afforded the desired compound as a colorless solid (45 mg, yield 85%). $C_{20}H_{18}FNO_2S$; MW 355; mp 120−121 °C; MS (ESI) 356 (M + H)$^+$; ^{1}H NMR (CD_3COCD_3) 2.36 (s, 3H), 3.38 (s, 3H), 3.90 (s, 3H), 6.58 (dd, *J* = 4.0, 1.0 Hz, 1H), 7.08−7.19 (m, 4H), 7.21 (dd, *J* = 4.1, 1.0 Hz, 1H), 7.23−7.27 (m, 2H), 7.36 (t, *J* = 7.7 Hz, 1H).

5-(3-Methoxyphenyl)-*N*-methyl-*N*-(3-(trifluoromethyl)-phenyl)thiophene-2-carboxamide (24). The title compound was prepared by reaction of 5-bromo-*N*-methyl-*N*-(3-(trifluoromethyl)-phenyl)thiophene-2-carboxamide **24b** (36 mg, 0.1 mmol) and 3-methoxyphenylboronic acid (20 mg, 0.13 mmol) with tetrakis-(triphenylphosphine)palladium (12 mg, 0.01 mmol) according to method B for 6 h. Purification by FC (*n*-hexane/ethyl acetate, 10:1 → 5:1) afforded the desired compound as a yellow solid (35 mg, yield 90%). $C_{20}H_{16}F_3NO_2S$; MW 391; mp 97−98 °C; MS (ESI) 392 (M + H)$^+$; ^{1}H NMR (CD_3COCD_3) 3.47 (s, 3H), 3.83 (s, 3H), 6.57 (d, *J* = 4.1 Hz, 1H), 6.91 (ddd, *J* = 8.2, 2.5, 0.9 Hz, 1H), 7.11 (t, *J* = 2.2 Hz, 1H), 7.14 (ddd, *J* = 7.6, 1.6, 0.9 Hz, 1H), 7.19 (d, *J* = 4.1 Hz, 1H), 7.31 (t, *J* = 8.2 Hz, 1H), 7.69−7.78 (m, 3H), 7.81−7.82 (m, 1H); ^{13}C NMR (CD_3COCD_3) 39.0, 55.6, 112.0, 115.0, 119.0, 124.1, 125.3, 125.4, 125.8, 125.9, 131.1, 131.7, 132.2, 132.5, 133.0, 133.5, 135.5, 138.2, 146.3, 149.2, 161.2, 162.6; IR (cm^{-1}) 3046, 2963, 1608, 1438, 1330, 1117, 707 .

***N*-(Biphenyl-3-yl)-5-(3-methoxyphenyl)-*N*-methylthiophene-2-carboxamide (26).** The title compound was prepared by reaction of *N*-(biphenyl-3-yl)-5-bromo-*N*-methylthiophene-2-carboxamide **26b** (37 mg, 0.1 mmol) and 3-methoxyphenylboronic acid (18 mg, 0.12 mmol) with tetrakis(triphenylphosphine)palladium (12 mg, 0.01 mmol) according to method B for 14 h. Purification by FC (*n*-hexane/ethyl acetate 8:1) afforded the desired compound as a yellow solid (38 mg, yield 95%). $C_{25}H_{21}NO_2S$; MW 399; mp 108−109 °C; MS (ESI) 400 (M + H)$^+$; ^{1}H NMR (CD_3COCD_3) 3.46 (s, 3H), 3.81

dx.doi.org/10.1021/jm3014053 | *J. Med. Chem.* 2013, 56, 167−181

(s, 3H), 6.65 (d, J = 4.0 Hz, 1H), 6.89 (dd, J = 8.0, 2.1 Hz, 1H), 7.09 (s, 1H), 7.12 (d, J = 7.6 Hz, 1H), 7.15 (d, J = 4.0 Hz, 1H), 7.28 (t, J = 8.0 Hz, 1H), 7.36−7.39 (m, 2H), 7.46 (t, J = 7.8 Hz, 2H), 7.57 (t, J = 7.8 Hz, 1H), 7.68 (d, J = 8.0 Hz, 2H), 7.71−7.74 (m, 2H).

log *P* Determination. The log P values were calculated from CambridgeSoft Chem & Bio Draw 11.0 using the ChemDrawPro 11.0 program.

2. Biological Methods. [2,4,6,7-^{3}H]E2, [6,7-^{3}H]E2, [2,4,6,7-^{3}H]E1, and [1,2,6,7-^{3}H]A-dione were bought from Perkin-Elmer, Boston, MA. Quickszint Flow 302 scintillator fluid was bought from Zinsser Analytic, Frankfurt, Germany. ReadyFlow III scintillation fluid was from Beckman. Other chemicals were purchased from Sigma, Serva, Roth, or Merck.

Cytosolic (17β-HSD1) and microsomal (17β-HSD2) fractions were obtained from human and *Callithrix jacchus* placenta according to previously described procedures[46,47,60] and from mouse liver tissues.[61] Fresh tissue was homogenized and centrifuged. The pellet fraction contains the microsomal 17β-HSD2 and was used for the determination of E1 formation, while 17β-HSD1 was obtained after precipitation with ammonium sulfate from the cytosolic fraction for use of testing of E2 formation.

Human 17β-HSD4 and 17β-HSD5 were cloned into the modified pGEX-2T vector.[50] For the multidomain enzyme 17β-HSD4, only the steroid converting SDR domain was subcloned.[50] The human 11β-HSD1 and 11β-HSD2 were stably transfected in HEK cells as described earlier by Odermatt.[62]

Inhibition of 17β-HSD2/E1 Formation in Cell-Free Assay. Inhibitory activities were evaluated by an established method with minor modifications.[23,63,64] Briefly, the enzyme preparation was incubated with NAD^+ [1500 μM] in the presence of potential inhibitors at 37 °C in a phosphate buffer (50 mM) supplemented with 20% of glycerol and EDTA, 1 mM. Inhibitor stock solutions were prepared in DMSO. Final concentration of DMSO was adjusted to 1% in all samples. The enzymatic reaction was started by addition of a mixture of unlabeled E2 and [^{3}H]E2 (final concentration of 500 nM, 0.11 μCi). After 20 min, the incubation was stopped with $HgCl_2$ and the mixture was extracted with ether. After evaporation, the steroids were dissolved in acetonitrile/water (45:55). E1 and E2 were separated using acetonitrile/water (45:55) as mobile phase in a C18 RP chromatography column (Nucleodur C18, 3 μm, Macherey-Nagel, Düren, Germany) connected to a HPLC system (Agilent 1100 series, Agilent Technologies, Waldbronn, Germany). Detection and quantification of the steroids were performed using a radioflow detector (Berthold Technologies, Bad Wildbad, Germany). The conversion rate was calculated according to the following equation: % conversion = [(% E1)/(% E1 + % E2)] × 100. Each value was calculated from at least three independent experiments.

Inhibition of 17β-HSD1/E2 Formation in Cell-Free Assay. The 17β-HSD1 inhibition assay was performed similarly to the 17β-HSD2 test. The microsomal fraction was incubated with NADH (500 μM), test compound, and a mixture of unlabeled E1 and [^{3}H]E1 (final concentration of 500 nM, 0.15 μCi) for 10 min at 37 °C. Further treatment of the samples and HPLC separation were carried out as mentioned above for 17β-HSD2.

Inhibition of Human 17β-HSD4 and 17β-HSD5. Inhibitory activity was assessed as described earlier.[50,51] Briefly, for 17β-HSD4 inhibition, an appropriate amount of bacteria containing recombinantly expressed human 17β-HSD4 (SDR domain)[50] was resuspended in 100 mM sodium phosphate buffer, pH 7.7. Substrate [6,7-^{3}H]E2 and inhibitor (dissolved in DMSO) were added in final concentrations of 21 nM and 1 μM (1% (v/v) DMSO), respectively. Controls contained 1% DMSO without inhibitor. The enzymatic reaction was started with the addition of NAD^+ (750 μM final).

For 17β-HSD5 inhibition, an appropriate amount of bacterial lysate containing recombinantly expressed human 17β-HSD556 was dissolved in 100 mM sodium phosphate buffer, pH 6.6. Substrate [1,2,6,7-^{3}H]A-dione and inhibitor (dissolved in DMSO) were added in final concentrations of 21 nM and 1 μM (1% (v/v) DMSO), respectively. Controls contained 1% DMSO without inhibitor. The enzymatic reaction was started with the addition of NADPH (600 μM final). The incubation at 37 °C was stopped with 0.21 M ascorbic acid in methanol/acetic acid (99:1) after the time needed to convert approximately 30% of the substrate in a control assay without inhibitor. Steroids were extracted from the assay mixture by SPE using Strata C18-E columns (Phenomenex), eluted with methanol, and separated by RP-HPLC (column Luna, 5 μm C18(2), 150 mm; Phenomenex) at a flow rate of 1 mL/min acetonitrile/water (43:57). Radioactivity was detected by online scintillation counting with a Berthold LB506D detector (Berthold Technologies, Bad Wildbad, Germany) after mixing with ReadyFlow III (Beckman). Conversion was calculated from integration of substrate and product peaks. For calculation of inhibitory potential, conversion of the control assays (assays without inhibitor) was set to 0% inhibition. Assays were run in triplicate.

Inhibition of 11β-HSD1 and 11β-HSD2 Using Cell Lysates. HEK-293 cells stably transfected with 11β-HSD1 or 11β-HSD2 were cultured in Dulbecco's modified Eagle medium (DMEM) containing 4.5 g/L glucose, supplemented with 10% fetal bovine serum, MEM nonessential amino acids, 100 U/mL penicillin, 0.1 mg/mL streptomycin, and 10 mM HEPES, pH 7.4. Cells were grown to 90% confluence, washed with PBS, suspended, and centrifuged for 4 min at 150g. Cell pellets were frozen and stored at −80 °C.

Inhibitors were dissolved in DMSO to obtain stock solutions of 10 mM and stored as 100 μL aliquots at −20 °C. [1,2-^{3}H]Cortisone was purchased from American Radiolabeled Chemicals (St. Louis, MO, U.S.), and [1,2,6,7-^{3}H]cortisol was from Amersham Pharmacia (Piscataway, NJ, U.S.). All other chemicals were obtained from Sigma-Aldrich Chemie GmbH (Buchs, Switzerland) of the highest grade available.

Activity assays were performed as described by Kratschmar et al.[54] Briefly, cell lysates were incubated for 10 min at 37 °C in TS2 buffer (100 mM NaCl, 1 mM EGTA, 1 mM EDTA, 1 mM $MgCl_2$, 250 mM sucrose, 20 mM Tris-HCl, pH 7.4) in a final volume of 22 μL, containing either vehicle (0.2% DMSO) or the corresponding inhibitor at 2 and 20 μM. To measure 11β-HSD1 activity, the reaction mixture contained 380 nM unlabeled cortisone, 20 nM [1,2-^{3}H]cortisone, and 500 μM NADPH. 11β-HSD2 activity was determined in a reaction mixture containing 80 nM unlabeled cortisol, 20 nM [1,2,6,7-^{3}H]cortisol, and 500 μM NAD^+. Reactions were stopped after 10 min by the addition of an excess of unlabeled cortisone and cortisol (2 mM, in methanol). Steroids were separated by TLC, followed by scintillation counting and calculation of substrate conversion. Data were obtained from three independent experiments.

Inhibition of 17β-HSD2 in a Cellular Assay. Cellular 17β-HSD2 activity is measured using the breast cancer cell-line MDA-MB-231[65] (17β-HSD1 activity negligible). [^{3}H]E2 (200 nM) is taken as substrate and is incubated with the inhibitor for 6 h at 37 °C. After ether extraction, substrate and product are separated by HPLC and detected with a radioflow detector. Potency is evaluated as percentage of inhibition (inhibitor concentration of 1 μM) and as IC_{50} values.

ER Affinity in a Cellular Free Assay. The binding affinity of selected compounds to the ERα and ERβ was determined according to Zimmermann et al.[49] using recombinant human proteins. Briefly, 0.25 pmol of ERα or ERβ was incubated with [^{3}H]E2 (10 nM) and test compound for 1 h at room temperature. The potential inhibitor was dissolved in DMSO (5% final concentration). Nonspecific binding was performed with diethylstilbestrol (10 μM). After incubation, ligand−receptor complexes were selectively bound to hydroxyapatite (5 g/60 mL of TE buffer). The formed complex was separated, washed, and resuspended in ethanol. For radiodetection, scintillator cocktail (Quickszint 212, Zinsser Analytic, Frankfurt, Germany) was added and samples were measured in a liquid scintillation counter (Rack Beta Primo 1209, Wallac, Turku, Finland). For determination of the relative binding affinity (RBA), inhibitor and E2 concentrations required to displace 50% of the receptor bound labeled E2 were determined: RBA (%) = IC_{50}(E2)/IC_{50}(compound) × 100. The RBA value for E2 was arbitrarily set at 100%.

Cytotoxicity. For evaluation of cytotoxicity, conversion of 3-(4,5-dimethylthiazol-2-yl)-2,5-diphenyltetrazolium bromide (MTT) is determined according to Denizot and Lang with minor modifica-

tions.[57] Experiments were performed in 96-well cell culture plates in DMEM supplemented with 10% FCS. MDA-MB-231 cells are incubated with the compounds for 3 h at 37 °C in 5% CO_2 humidified atmosphere. After an MTT incubation of another 3 h the cleavage of MTT to a blue formazane by mitochondrial succinate dehydrogenase was stopped and cell lysis was carried out by addition of sodium dodecyl sulfate (SDS) in 0.01 N HCl (10%). The produced blue formazane was quantified spectrophotometrically at 590 nm.

■ ASSOCIATED CONTENT

Supporting Information

Chemical synthesis and characterization of all compounds and HPLC purity determination. This material is available free of charge via the Internet at http://pubs.acs.org.

■ AUTHOR INFORMATION

Corresponding Author

*Phone: +49 681 302 70300. Fax: +49 681 302 70308. E-mail: rwh@mx.uni-saarland.de. Web site: http://www.pharmmedchem.de.

Author Contributions

#S.M.-O. and K.X. contributed equally to this work.

Notes

The authors declare no competing financial interest.

■ ACKNOWLEDGMENTS

We thank Josef Zapp for the NMR measurements, Martina Jankowski for the LC mass spectra, and Jannine Ludwig, Jeannine Jung, Laura Schrobildgen, and Jörg Haupenthal for the biological tests. K.X. is grateful to the Alexander von Humboldt Foundation (AvH) for a fellowship. We are thankful to Prof. A. Einspanier for the gift of monkey placentas. We acknowledge the Deutsche Forschungsgemeinschaft (DFG) for financial support (Grants HA1315/12-1 and AD 127/10-1).

■ ABBREVIATIONS USED

17β-HSD2, 17β-hydroxysteroid dehydrogenase type 2; 17β-HSD1, 17β-hydroxysteroid dehydrogenase type 1; E1, estrone; E2, 17β-estradiol; T, testosterone; DHT, dihydrotestosterone; DHEA, dehydroepiandrosterone; Δ^4-AD, Δ^4-androstene-3,17-dione; FC, flash chromatography; SF, selectivity factor; RBA, relative binding affinity; ER, estrogen receptor; ERT, estrogen replacement therapy; RBA, relative binding affinity; inh, inhibition; MEP, molecular electrostatic potential

■ ADDITIONAL NOTE

For the sake of clarity, IUPAC nomenclature is not strictly followed except for the experimental part where the correct IUPAC names are given.

■ REFERENCES

(1) Wu, L.; Einstein, M.; Geissler, W. M.; Chan, H. K.; Elliston, K. O.; Andersson, S. Expression cloning and characterization of human 17 beta-hydroxysteroid dehydrogenase type 2, a microsomal enzyme possessing 20 alpha-hydroxysteroid dehydrogenase activity. *J. Biol. Chem.* **1993**, *268*, 12964−12969.

(2) Suzuki, T.; Sasano, H.; Andersson, S.; Mason, J. I. 3β-Hydroxysteroid dehydrogenase/Δ5→4-isomerase activity associated with the human 17β-hydroxysteroid dehydrogenase type 2 isoform. *J. Clin. Endocrinol. Metab.* **2000**, *85*, 3669−3672.

(3) Bodine, P. V. N.; Komm, B. S. Tissue culture models for studies of hormone and vitamin action in bone cells. *Vitam. Horm.* **2002**, *64*, 101−151.

(4) Vanderschueren, D.; Gaytant, J.; Boonen, S.; Venken, K. Androgens and bone. *Curr. Opin. Endocrinol., Diabetes Obes.* **2008**, *15*, 250−254.

(5) Vanderschueren, D.; Vandenput, L.; Boonen, S.; Lindberg, M. K.; Bouillon, R.; Ohlsson, C. Androgens and bone. *Endocr. Rev.* **2004**, *25*, 389−425.

(6) Cree, M.; Soskolne, C. L.; Belseck, E.; Hornig, J.; McElhaney, J. E.; Brant, R.; Suarez-Almazor, M. Mortality and institutionalization following hip fracture. *J. Am. Geriatr. Soc.* **2000**, *48*, 283−288.

(7) McCloskey, E. Effects of third-generation aromatase inhibitors on bone. *Eur. J. Cancer* **2006**, *42*, 1044−1051.

(8) Marcus, R.; Wong, M.; Heath, H., 3rd; Stock, J. L. Antiresorptive treatment of postmenopausal osteoporosis: comparison of study designs and outcomes in large clinical trials with fracture as an endpoint. *Endocr. Rev.* **2002**, *23*, 16−37.

(9) Orwoll, E.; Ettinger, M.; Weiss, S.; Miller, P.; Kendler, D.; Graham, J.; Adami, S.; Weber, K.; Lorenc, R.; Pietschmann, P.; Vandormael, K.; Lombardi, A. Alendronate for the treatment of osteoporosis in men. *N. Engl. J. Med.* **2000**, *343*, 604−610.

(10) Ringe, J. D.; Faber, H.; Farahmand, P.; Dorst, A. Efficacy of risedronate in men with primary and secondary osteoporosis: results of a 1-year study. *Rheumatol. Int.* **2006**, *26*, 427−31.

(11) Ettinger, B.; Black, D. M.; Mitlak, B. H.; Knickerbocker, R. K.; Nickelsen, T.; Genant, H. K.; Christiansen, C.; Delmas, P. D.; Zanchetta, J. R.; Stakkestad, J.; Glüer, C. C.; Krueger, K.; Cohen, F. J.; Eckert, S.; Ensrud, K. E.; Avioli, L. V.; Lips, P.; Cummings, S. R. Reduction of vertebral fracture risk in postmenopausal women with osteoporosis treated with raloxifene: results from a 3-year randomized clinical trial. Multiple Outcomes of Raloxifene Evaluation (MORE) Investigators. *JAMA, J. Am. Med. Assoc.* **1999**, *282*, 637−645.

(12) Felson, D. T.; Zhang, Y.; Hannan, M. T.; Kiel, D. P.; Wilson, P. W.; Anderson, J. J. The effect of postmenopausal estrogen therapy on bone density in elderly women. *N. Engl. J. Med.* **1993**, *329*, 1141−1146.

(13) Chen, C.-L.; Weiss, N. S.; Newcomb, P.; Barlow, W.; White, E. Hormone replacement therapy in relation to breast cancer. *JAMA, J. Am. Med. Assoc.* **2002**, *287*, 734−741.

(14) Beresford, S. A.; Weiss, N. S.; Voigt, L. F.; McKnight, B. Risk of endometrial cancer in relation to use of oestrogen combined with cyclic progestagen therapy in postmenopausal women. *Lancet* **1997**, *349*, 458−61.

(15) Grady, D.; Gebretsadik, T.; Kerlikowske, K.; Ernster, V.; Petitti, D. Hormone replacement therapy and endometrial cancer risk: a meta-analysis. *Obstet. Gynecol.* **1995**, *85*, 304−313.

(16) Dong, Y.; Qiu, Q. Q.; Debear, J.; Lathrop, W. F.; Bertolini, D. R.; Tamburini, P. P. 17Beta-hydroxysteroid dehydrogenases in human bone cells. *J. Bone Miner. Res.* **1998**, *13*, 1539−1546.

(17) Feix, M.; Wolf, L.; Schweikert, H. U. Distribution of 17beta-hydroxysteroid dehydrogenases in human osteoblast-like cells. *Mol. Cell. Endocrinol.* **2001**, *171*, 163−164.

(18) Eyre, L. J.; Bland, R.; Bujalska, I. J.; Sheppard, M. C.; Stewart, P. M.; Hewison, M. Characterization of aromatase and 17 beta-hydroxysteroid dehydrogenase expression in rat osteoblastic cells. *J. Bone Miner. Res.* **1998**, *13*, 996−1004.

(19) van Grunsven, E G; van Berkel, E.; Ijlst, L.; Vreken, P.; de Klerk, J. B.; Adamski, J.; Lemonde, H.; Clayton, P. T.; Cuebas, D. A.; Wanders, R. J. Peroxisomal D-hydroxyacyl-CoA dehydrogenase deficiency: resolution of the enzyme defect and its molecular basis in bifunctional protein deficiency. *Proc. Natl. Acad. Sci. U.S.A.* **1998**, *95*, 2128−2133.

(20) Blomquist, C. H.; Lindemann, N. J.; Hakanson, E. Y. 17 beta-Hydroxysteroid and 20 alpha-hydroxysteroid dehydrogenase activities of human placental microsomes: kinetic evidence for two enzymes differing in substrate specificity. *Arch. Biochem. Biophys.* **1985**, *239*, 206−215.

(21) Bydal, P.; Auger, S.; Poirier, D. Inhibition of type 2 17β-hydroxysteroid dehydrogenase by estradiol derivatives bearing a lactone on the D-ring: structure−activity relationships. *Steroids* **2004**, *69*, 325−342.

(22) Poirier, D.; Bydal, P.; Tremblay, M. R.; Sam, K. M.; Luu-The, V. Inhibitors of type II 17beta-hydroxysteroid dehydrogenase. *Mol. Cell. Endocrinol.* **2001**, *171*, 119−128.
(23) Sam, K. M.; Auger, S.; Luu-The, V.; Poirier, D. Steroidal spirogamma-lactones that inhibit 17 beta-hydroxysteroid dehydrogenase activity in human placental microsomes. *J. Med. Chem.* **1995**, *38*, 4518−4528.
(24) Tremblay, M. R.; Luu-The, V.; Leblanc, G.; Noël, P.; Breton, E.; Labrie, F.; Poirier, D. Spironolactone-related inhibitors of type II 17beta-hydroxysteroid dehydrogenase: chemical synthesis, receptor binding affinities, and proliferative/antiproliferative activities. *Bioorg. Med. Chem.* **1999**, *7*, 1013−1023.
(25) Cook, J. H.; Barzya, J.; Brennan, C.; Lowe, D.; Wang, Y.; Redman, A.; Scott, W. J.; Wood, J. E. 4,5-Disubstituted cis-pyrrolidinones as inhibitors of 17β-hydroxysteroid dehydrogenase II. Part 1: Synthetic approach. *Tetrahedron Lett.* **2005**, *46*, 1525−1528.
(26) Gunn, D.; Akuche, C.; Baryza, J.; Blue, M.-L.; Brennan, C.; Campbell, A.-M.; Choi, S.; Cook, J.; Conrad, P.; Dixon, B.; Dumas, J.; Ehrlich, P.; Gane, T.; Joe, T.; Johnson, J.; Jordan, J.; Kramss, R.; Liu, P.; Levy, J.; Lowe, D.; McAlexander, I.; Natero, R.; Redman, A. M.; Scott, W.; Seng, T.; Sibley, R.; Wang, M.; Wang, Y.; Wood, J.; Zhang, Z. 4,5-Disubstituted cis-pyrrolidinones as inhibitors of type II 17beta-hydroxysteroid dehydrogenase. Part 2. SAR. *Bioorg. Med. Chem. Lett.* **2005**, *15*, 3053−3057.
(27) Wood, J.; Bagi, C. M.; Akuche, C.; Bacchiocchi, A.; Baryza, J.; Blue, M.-L.; Brennan, C.; Campbell, A.-M.; Choi, S.; Cook, J. H.; Conrad, P.; Dixon, B. R.; Ehrlich, P. P.; Gane, T.; Gunn, D.; Joe, T.; Johnson, J. S.; Jordan, J.; Kramss, R.; Liu, P.; Levy, J.; Lowe, D. B.; McAlexander, I.; Natero, R.; Redman, A. M.; Scott, W. J.; Town, C.; Wang, M.; Wang, Y.; Zhang, Z. 4,5-Disubstituted cis-pyrrolidinones as inhibitors of type II 17beta-hydroxysteroid dehydrogenase. Part 3. Identification of lead candidate. *Bioorg. Med. Chem. Lett.* **2006**, *16*, 4965−4968.
(28) Wetzel, M.; Marchais-Oberwinkler, S.; Hartmann, R. W. 17β-HSD2 inhibitors for the treatment of osteoporosis: identification of a promising scaffold. *Bioorg. Med. Chem.* **2011**, *19*, 807−815.
(29) Wetzel, M.; Marchais-Oberwinkler, S.; Perspicace, E.; Möller, G.; Adamski, J.; Hartmann, R. W. Introduction of an electron withdrawing group on the hydroxyphenylnaphthol scaffold improves the potency of 17β-hydroxysteroid dehydrogenase type 2 (17β-HSD2) inhibitors. *J. Med. Chem.* **2011**, *54*, 7547−7557.
(30) Wetzel, M.; Gargano, E. M.; Hinsberger, S.; Marchais-Oberwinkler, S.; Hartmann, R. W. Discovery of a new class of bicyclic substituted hydroxyphenylmethanones as 17β-hydroxysteroid dehydrogenase type 2 (17β-HSD2) inhibitors for the treatment of osteoporosis. *Eur. J. Med. Chem.* **2012**, *47*, 1−17.
(31) Al-Soud, Y. A.; Marchais-Oberwinkler, S.; Frotscher, M.; Hartmann, R. W. Synthesis and biological evaluation of phenyl substituted 1*H*-1,2,4-triazoles as non-steroidal inhibitors of 17β-hydroxysteroid dehydrogenase type 2. *Arch. Pharm.* **2012**, *345*, 610−621.
(32) Xu, K.; Al-Soud, Y. A.; Wetzel, M.; Hartmann, R. W.; Marchais-Oberwinkler, S. Triazole ring-opening leads to the discovery of potent nonsteroidal 17β-hydroxysteroid dehydrogenase type 2 inhibitors. *Eur. J. Med. Chem.* **2011**, *46*, 5978−5990.
(33) Bagi, C. M.; Wood, J.; Wilkie, D.; Dixon, B. Effect of 17beta-hydroxysteroid dehydrogenase type 2 inhibitor on bone strength in ovariectomized cynomolgus monkeys. *J. Musculoskeletal Neuronal Interact.* **2008**, *8*, 267−280.
(34) Frotscher, M.; Ziegler, E.; Marchais-Oberwinkler, S.; Kruchten, P.; Neugebauer, A.; Fetzer, L.; Scherer, C.; Müller-Vieira, U.; Messinger, J.; Thole, H.; Hartmann, R. W. Design, synthesis, and biological evaluation of (hydroxyphenyl)naphthalene and -quinoline derivatives: potent and selective nonsteroidal inhibitors of 17beta-hydroxysteroid dehydrogenase type 1 (17beta-HSD1) for the treatment of estrogen-dependent diseases. *J. Med. Chem.* **2008**, *51*, 2158−2169.
(35) Marchais-Oberwinkler, S.; Kruchten, P.; Frotscher, M.; Ziegler, E.; Neugebauer, A.; Bhoga, U.; Bey, E.; Müller-Vieira, U.; Messinger, J.; Thole, H.; Hartmann, R. W. Substituted 6-phenyl-2-naphthols. Potent and selective nonsteroidal inhibitors of 17beta-hydroxysteroid dehydrogenase type 1 (17beta-HSD1): design, synthesis, biological evaluation, and pharmacokinetics. *J. Med. Chem.* **2008**, *51*, 4685−4698.
(36) Marchais-Oberwinkler, S.; Wetzel, M.; Ziegler, E.; Kruchten, P.; Werth, R.; Henn, C.; Hartmann, R. W.; Frotscher, M. New drug-like hydroxyphenylnaphthol steroidomimetics as potent and selective 17β-hydroxysteroid dehydrogenase type 1 inhibitors for the treatment of estrogen-dependent diseases. *J. Med. Chem.* **2011**, *54*, 534−547.
(37) Bey, E.; Marchais-Oberwinkler, S.; Kruchten, P.; Frotscher, M.; Werth, R.; Oster, A.; Algül, O.; Neugebauer, A.; Hartmann, R. W. Design, synthesis and biological evaluation of bis(hydroxyphenyl) azoles as potent and selective non-steroidal inhibitors of 17beta-hydroxysteroid dehydrogenase type 1 (17beta-HSD1) for the treatment of estrogen-dependent diseases. *Bioorg. Med. Chem.* **2008**, *16*, 6423−6435.
(38) Bey, E.; Marchais-Oberwinkler, S.; Werth, R.; Negri, M.; Al-Soud, Y. A.; Kruchten, P.; Oster, A.; Frotscher, M.; Birk, B.; Hartmann, R. W. Design, synthesis, biological evaluation and pharmacokinetics of bis(hydroxyphenyl) substituted azoles, thiophenes, benzenes, and aza-benzenes as potent and selective nonsteroidal inhibitors of 17beta-hydroxysteroid dehydrogenase type 1 (17beta-HSD1). *J. Med. Chem.* **2008**, *51*, 6725−6739.
(39) Bey, E.; Marchais-Oberwinkler, S.; Negri, M.; Kruchten, P.; Oster, A.; Klein, T.; Spadaro, A.; Werth, R.; Frotscher, M.; Birk, B.; Hartmann, R. W. New insights into the SAR and binding modes of bis(hydroxyphenyl)thiophenes and -benzenes: influence of additional substituents on 17beta-hydroxysteroid dehydrogenase type 1 (17beta-HSD1) inhibitory activity and selectivity. *J. Med. Chem.* **2009**, *52*, 6724−6743.
(40) Oster, A.; Klein, T.; Werth, R.; Kruchten, P.; Bey, E.; Negri, M.; Marchais-Oberwinkler, S.; Frotscher, M.; Hartmann, R. W. Novel estrone mimetics with high 17beta-HSD1 inhibitory activity. *Bioorg. Med. Chem.* **2010**, *18*, 3494−3505.
(41) Oster, A.; Hinsberger, S.; Werth, R.; Marchais-Oberwinkler, S.; Frotscher, M.; Hartmann, R. W. Bicyclic substituted hydroxyphenyl-methanones as novel inhibitors of 17β-hydroxysteroid dehydrogenase type 1 (17β-HSD1) for the treatment of estrogen-dependent diseases. *J. Med. Chem.* **2010**, *53*, 8176−8186.
(42) Oster, A.; Klein, T.; Henn, C.; Werth, R.; Marchais-Oberwinkler, S.; Frotscher, M.; Hartmann, R. W. Bicyclic substituted hydroxyphenylmethanone type inhibitors of 17β-hydroxysteroid dehydrogenase type 1 (17 β-HSD1): the role of the bicyclic moiety. *ChemMedChem* **2011**, *6*, 476−487.
(43) Spadaro, A.; Negri, M.; Marchais-Oberwinkler, S.; Bey, E.; Frotscher, M. Hydroxybenzothiazoles as new nonsteroidal inhibitors of 17β-hydroxysteroid dehydrogenase type 1 (17β-HSD1). *PLoS One* **2012**, *7*, e29252.
(44) Spadaro, A.; Frotscher, M.; Hartmann, R. W. Optimization of hydroxybenzothiazoles as novel potent and selective inhibitors of 17β-HSD1. *J. Med. Chem.* **2012**, *55*, 2469−2473.
(45) Henn, C.; Einspanier, A.; Marchais-Oberwinkler, S.; Frotscher, M.; Hartmann, R. W. Lead optimization of 17β-HSD1 inhibitors of the (hydroxyphenyl)naphthol sulfonamide type for the treatment of endometriosis. *J. Med. Chem.* **2012**, *55*, 3307−3318.
(46) Qiu, W.; Campbell, R. L.; Gangloff, A.; Dupuis, P.; Boivin, R. P.; Tremblay, M. R.; Poirier, D.; Lin, S.-X. A concerted, rational design of type 1 17beta-hydroxysteroid dehydrogenase inhibitors: estradiol-adenosine hybrids with high affinity. *FASEB J.* **2002**, *16*, 1829−1831.
(47) Kruchten, P.; Werth, R.; Marchais-Oberwinkler, S.; Frotscher, M.; Hartmann, R. W. Development of a biological screening system for the evaluation of highly active and selective 17beta-HSD1-inhibitors as potential therapeutic agents. *Mol. Cell. Endocrinol.* **2009**, *301*, 154−157.
(48) Negri, M.; Recanatini, M.; Hartmann, R. W. Computational investigation of the binding mode of bis(hydroxylphenyl)arenes in 17β-HSD1: molecular dynamics simulations, MM-PBSA free energy calculations, and molecular electrostatic potential maps. *J. Comput.-Aided Mol. Des.* **2011**, *25*, 795−811.

(49) Zimmermann, J.; Liebl, R.; von Angerer, E. 2,5-Diphenylfuran-based pure antiestrogens with selectivity for the estrogen receptor alpha. *J. Steroid Biochem. Mol. Biol.* **2005**, *94*, 57−66.
(50) Schuster, D.; Kowalik, D.; Kirchmair, J.; Laggner, C.; Markt, P.; Aebischer-Gumy, C.; Ströhle, F.; Möller, G.; Wolber, G.; Wilckens, T.; Langer, T.; Odermatt, A.; Adamski, J. Identification of chemically diverse, novel inhibitors of 17β-hydroxysteroid dehydrogenase type 3 and 5 by pharmacophore-based virtual screening. *J. Steroid Biochem. Mol. Biol.* **2011**, *125*, 148−161.
(51) Möller, G.; Deluca, D.; Gege, C.; Rosinus, A.; Kowalik, D.; Peters, O.; Droescher, P.; Elger, W.; Adamski, J.; Hillisch, A. Structure-based design, synthesis and in vitro characterization of potent 17beta-hydroxysteroid dehydrogenase type 1 inhibitors based on 2-substitutions of estrone and D-homo-estrone. *Bioorg. Med. Chem. Lett.* **2009**, *19*, 6740−6744.
(52) Thomas, M. P.; Potter, B. V. L Crystal structures of 11β-hydroxysteroid dehydrogenase type 1 and their use in drug discovery. *Future Med. Chem.* **2011**, *3*, 367−390.
(53) Baker, M. E. Unusual evolution of 11beta- and 17beta-hydroxysteroid and retinol dehydrogenases. *BioEssays* **1996**, *18*, 63−70.
(54) Kratschmar, D. V.; Vuorinen, A.; Da Cunha, T.; Wolber, G.; Classen-Houben, D.; Doblhoff, O.; Schuster, D.; Odermatt, A. Characterization of activity and binding mode of glycyrrhetinic acid derivatives inhibiting 11β-hydroxysteroid dehydrogenase type 2. *J. Steroid Biochem. Mol. Biol.* **2011**, *125*, 129−142.
(55) Ahasan, M. M.; Hardy, R.; Jones, C.; Kaur, K.; Nanus, D.; Juarez, M.; Morgan, S. A.; Hassan-Smith, Z.; Bénézech, C.; Caamaño, J. H.; Hewison, M.; Lavery, G.; Rabbitt, E. H.; Clark, A. R.; Filer, A.; Buckley, C. D.; Raza, K.; Stewart, P. M.; Cooper, M. S. Inflammatory regulation of glucocorticoid metabolism in mesenchymal stromal cells. *Arthritis Rheum.* **2012**, *64*, 2404−2413.
(56) Lipinski, C. A.; Lombardo, F.; Dominy, B. W.; Feeney, P. J. Experimental and computational approaches to estimate solubility and permeability in drug discovery and development settings. *Adv. Drug Delivery Rev.* **2001**, *46*, 3−26.
(57) Denizot, F.; Lang, R. Rapid colorimetric assay for cell growth and survival. Modifications to the tetrazolium dye procedure giving improved sensitivity and reliability. *J. Immunol. Methods* **1986**, *89*, 271−277.
(58) Pogoda, P.; Priemel, M.; Schilling, A.; Gebauer, M.; Catalá-Lehnenf, P.; Barvencik, F.; Beil, F.; Münch, C.; Rupprecht, M.; Müldner, C.; Rueger, J.; Schinke, T.; Amling, M.; Pogoda, P.; Priemel, M.; Schilling, A.; Gebauer, M.; Catalá-Lehnen, P.; Barvencik, F.; Beil, F.; Munch, C.; Rupprecht, M.; Miildner, C.; Rueger, J.; Schinke, T.; Amling, M. Mouse models in skeletal physiology and osteoporosis: experiences and data on 14839 cases from the Hamburg Mouse Archives. *J. Bone Miner. Metab.* **2005**, *23*, 97−102.
(59) Joerg, H.; Holstein, P. G. Mouse Models for the Study of Fracture Healing and Bone Regeneration. In *Osteoporosis Research: Animal Models*; Duque, G., Watanabe, K., Eds.; Springer: London, 2011; pp 175−191.
(60) Zhu, D. W.; Lee, X.; Breton, R.; Ghosh, D.; Pangborn, W.; Daux, W. L.; Lin, S. X. Crystallization and preliminary X-ray diffraction analysis of the complex of human placental 17 beta-hydroxysteroid dehydrogenase with NADP. *J. Mol. Biol.* **1993**, *234*, 242−244.
(61) Jazbutyte, V.; Hu, K.; Kruchten, P.; Bey, E.; Maier, S. K. G.; Fritzemeier, K.-H.; Prelle, K.; Hegele-Hartung, C.; Hartmann, R. W.; Neyses, L.; Ertl, G.; Pelzer, T. Aging reduces the efficacy of estrogen substitution to attenuate cardiac hypertrophy in female spontaneously hypertensive rats. *Hypertension* **2006**, *48*, 579−586.
(62) Odermatt, A.; Arnold, P.; Stauffer, A.; Frey, B. M.; Frey, F. J. The N-terminal anchor sequences of 11beta-hydroxysteroid dehydrogenases determine their orientation in the endoplasmic reticulum membrane. *J. Biol. Chem.* **1999**, *274*, 28762−28770.
(63) Lin, S. X.; Yang, F.; Jin, J. Z.; Breton, R.; Zhu, D. W.; Luu-The, V.; Labrie, F. Subunit identity of the dimeric 17 beta-hydroxysteroid dehydrogenase from human placenta. *J. Biol. Chem.* **1992**, *267*, 16182−16187.
(64) Sam, K. M.; Boivin, R. P.; Tremblay, M. R.; Auger, S.; Poirier, D. C16 and C17 derivatives of estradiol as inhibitors of 17 beta-hydroxysteroid dehydrogenase type 1: chemical synthesis and structure−activity relationships. *Drug Des. Discovery* **1998**, *15*, 157−180.
(65) Day, J. M.; Tutill, H. J.; Newman, S. P.; Purohit, A.; Lawrence, H. R.; Vicker, N.; Potter, B. V. L; Reed, M. J. 17Beta-hydroxysteroid dehydrogenase type 1 and type 2: association between mRNA expression and activity in cell lines. *Mol. Cell. Endocrinol.* **2006**, *248*, 246−249.

Appendix

Protocol: Preparation of intact liver microsomes & cytochrome C reductase assay

IMPORTANT: Work always on ice!

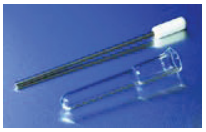

Solution A: 10 mM imidazole, 0.3 M sucrose, pH 7.0

Solution B: 20 mM tris-maleate, 0.6 M KCl, 0.3 M sucrose, pH 7.0

Solution C: 10 mM tris-maleate, 0.15 M KCl, 0.25 M sucrose, pH 7.0

Per 100 mg tissue use 2 mL sol. A, 0.5 mL sol. B and 0.2 mL sol. C. All solutions are supplemented with 1 % protease inhibitor (7x stock of complete®, Mini Protease Inhibitor Cocktail, Roche)

1. Use 100 mg fresh or frozen liver tissue and 2 mL **solution A,** homogenize with a Potter-Elvehjem PTFE pestle and glass tube applying approximately 10 - 12 strokes with rotations (220 rpm) with the polytron, transfer homogenate to a plastic tube
2. centrifuge at 4˚C, 10 min, 1'000 × g, transfer supernatant into new plastic tube, repeat centrifugation transfer supernatant into new plastic tube
3. centrifuge at 4˚C, 10 min, 12'000 × g, transfer supernatant into ultracentrifugation tube (Microfuge Tube Polyallomer® from Beckman in lab 5007)
4. centrifuge at 4˚C, 60 min, 100'000 × g with ultracentrifuge (BZ 5th floor)
5. resuspend pellet in 0.5 mL of **solution B** (will be difficult to resuspend)
6. centrifuge at 4˚C, 60 min, 100'000 × g with ultracentrifuge (BZ 5th floor)
7. resuspend pellet in 0.2 mL of **solution C** (that will yield approx. 2 mg/mL)
8. spin 5 sec, at 4˚C (maximal speed) table top centrifuge, remove white chunks, transfer supernatant to new tube, make aliquots and freeze at – 80 °C.
9. Characterize microsomes by total protein assay (BCA) and test for activity with cytochrome C reductase assay kit.

Cytochrome C reductase assay kit from Sigma in 96-well plate (Sigma CY0100)

1. 95 µL working solution (0.9 mg cytochrome C + 2 ml assay buffer)
2. 5 µL of enzyme (approx. 10 µg, dilute as needed with dilution buffer)
3. 10 µL NADPH (0.85 mg/mL) (22 µL of NADPH aliquot + 1 mL H_2O)
4. Positive control - Dilute an aliquot of the cytochrome c reductase (NADPH) (Catalog Number C9363) 10-fold with the enzyme dilution buffer just before assaying
5. Set the spectrophotometer to 550 nm and run the kinetic program at 25°C:
    a. Initial delay = 5 seconds
    b. interval= 10 seconds
    c. readings = 7

Calculate activity (Units/mL) = (ΔA_{550}/min * dilution factor * 0.11) / (21.1 * volume of the enzyme sample (mL))
Should be over 3 Units/mL for microsomes.

References

[1] Atanasov AG, Nashev LG, Gelman L, Legeza B, Sack R, Portmann R, et al. Direct protein-protein interaction of 11beta-hydroxysteroid dehydrogenase type 1 and hexose-6-phosphate dehydrogenase in the endoplasmic reticulum lumen. Biochim Biophys Acta 2008;1783:1536-43.

[2] Zhang Y-l, Zhong X, Gjoka Z, Li Y, Stochaj W, Stahl M, et al. H6PDH interacts directly with 11β-HSD1: Implications for determining the directionality of glucocorticoid catalysis. Archives of Biochemistry and Biophysics 2009;483:45-54.

[3] Bánhegyi G, Benedetti A, Fulceri R, Senesi S. Cooperativity between 11β-Hydroxysteroid Dehydrogenase Type 1 and Hexose-6-phosphate Dehydrogenase in the Lumen of the Endoplasmic Reticulum. Journal of Biological Chemistry 2004;279:27017-21.

[4] Nyfeler B, Michnick SW, Hauri H-P. Capturing protein interactions in the secretory pathway of living cells. Proceedings of the National Academy of Sciences of the United States of America 2005;102:6350-5.

[5] Atanasov AG, Odermatt A. Readjusting the glucocorticoid balance: an opportunity for modulators of 11beta-hydroxysteroid dehydrogenase type 1 activity? Endocr Metab Immune Disord Drug Targets 2007;7:125-40.

[6] Hughes KA, Webster SP, Walker BR. 11-Beta-hydroxysteroid dehydrogenase type 1 (11beta-HSD1) inhibitors in type 2 diabetes mellitus and obesity. Expert Opin Investig Drugs 2008;17:481-96.

[7] Sun D, Wang M, Wang Z. Small molecule 11beta-hydroxysteroid dehydrogenase type 1 inhibitors. Curr Top Med Chem 2011;11:1464-75.

[8] Masuzaki H, Flier JS. Tissue-specific glucocorticoid reactivating enzyme, 11 beta-hydroxysteroid dehydrogenase type 1 (11 beta-HSD1)--a promising drug target for the treatment of metabolic syndrome. Curr Drug Targets Immune Endocr Metabol Disord 2003;3:255-62.

[9] Nashev LG, Chandsawangbhuwana C, Balazs Z, Atanasov AG, Dick B, Frey FJ, et al. Hexose-6-phosphate dehydrogenase modulates 11beta-hydroxysteroid dehydrogenase type 1-dependent metabolism of 7-keto- and 7beta-hydroxy-neurosteroids. PLoS One 2007;2:e561.

[10] Schweizer RA, Zurcher M, Balazs Z, Dick B, Odermatt A. Rapid hepatic metabolism of 7-ketocholesterol by 11beta-hydroxysteroid dehydrogenase type 1: species-specific differences between the rat, human, and hamster enzyme. J Biol Chem 2004;279:18415-24.

[11] Odermatt A, Da Cunha T, Penno CA, Chandsawangbhuwana C, Reichert C, Wolf A, et al. Hepatic reduction of the secondary bile acid 7-oxolithocholic acid is mediated by 11beta-hydroxysteroid dehydrogenase 1. Biochem J 2011;436:621-9.

[12] Wsol V, Szotakova B, Skalova L, Maser E. Stereochemical aspects of carbonyl reduction of the original anticancer drug oracin by mouse liver microsomes and purified 11beta-hydroxysteroid dehydrogenase type 1. Chemico-Biological Interactions 2003;143-144:459-68.

[13] Maser E, Bannenberg G. 11 beta-hydroxysteroid dehydrogenase mediates reductive metabolism of xenobiotic carbonyl compounds. Biochem Pharmacol 1994;47:1805-12.

[14] Hult M, Nobel CS, Abrahmsen L, Nicoll-Griffith DA, Jornvall H, Oppermann UC. Novel enzymological profiles of human 11beta-hydroxysteroid dehydrogenase type 1. Chem Biol Interact 2001;130-132:805-14.
[15] Kenneke JF, Mazur CS, Ritger SE, Sack TJ. Mechanistic investigation of the noncytochrome P450-mediated metabolism of triadimefon to triadimenol in hepatic microsomes. Chem Res Toxicol 2008;21:1997-2004.
[16] Crowell SR, Henderson WM, Fisher JW, Kenneke JF. Gender and species differences in triadimefon metabolism by rodent hepatic microsomes. Toxicol Lett 2010;193:101-7.
[17] Barton HA, Tang J, Sey YM, Stanko JP, Murrell RN, Rockett JC, et al. Metabolism of myclobutanil and triadimefon by human and rat cytochrome P450 enzymes and liver microsomes. Xenobiotica; the fate of foreign compounds in biological systems 2006;36:793-806.
[18] Fang H, Tang FF, Zhou W, Cao ZY, Wang DD, Liu KL, et al. Persistence of repeated triadimefon application and its impact on soil microbial functional diversity. J Environ Sci Health B 2012;47:104-10.
[19] Wang X, Abdelrahman DR, Fokina VM, Hankins GD, Ahmed MS, Nanovskaya TN. Metabolism of bupropion by baboon hepatic and placental microsomes. Biochem Pharmacol 2011;82:295-303.
[20] Wang X, Abdelrahman DR, Zharikova OL, Patrikeeva SL, Hankins GDV, Ahmed MS, et al. Bupropion metabolism by human placenta. Biochem Pharmacol 2010;79:1684-90.
[21] Molnari JC, Myers AL. Carbonyl reduction of bupropion in human liver. Xenobiotica 2012;42:550-61.
[22] Fava M, Rush AJ, Thase ME, Clayton A, Stahl SM, Pradko JF, et al. 15 years of clinical experience with bupropion HCl: from bupropion to bupropion SR to bupropion XL. Prim Care Companion J Clin Psychiatry 2005;7:106-13.
[23] Holm KJ, Spencer CM. Bupropion: A Review of its Use in the Management of Smoking Cessation. Drugs 2000;59:1007-24.
[24] Faucette SR, Hawke RL, Lecluyse EL, Shord SS, Yan B, Laethem RM, et al. Validation of Bupropion Hydroxylation as a Selective Marker of Human Cytochrome P450 2B6 Catalytic Activity. Drug Metabolism and Disposition 2000;28:1222-30.
[25] Hesse LM, Venkatakrishnan K, Court MH, von Moltke LL, Duan SX, Shader RI, et al. CYP2B6 Mediates the In Vitro Hydroxylation of Bupropion: Potential Drug Interactions with Other Antidepressants. Drug Metabolism and Disposition 2000;28:1176-83.
[26] Atanasov AG, Nashev LG, Tam S, Baker ME, Odermatt A. Organotins disrupt the 11beta-hydroxysteroid dehydrogenase type 2-dependent local inactivation of glucocorticoids. Environ Health Perspect 2005;113:1600-6.
[27] Atanasov AG, Tam S, Rocken JM, Baker ME, Odermatt A. Inhibition of 11 beta-hydroxysteroid dehydrogenase type 2 by dithiocarbamates. Biochemical and Biophysical Research Communications 2003;308:257-62.
[28] Kusakabe M, Nakamura I, Young G. 11β-Hydroxysteroid Dehydrogenase Complementary Deoxyribonucleic Acid in Rainbow Trout: Cloning, Sites of Expression, and Seasonal Changes in Gonads. Endocrinology 2003;144:2534-45.
[29] Jiang JQ, Wang DS, Senthilkumaran B, Kobayashi T, Kobayashi HK, Yamaguchi A, et al. Isolation, characterization and expression of 11beta-hydroxysteroid dehydrogenase type 2 cDNAs from the testes of Japanese eel (Anguilla japonica) and Nile tilapia (Oreochromis niloticus). J Mol Endocrinol 2003;31:305-15.
[30] Rasheeda MK, Kagawa H, Kirubagaran R, Dutta-Gupta A, Senthilkumaran B. Cloning, expression and enzyme activity analysis of testicular 11beta-hydroxysteroid

dehydrogenase during seasonal cycle and after hCG induction in air-breathing catfish Clarias gariepinus. The Journal of Steroid Biochemistry and Molecular Biology 2010;120:1-10.
[31] Miura T, Yamauchi K, Takahashi H, Nagahama Y. Hormonal induction of all stages of spermatogenesis in vitro in the male Japanese eel (Anguilla japonica). Proceedings of the National Academy of Sciences of the United States of America 1991;88:5774-8.
[32] Castro IB, Rossato M, Fillmann G. Imposex reduction and residual butyltin contamination in southern Brazilian harbors. Environ Toxicol Chem 2012.
[33] Kannan K, Tanabe S, Iwata H, Tatsukawa R. Butyltins in muscle and liver of fish collected from certain Asian and Oceanian countries. Environmental Pollution 1995;90:279-90.
[34] Jadhav S, Bhosale D, Bhosle N. Baseline of organotin pollution in fishes, clams, shrimps, squids and crabs collected from the west coast of India. Marine Pollution Bulletin 2011;62:2213-9.
[35] Mindnich R, Adamski J. Zebrafish 17beta-hydroxysteroid dehydrogenases: An evolutionary perspective. Mol Cell Endocrinol 2009;301:20-6.
[36] Nashev LG, Schuster D, Laggner C, Sodha S, Langer T, Wolber G, et al. The UV-filter benzophenone-1 inhibits 17beta-hydroxysteroid dehydrogenase type 3: Virtual screening as a strategy to identify potential endocrine disrupting chemicals. Biochem Pharmacol 2010;79:1189-99.
[37] Baker ME. Evolutionary analysis of 11[beta]-hydroxysteroid dehydrogenase-type 1, -type 2, -type 3 and 17[beta]-hydroxysteroid dehydrogenase-type 2 in fish. FEBS Letters 2004;574:167-70.
[38] Baker ME. Evolution of 11[beta]-hydroxysteroid dehydrogenase-type 1 and 11[beta]-hydroxysteroid dehydrogenase-type 3. FEBS Letters 2010;584:2279-84.
[39] Bagi CM, Wood J, Wilkie D, Dixon B. Effect of 17beta-hydroxysteroid dehydrogenase type 2 inhibitor on bone strength in ovariectomized cynomolgus monkeys. J Musculoskelet Neuronal Interact 2008;8:267-80.
[40] Vihko P, Isomaa V, Ghosh D. Structure and function of 17beta-hydroxysteroid dehydrogenase type 1 and type 2. Mol Cell Endocrinol 2001;171:71-6.
[41] Sinnesael M, Boonen S, Claessens F, Gielen E, Vanderschueren D. Testosterone and the Male Skeleton: A Dual Mode of Action. Journal of Osteoporosis 2011;2011.
[42] Vanderschueren D, Gaytant J, Boonen S, Venken K. Androgens and bone. Curr Opin Endocrinol Diabetes Obes 2008;15:250-4.